TAMPEREEN TEKNILLINEN YLIOPISTO
TAMPERE UNIVERSITY OF TECHNOLOGY

SANTHOSH KUMAR PANDIAN

PREPARATION AND CHARACTERIZATION OF TITANIUM BASED COATINGS BY DIRECT-CURRENT (DC) MAGNETRON SPUTTERING PROCESS

Master of Science thesis

**Examiners: Prof. Petri Vuoristo,
Dr. Minna Kotilainen**

Examiners and topic approved
by the Council of the Faculty
of Engineering Sciences on
7th October 2015

ABSTRACT

SANTHOSH KUMAR PANDIAN: Preparation and characterization of titanium based coatings by Direct-Current (DC) magnetron sputtering process
Tampere University of technology
Master of Science Thesis, 133 pages
November 2016
Master's Degree Programme in Material Science
Major: Metallic and ceramic materials
Examiner: Professor Petri Vuoristo, Dr. Minna Kotilainen

Keywords: Thin films, DC magnetron sputtering, sputtering parameters, titanium, titanium nitride, microstructure, film properties

Thin film coatings by sputtering process are widely used in numerous industries due to their superior qualities such as improvement in wear and corrosion resistance, enhancement of the surface quality, functional properties enrichment and increased life-time. So withstanding the above mentioned conditions is essential for numerous industrial and medical applications. One of the most effective ways to create thin film materials of desired composition is sputtering process. Nordiko sputtering (NS) 2500 equipment is used in this thesis work to carry out the sputtering experiments.

The aim of the thesis work is to study the relationship between depositions parameters used for DC magnetron sputtering process using Nordiko sputtering (NS-2500) equipment. The study is mainly focused to explain the relationship between deposition rates of thin film depositions with respect to sputtering parameters involved. One of the main objective is to study the effect of deposition parameters on the resultant microstructures and properties such as adhesion strength and surface roughness. This research work also deals with investigating the operation of Nordiko sputtering equipment and obtaining relevant experience related to it. The study is also focused on to briefly analyze the effect of substrate heating and etching to understand the morphological changes observed during sputtering depositions

The thin film coating formation of titanium and titanium nitride compositions is successfully deposited using Nordiko sputtering equipment. Typical deposition rates were able to achieve in this DC magnetron sputtering process. In this thesis work, the relationship between deposition parameters is studied in detail and verified using various experimentation techniques. The effect of deposition parameters on the resultant microstructures and properties such as adhesion strength and surface roughness is successfully studied using several characterization techniques such as FESEM, adhesion strength, optical profilometer and XRD analysis. The effect of substrate etching and heating is studied briefly in this thesis work and the results established significant improvement in deposition rates and adhesion strength values. The sputtering equipment used in this experiment work is studied completely and it can be used for versatile operations. A short operational guide regarding the user manual is also prepared in this thesis report.

PREFACE

This work was carried out at the department of Material Science, Tampere University of Technology (TUT) Tampere, Finland. I wish to express my sincere and greatest gratitude to my supervisor, Prof. Petri Vuoristo for his continuous encouragement and helpful discussions during this thesis work. It is with great pleasure I thank Professor Petri Vuoristo for providing me a great opportunity to work in my area of interest. My sincere thanks to Dr. Minna Kotilainen (VTT) for her valuable discussions and support during this thesis study.

My special thanks to people who assisted me in finishing the research tasks during this thesis work. I would like to thank Dr. Minna Kotilainen (VTT) and Mr. Jarmo Laakso (TUT) for their support and valuable comments during FESEM analysis. I would also like to express my gratitude to researchers Davide Fantozzi and Leo Hyvärinen for X-ray diffraction studies and Mr. Jarmo Laakso for optical profilometer trainings. I am also grateful to Mr. Mikko Kylmälahti and Mr. Ari Varttila for their support in assembling the sputtering system. I would like to express my sincere gratitude to all those people who aided me in various ways to complete this project successfully. I would like to take this opportunity to thank and acknowledge Fortum Foundation for their financial support during this master thesis study.

I wish to thank my parents and family, for their encouraging support all through my thesis work and motivated me towards achieving my goal and completing this research work by providing moral support.

Many thanks to my supervisor, all my co-workers from surface engineering laboratory for their support during this thesis study.

Tampere, 23.11.2016

Santhosh Kumar Pandian

TABLE OF CONTENTS

LIST OF SYMBOLS AND ABBREVIATIONS

α	Alpha
°	Degree
θ	Theta
ε	Field amplitude
ω_c	Cyclotron frequency
%	Percentage
”	Inches
μm	Micrometer
316L	Low carbon version of the 316 steel alloy
2D	2-dimensional
3D	3-dimensional
α-Ti	Alpha-titanium phase
γ-Fe	Austenite phase

A	Amperes
AISI	American Iron and Steel Institute
Al	Aluminum
AlN	Aluminum nitride
Ar^+	Argon ions
Ar	Argon
Ar. Pr	Argon pressure
B	Magnetic field
BCC	Body centered cubic
Cu-Kα	Copper radiation
℃	Degree Celsius
C	Celsius
CCP	Cubic close packed
cm	Centimetre
CO	Carbon monoxide
CO_2	Carbon dioxide
Cu	Copper
CVD	Chemical vapor deposition
DC	Direct-Current
DC 704	Diffusion oil type
Dep.rate	Deposition rate
DSC	Dye-sensitized solar cells
E	Electric field
EDS	Energy dispersive X-ray spectrometer
FCC	Face cantered cubic
FESEM	Field Emission Scanning Electron Microscopy
FIM	Focused ion microscopy
G	Gauss
g/cm^3	Gram/cubic centimeter
HASTINGS EVT-5	Thermocouple gauge type
HCP	Hexagonal close packed

Hi-Vac	High-vacuum valve
H.T. on	High tension control switch ON
H.V gauge	High Voltage gauge
I	Current
ICDD	International center for diffraction data
IR	Infrared
kW	Kilowatts
liq. N_2	Liquid nitrogen
l/s	Litre/second
mA/cm^2	Milliampere per square centimetre
mbar	Millibar
m_e	Mass
mins	Minutes
mm	Millimetre
mtorr	Millitorr
N_2	Nitrogen
N4 700-1400	Nordiko sputtering equipment model types
Nm	Nanometer
NM 400-2000	Nordiko sputtering equipment model types
NS	Nordiko sputtering
NS-2500	Nordiko Sputtering equipment
O_2	Oxygen
OFC	Oxygen-free copper
P	Pressure/Sputtering pressure
PCD	Pitch circle diameter
PVD	Physical Vapor depositions
q	Charge
Q	Outgassing rate
Ra	Surface roughness
RF	Radio-frequency
S/N curves	Stress (S) against the number of cycles to failure (N) or Fatigue
S	Pumping speed
SE1	Substrate electrode
SEM	Scanning electron microscopy
Si	Silicon
Sp	Speed
SS	Stainless steel
SZD	Structure-zone diagrams
SZM	Structure Zone Model
t	Time
Ta_2O_5	Tantalum oxide
TC1	Thermocouple gauge 1
TC2	Thermocouple gauge 2
TEM	Transmission electron microscopy
TFT	Thin film transistors
TiO_2	Titanium dioxide
Ti	Titanium
TiN	Titanium nitride
TiN_{1-x}	Titanium nitride sub stoichiometric compositions
$T_м$	Melting point of condensate

Ts	Substrate temperature
TUT	Tampere university of technology
U	Voltage
V	Volts
V	Voltage
V_b/Vs	Bias voltage
VLSI	Very-large scale integration
W	Watt
Wcm^{-2}	Watt per square centimetre
XRD	X-ray diffraction
x	Electron displacement
+Z	Positive Z-axis direction
ZnO	Zinc oxide
Zone Ib/ Ic	Extended SZD
Zone T	Transition zone

1. INTRODUCTION

The demand for deposition of coating materials with magnificent physical properties is always critical. The focus on developing thin film materials which are suitable for high temperature applications, high corrosive and erosive environments applications is highly increasing. So withstanding the above mentioned conditions is necessary for various industrial applications. This research work studies efficient methods to create new coating materials which can be used for various types of applications. One of the most effective ways to create thin film materials of desired composition is sputtering process. In general, sputtering deposition is used for depositing thin film coatings over the substrate from the target material. The sputtering process principle is similar to the game of billiards, where the cue ball hits the group of balls (break shot) and the object balls gets scattered along with the angle of impact [1-3]**.** As similar to this principle, generated plasma is used to ionize gas atoms which in turn strike the target surface. The impact emits atoms from the target material that will be transferred to the substrate surface and deposit coatings of required composition. In this research work, the coatings are developed using Direct-Current (DC) magnetron reactive sputtering process. The technique allows the deposition of compound materials of various composition. The main advantage of using this process is high deposition rate, excellent uniformity of coating, and control over the deposition parameters. Nordiko sputtering (NS) 2500 equipment is used in this thesis work to carry out the sputtering experiments. This equipment can be used for different sputtering process such as Direct-Current (DC) magnetron sputtering, Radio-frequency (RF) magnetron sputtering and bias sputtering process. The objectives of the research work are to develop thin film coatings with superior physical properties by DC magnetron sputtering process. To accomplish this, the relationship between the deposition parameters such as deposition rate, sputtering pressure, deposition time and their effect on the microstructural changes during thin film deposition is studied in detail. The titanium and titanium nitride coatings is deposited using DC magnetron sputtering process in this thesis work. Thus, depositing thin film coating materials with sputtering process is accomplished in this research study. One of the main objectives of this research work is to study operation of the sputtering equipment. The material chosen for sputtering thin film depositions are titanium (Ti) and titanium nitride (TiN) composition, and these materials does not have any negative impact towards environment [4]. In developing thin films by sputter deposition, there is no environmental hazard as the process is very safe and can be converted easily to large scale of industrial production [4]. The energy used for development of coating using sputtering deposition is considered quite negligible when

compared to other physical vapor deposition techniques such as evaporation [5; 6]. The thesis work focusses on optimizing the sputtering parameters used in reactive and non-reactive magnetron sputtering process. The microstructure of the coatings, types of coatings, composition present in the coatings are studied in detail to optimize the DC reactive magnetron sputtering process. The applications of the thin film coatings are varied greatly from biomedical applications to very high load applications .[1; 2; 7-11]

Magnetron sputtering is considered efficient and effective process when compared to other physical vapor depositions (PVD) such as evaporation, pulsed laser ablation, chemical vapor depositions (CVD) and sol-gel methods .[4] As magnetron sputtering have many advantages such as high deposition rate, deposition over large scale and repeatability of results is achieved. In general, polycrystalline films are also attained during sputtering process and the physical properties of the sputtered films are superior to other PVD process.[4; 5] The factors such as crystallographic orientation, deposition parameters and substrate materials used in the sputtering process significantly influences the morphological changes observed during film growth. This is one of the main benefits of sputtering as by controlling the parameters used in the deposition, the properties of deposited thin films is modified .[12] The advantages of using sputtering process is that it is cost-effective, simple in nature, increased rate of deposition and higher quality of thin films is achieved as end result. The deposition parameters play an important role in influencing the electrical and optical properties of thin films. [13] According to numerous research articles, it is clear that sputtering parameters used in magnetron sputtering process highly influence the structural, electrical and optical properties of deposited thin films. The other notable advantages of using sputtering process are increased mechanical stability of thin films, excellent uniformity in thin film coating and even at low temperature, superior deposition rate is accomplished [14].

The titanium thin film coatings are used in many industrial and medical applications owing to its superior properties such as high corrosion resistance, increase in mechanical properties, high thermal properties [11; 15; 16]. Titanium nitride (TiN) composition has various distinctive advantages such as wear resistant coatings, tools used for cutting, diffusion barriers and integrated circuits. TiN composition also have outstanding physical properties such as high hardness, inert, high corrosion resistance, low electrical resistivity, excellent thermal stability. These titanium and TiN coating materials have the combination of toughness, inertness, adhesion and hardness, owing to its excellent reflective nature and also used in jewelry and optics. [1] So, titanium and titanium nitride coatings have various advantages over other coating material and the applications ranges from microelectronics, light detectors, cutting tools and medical instrumentation. Therefore, special interest has been developed over the years about these Ti and TiN coatings and effective ways to deposit them is also analyzed in this thesis work.

2. DEPOSITION METHODS BASED ON SPUTTERING TECHNIQUES

This section will deal with the different types of sputtering processes and their subsequent development from one another. The sputtering process can be divided into four different types which as classified as follows i) DC ii) RF iii) Reactive and iv) Magnetron sputtering process [1; 9; 17-19]. There are several mechanisms where these sputtering processes are used to produce thin film coating over the substrate such as DC magnetron sputtering, RF magnetron sputtering, RF and DC diode sputtering process. [2] The most efficient ways to produce quality coatings are well established nowadays. In this part different types of sputtering process are considered and how it evolved to the modern technology to produce efficient coating material. The basic science behind the process is explained here, sputtering in general is a momentum transfer process, in which the atoms will be ejected from the surface of the target material by means of bombardment of energetic particles [2; 17; 20; 21]. The desired layer is obtained after the sputtered atoms reach the substrate surface [17; 20].

2.1 DC diode sputtering process

This is one of the oldest technologies to produce thin film coatings using sputtering technique. Initially, the coatings were mainly concentrating on metallic films over the metallic substrate, so until 1960s this DC diode sputtering process was one of the most common sputtering techniques available in the market. In 1852, W.R. Grove studied about sputter deposition for the first time. The significant achievement in the process was achieved by Leslie Holland in cathodic sputtering in the year 1956. L. Holland, detected an occurrence where due to the ionic bombardment of gas molecules the electrode (cathode) was degenerated, these particular phenomenon was observed when electrical current is delivered at low pressure. There was some notable accomplishment in the sputtering field, in 1933 C. J. Overbeck noted the formation of certain compounds which was used for coating and this happened in a reactive gas atmosphere. F.M. Penning suggested in 1936, if the plasma content used in the sputtering process needs to be increased, then electron trap (crossed field) was used. [19]

The mechanism involved in the DC diode sputtering is described as follows. The equipment comprises of a vacuum chamber, where two electrodes are present in it. [18] The target material usually used are metals, however other materials can be used too. The target materials used are of disk-shaped and it is connected to a backing plate which

cools the target material so that it does not crack due to overheating. The distance between target and the anode materials is around 8-10 (cm) centimeters. [19] This vacuum chamber should have perfect functioning gas stream and pumping system. The two different electrodes used is cathode (negative potential) which is the target material and anode is the substrate. The anode electrode can be connected to the ground or even biased depending on the process requirement. [18] In this sputtering process, the most important factor to be taken care is about the discharge. The discharge needs to be sustained so that the sputtering process takes place smoothly. The plasma is used to generate discharge and this discharge is termed as DC diode discharge. [1; 9]

The DC diode discharge is created in the vacuum chamber, usually the chamber is connected to the series of vacuum pumps. The vacuum produced inside the chamber will be controlled appropriately by various controllers such as leak valves, flow controllers, gauges and so on. The pressure created by the chamber is usually lower than the normal operating pressure used for the process. This is because working gases such as argon which will be added later in the chamber and these gases will be helping in achieving the required pressure. The electric field will be applied in between cathode and anode, which help in the process of accelerating the electrons towards the substrate material. The gas discharge produced will be collected in the cathode region and the electrons produced will acquire necessary energy to ionize the gas atoms present in the discharge. These ions try to impinge on the surface of the anode material thus coating occurs. In the meantime, when the electron comes in contact with gaseous atom present in the discharge, secondary electrons are produced along with the ions and these secondary electrons also help in maintaining the diode discharge. [9]

DC diode sputtering process is explained in this section, as mentioned previously the target material is connected to the negative potential of the power supply and the anode material is grounded. The pumps are connected to the chamber to create necessary pressure (usually low pressure) and vacuum conditions. The plasma discharge produced will be accumulated near the cathode region as shown in the Figure 1. The target cathode electrode material will be bombarded by the positive argon ions (Ar^+) and the result will be the production of neutral atoms. At certain point during the diode sputtering, the voltage is dropped near the cathode, which will help the ions to accelerate towards the anode and gets accumulated over the substrate material. These ions will collide with the gas atoms near the cathode region to produce secondary electrons which is used for maintain the discharge in the plasma. The main disadvantages of this sputtering would be deposition rates are very low, conductor materials can only be used, the plasma densities achieved will be very less when compared with the magnetron sputtering process. [18]

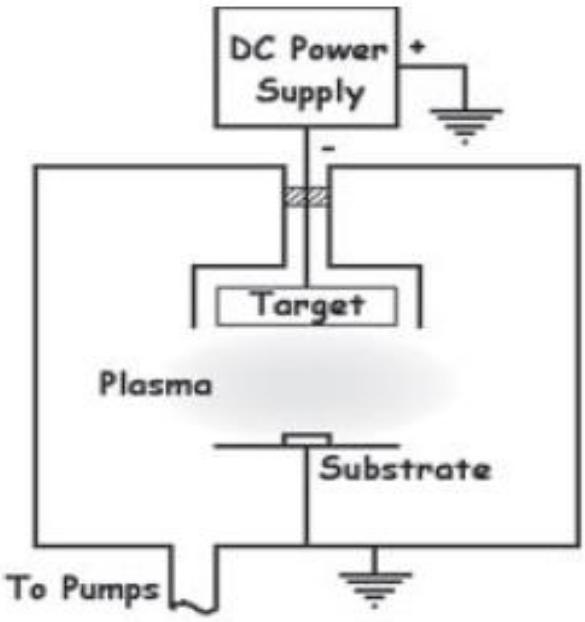

Figure 1. Typical schematic representation of DC diode sputtering process, displaying substrate material which is subjected to target ion bombardment by plasma ions. [18]

2.2 Triode sputtering process

The advancement in DC diode sputtering process in 1960 led to increase the efficiency of the deposition rate by including one more electrode to the DC diode setup. So the name and process 'Triode sputtering' came into existence. The extra electrode used in the process will be very hot in nature and can emit electrons into the plasma. The electrons are relatively emitted thermionically from the target surface. So by this the electron density is increased tremendously and thus the plasma ionization is also increased rapidly. Using this process led to the achievement of deposition rate of around hundred nm/min. The normal operating conditions for triode sputtering are pressure 0.5 -1 mtorr (millitorr) and the applied voltage is 50-100 V(volts) which are comparatively low with respect to magnetron sputtering process. The other advantage be thick coatings can be deposited by the triode sputtering. However, this triode sputtering has many disadvantages such as the hot electrode might react with the atoms present in the plasma, erosion of electrode, quality of coating is low, and uniformity of film coating is also not achieved properly. The practical difficulties were the thermionic emitter is susceptible to reactive gases present in the chamber, also the industrial scaling of the process is very limited. Over the development of magnetron sputtering process, triode sputtering lost its significance owing to the high rate sputtering of magnetron process. [18] The below mentioned Figure 2 represents the DC triode sputtering process.

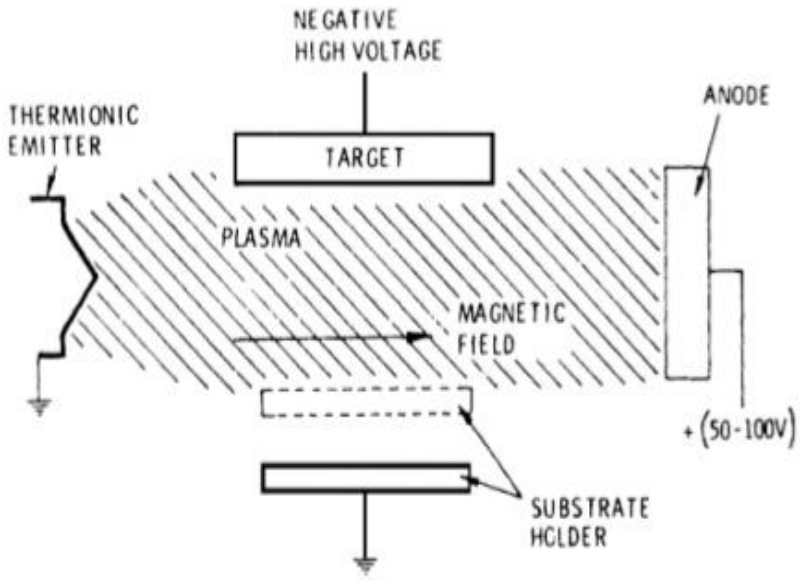

Figure 2. General schematic representation of Triode (hot-cathode assisted) sputtering process, simply demonstrating with a target (cathode) material and substrate (anode) material with an additional setup of Thermionic emitter (to emit hot electrons) in a plasma environment. [18]

2.3 Magnetron sputtering process

The planar magnetron was first designed by J.S Chapin in the year 1974. The process used sputter gun which was used as sputtering source and it was developed by Clarke in 1968. During 1970, planar magnetron was widely used in magnetron sputtering experiment. [18] The magnetron sputtering process is generally divided into three types 1) Planar magnetron 2) cylindrical magnetron and 3) Unbalanced magnetron sputtering process. The main difference between DC diode and magnetron process is that the cathode in latter process is being connected to a magnetic field. So that the electrons present in the process would follow the E*B drift path as shown in Figure 3 [18]. Due to magnetic field the electrons is concentrated near to the cathode surface, so more ionization. The secondary electrons also be present near the cathode surface and these electrons too will move in a circular path as shown in Figure 3**.** The electron circulating in the path will have higher radius if it has very high speed as shown in Figure 3 and vice-versa for the case with low speed electrons. When the electric field and magnetic field is influencing the electrons movement above the cathode surface, electrons interacting with the process gas to produce more ionizing atoms thus resulting in more collisions. The electrons also lose its energy due to interaction with the anode surface and the chamber surface. However, due to magnetic field the ionic density is increased conveniently and thereby increasing the deposition rate, uniformity of the coating with low substrate heating. The magnetron sputtering process can also be used in low

pressure. In general, the electrons will follow a cycloidal path near the cathode surface as shown in Figure 3 due to the linearly decreasing electric field. [18]

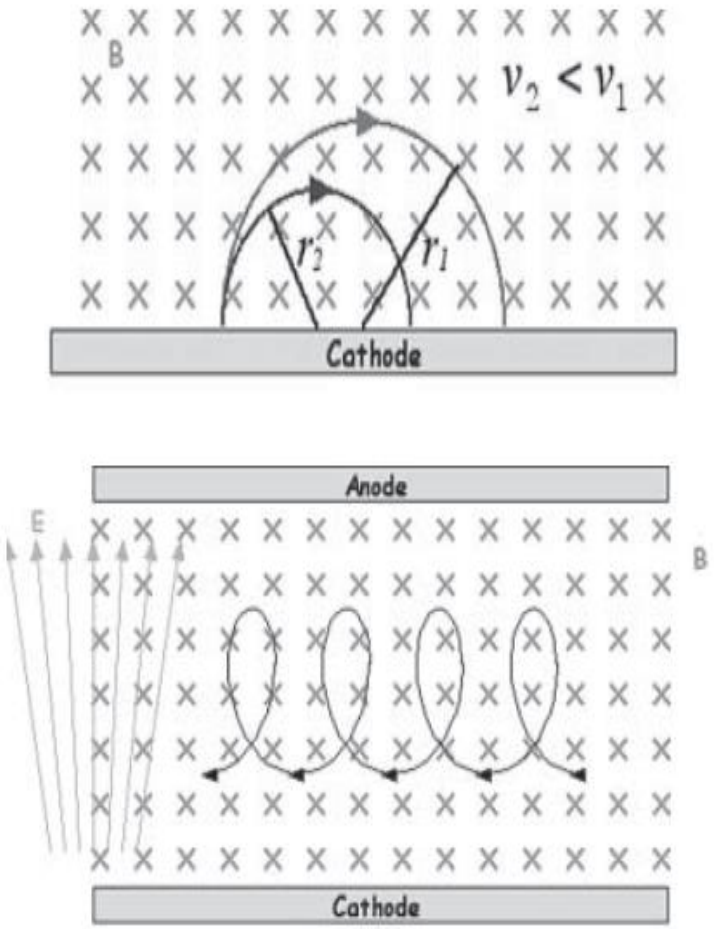

Figure 3. Electrons movement under electric and magnetic field in magnetron sputtering process is illustrated in the Figure. [18]

The relationship between plasma current (I) and the voltage (V) which is applied in the sputtering process is given by the following equation i,

$$I = kV^n \quad \text{———>i}$$

Equation i, explains the plasma current and voltage association with each other, the constants K and n will be dependent on the cathode, sputtering gas and magnetron type used. The optimal characteristics of magnetron sputtering process are as follows pressure around 1 mtorr, current density of cathode around 20 mA/cm^2 (milliampere per square centimeter), discharge voltage is around 250-800 V and distance between target and substrate is about 10 cm approximately. [18] The different types of magnetron sputtering process is explained in the following section.

2.3.1 Planar magnetron sputtering process

The most commonly used magnetron configuration is planar magnetron sputtering process. The mechanism behind this configuration is explained in this section. The typical magnetic arrangements of planar magnetron are shown in the following Figure 4. It is known that both the electric field (E) and magnetic field (B) is generally applied perpendicular to each other. The intensity of electric field decreases when the distance from the surface is increased. The magnets are placed below the cathode surface so that the magnetic field is traversing radially. This particular arrangement makes the E*B drift to form a circular path over the surface of the target. This path is generally referred to as 'racetrack' as shown in Figure 5. The cooling arrangement is an essential setup in magnetron sputtering process, else during the process the target is overheated and result in cracking. There will be certain combination of permanent, electromagnets which can be used in the actual magnetron setup as shown in the Figure 4. The normal magnetic field produced in the process is around 500 Gauss (G). The one main disadvantage of the process is that the target utilization, in general only 45 % (percentage) of the target is consumed in the process. This is because of the circular path of the magnetic field flowing through the target. In 1991, Krug et al developed new design for high rate planar magnetron process in which the target and magnet will be placed side by side as shown in the Figure 6. This particular setup will make use of more target surface because of the flat magnetic field produced. [18]

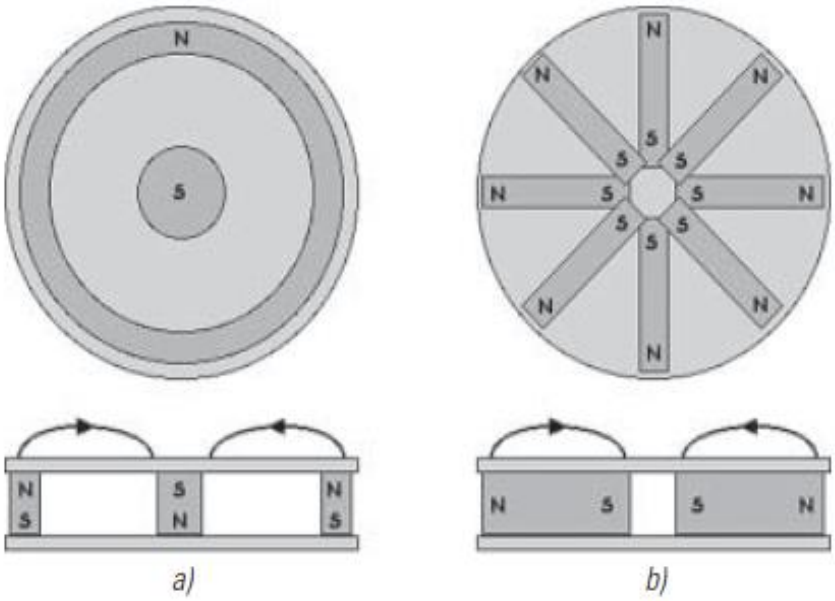

Figure 4. Schematic representations of typical planar magnetron magnet arrangements setup used in sputtering process [18].

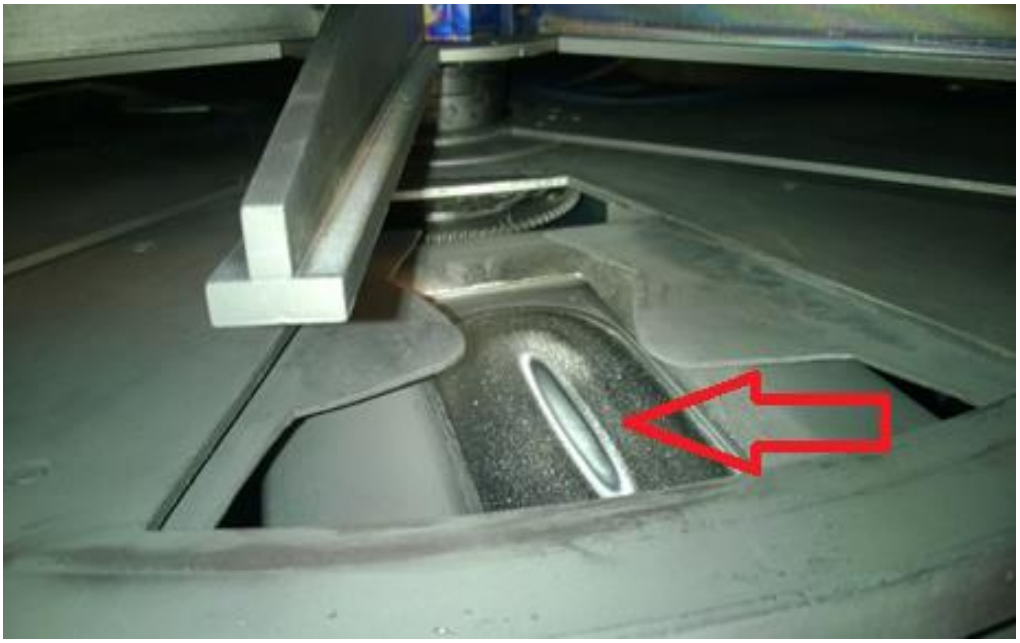

Figure 5. "Racetrack" present in our planar magnetron sputtering target material. The arrow marked in the Figure represents the path of sputtering process, following the confined path of magnetrons used.

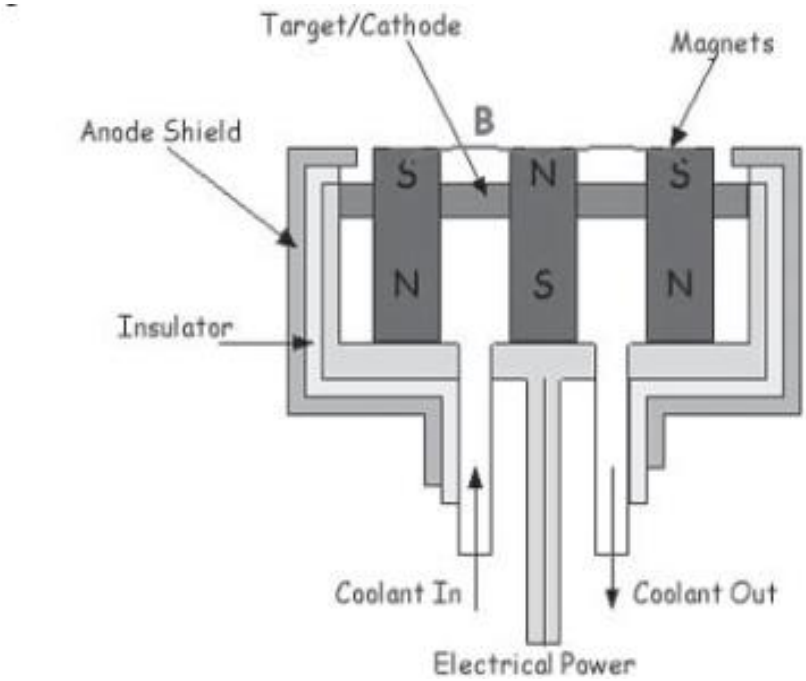

Figure 6. Schematic representation of model developed by Krug, et.al is shown in which cathode and magnets are placed side by side as shown. [18]

The mechanism of how the electron moves to the anode (substrate) with respect to the magnetic field will be discussed briefly in this section. Consider a planar magnetron as shown in Figure 7. In this setup, electric field is applied between the cathode (target) and the anode. The electric field applied is of DC in nature and it is around 100 V/cm. The magnets which are placed behind the cathode will be of circular or elliptical in nature based on the circular or rectangular nature of the target used. The mechanism of magnetic field generation is similar to that of a normal bar magnet. In this from the north Pole end, the magnetic field rises perpendicular to the target surface and it continues to rise in the shape of arch, where it is almost parallel to the surface. As discussed earlier the electric field decreases when the distance between the target is increased. So at that point where the magnetic field (B) is parallel to the cathode surface, field B returns to the South Pole. This is the magnetron mechanism and by which it forms an array of magnetic tunnel lines over the cathode so that the ionization is high in this area. The electrons which will be released from the cathode will move in this spiral path along the B field. When the electric field (E) and B are applied perpendicular, then the electrons will follow the cycloidal motion as discussed earlier. This movement of electrons across the target, together with the strong magnetic field explains the "racetrack" formation in the target. The plasma produced will be very high owing to the high ionization in this region. [22]

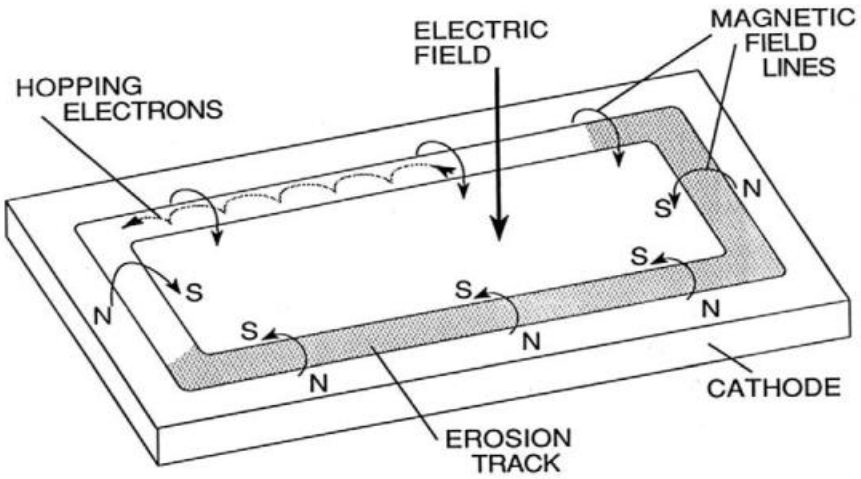

Figure 7. Typical representation of movement of electrons in planar magnetron setup with respect to both electric and magnetic field is presented .[22]

The knowledge about perpendicular fields will get to understand how the electrons will reach the anode from the target material. The electric field (E) and magnetic field (B) is applied perpendicular to each other so that the confinement of electrons is obtained in the process. Consider the anode (substrate) and the cathode as shown on Figure 8 with B applied in the '+Z' direction (Positive Z-axis direction) and E applied normal to the target surface. The electrons which are emitted from the cathode are being enhanced on the way to anode. The electrons movement will be a helical motion as shown in Figure

8, and this motion is because of the combined electric and magnetic field. The electrons will follow the magnetic lines from north to south pole and thereby increasing the electron confinement as discussed earlier. The electrons will try to reach the anode till it encounters the parallel magnetic field at this point the electrons is bent towards to form an orbit as shown in Figure 8. This particular electron motions are explained by the following equations in three directions which are perpendicular to each other. The x and y coordinates in the equation represents their positions along and above the cathode surface respectively. [22] Using the Lorentz equation, three differential equations are given below,

$$m_e\, dx^2/dt^2 = qB\, dy/dt \quad \rightarrow \quad 1$$

$$m_e\, dy^2/dt^2 = q\mathscr{E} - qB\, dx/dt \quad \rightarrow \quad 2$$

$$m_e\, dz^2/dt^2 = 0. \quad \rightarrow \quad 3$$

The equations 1, 2, 3 are being solved to obtain the parametric equations which gives the explanation about the electron cycloidal motion. The notions used in the above equations is given as follows m_e –mass, x- electron displacement, t- time, q- charge, ε- field amplitude and ω_c- cyclotron frequency. From equation 4 and 5, the frequency of cyclotron is obtained and the time interval at which the electron returns back to the cathode is noted. The cathode dark space is the area where both the fields influence the electron motion and in the negative glow region the electrons move randomly because at this point the E is low. The electrons follow a circular path and upon collisions with each other, the electrons move to anode surface or to the dark space. In this area above the parallel fields the ionization is high with respect to the cathode region which also increases the lifetime of the electron. The ionization and increased lifetime of electrons, results in the efficient plasma generation and significant discharge current which is used mainly in magnetron sputtering process. [22]

$$y = -\frac{q\mathscr{E}(1 - \cos \omega_c t)}{m_e \omega_c^2} \quad \rightarrow \quad 4$$

$$x = \frac{\mathscr{E} t}{B}\left(1 - \frac{\sin \omega_c t}{\omega_c t}\right), \quad \rightarrow \quad 5$$

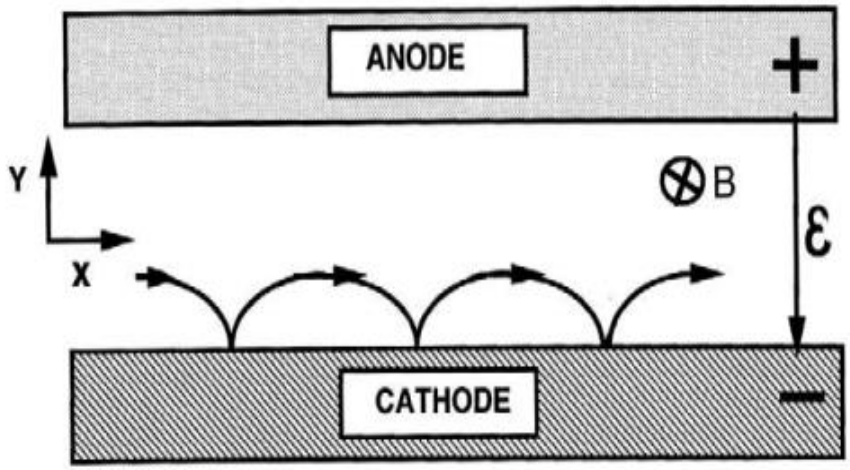

Figure 8. The cycloidal electron motion on cathode surface which displays helical type motion with respect to electric and magnetic field is represented in this Figure. [22]

2.3.2 Cylindrical magnetron sputtering process

The main advantage of using cylindrical magnetron sputtering process over planar magnetron sputtering process is the effective target utilization for deposition process. In cylindrical post magnetron sputtering configuration, the target (cathode) is of cylinder shape and cathode is surrounded by substrate (anode) which in turn will be used for depositing thin films. As shown in the following Figure 9, a uniform magnetic field is applied by using permanent or electromagnets or by coaxial solenoid. The magnetic field is applied parallel in z direction as shown in below Figure 9. From the cathode, electrons are emitted radially and travelling in closed orbits along the target circumference. The typical reason for this behavior of electron movement is lorentz-force. [22] In brief, the applied parallel magnetic field is in contact with the electrons emitted from the cathode, but the plasma ions are not affected by the field. The solenoid coil is used in case of non-magnetic materials is used for sputtering. The electrons which are emitted from the target are drifted radially to reach the substrate surface. The plasma discharge generated during the sputtering process is sustained due to electronic collisions as discussed previously in this section. [1; 10; 22]

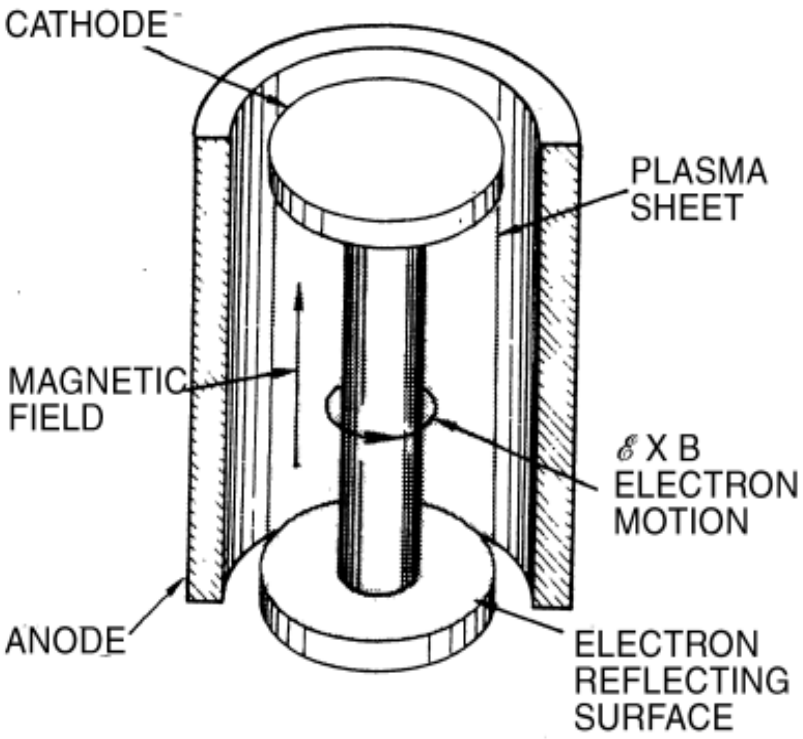

Figure 9. General view of cylindrical-post magnetron sputtering process with applied magnetic fields and electric field is represented in this Figure. [10; 22]

2.4 Reactive sputtering

One of the most important modes of operation for sputter deposition is reactive sputtering process. This reactive sputtering process is preferred in cases where film microstructure and properties needs to be controlled precisely [1]. Reactive deposition of thin films is achieved by two methods, in one such process metallic cathode is chosen for the sputtering process whereas in second method, a specific compound of interest is chosen as cathode. This compound material chosen is either oxide or nitride compounds based upon requirement of thin films. When comparing the two processes, metallic cathode is more preferred to metallic compound cathode as it achieves better deposition rate and control over the deposition is more accurate. Owing to these many advantages, reactive sputtering is still considered to be more complicated than other sputtering process as nitride/oxide film will be formed upon reaction with metallic cathode on its surface. So, the deposition rate is reduced to considerable extent. [1; 23] The other thin film compounds which are deposited using the reactive sputtering are carbides, sulfides, oxycarbides and oxynitrides. In any case the thin films which is sputter deposited is either a compound film namely TiN, AlN (aluminum nitride) otherwise it would be a solid solution of target metal doped with reactive gas compositions [24]. The most interesting aspect of reactive sputtering is either one or fraction of that element used in deposition is in gaseous state [1]. During the reactive sputtering process, there is also a

possibility that at higher working pressure in the gas phase the thin film formation can even occur at the target surface leading to target poisoning, substrate can even react with the gaseous elements to form some other unwanted compounds. So usually the sputtering gas will be the inert gas such as argon (Ar) and the reactive gases would be nitrogen (N_2) or oxygen (O_2). The properties of thin film deposited using reactive sputtering is not directly related to the amount of the reactive gas injected into the system. The relationship between properties of film and reactive gas is so complicated owing to so many factors involved in it such as temperature involved, composition of film, structure of film achieved, and deposition rate. [1; 23; 24] The typical representation of reactive sputtering is explained in Figure 10.

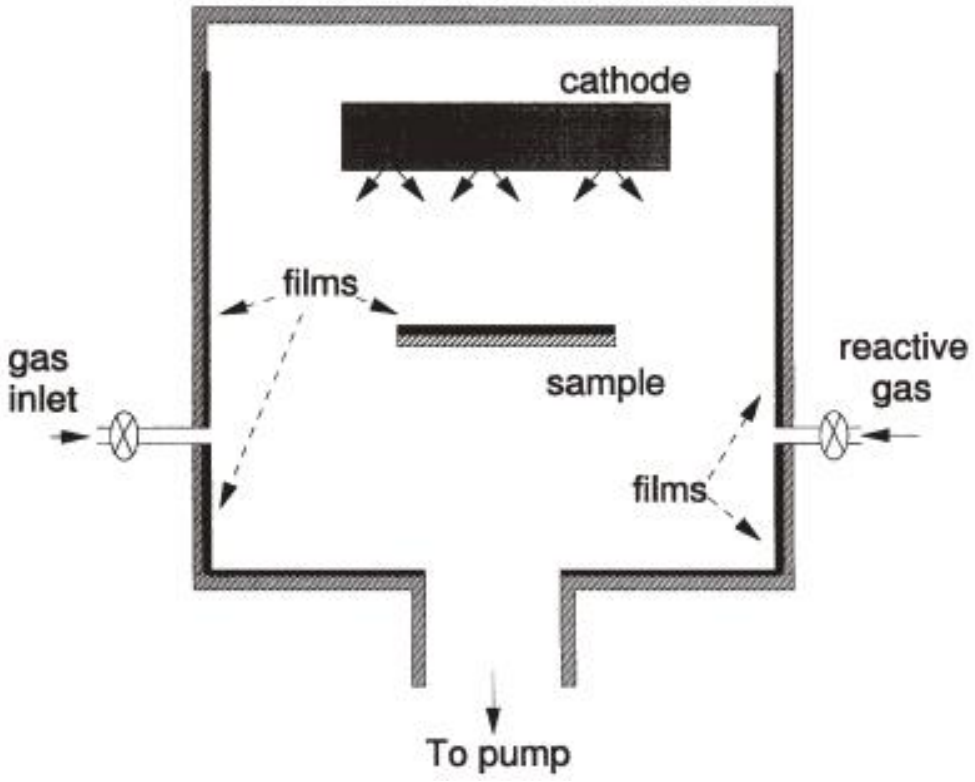

Figure 10. Schematic representation of reactive sputter deposition process setup is shown with separate inlets for sputtering and reactive gas. [23]

Consider a scenario where the reactive gas flow in the gas mixture (O_2+Ar) is minimized in reactive sputtering process, which means every available oxygen gas is reacted with thin film. So consumption of oxygen gas is higher when compared to argon gas in the gas mixture. The remaining argon gas reacts with cathode or target to form metallic thin film coatings. When the oxygen rate supply is increased in the gas mixture to achieve stoichiometric coating, there is decrease in the deposition rate of metallic or compound thin film coatings. This marks the transition between the metal to compound thin film formation shift with respect to the reactive gas mixture, which can be observed

in the Figure 11 below. In this particular point, the cathode or target surface have high energetic flux of reactive gas fractions which makes effective sputtering of various compounds highly possible. The sputtering parameter such as discharge voltage is also studied with respect to reactive sputtering process. As oxygen intake is increased due to shift from metal to compound the discharge voltage is reduced and vice versa, this particular transition resembles the hysteresis cycle present in magnetic materials. The hysteresis effect can also be mentioned in the below Figure 11 [1].

The compound formation on cathode or target surface is referred to as “poisoned”. This poisoning effect of cathode will lead to difficulties such as reduced deposition rate, shift between metal to compound will occur more abruptly so required composition of particular suboxides cannot be achieved properly. However, the positive sides of reactive sputtering are insulating or metallic compounds can be formed with DC source, any variety of graded structure composition can be deposited, all these can be achieved using metal targets. [1]

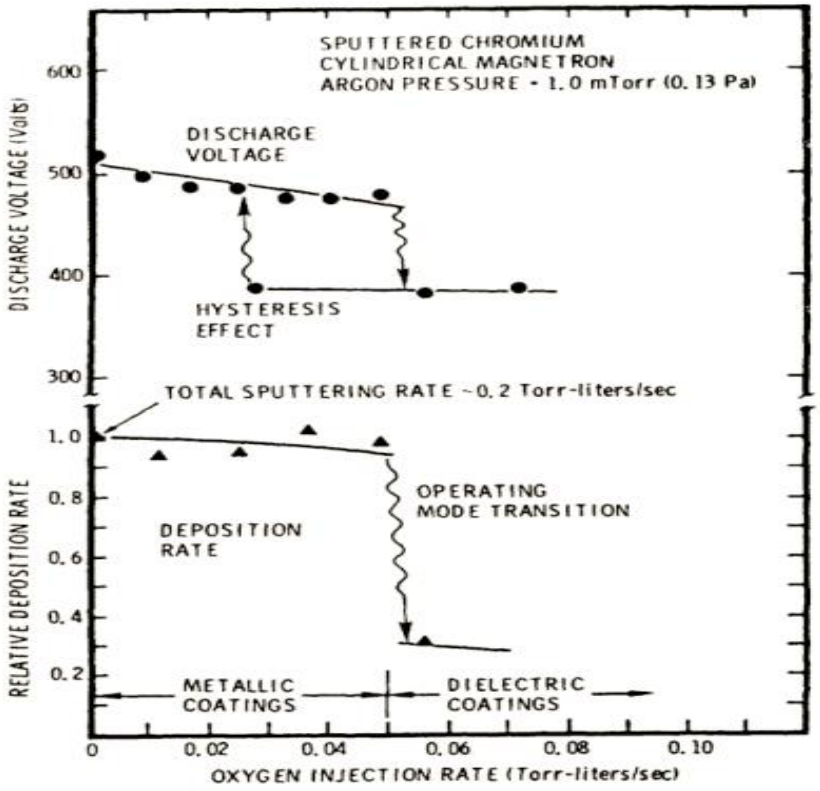

Figure 11. The standard relationship between the deposition rate and discharge voltage effects with respect to reactive gas flow rate is represented above as explained by Bunshah F.R. [1]

2.5 Bias sputtering

In year 1962, bias sputtering process was patented by Wehner, in this sputtering setup the anode or the substrate material is being connected to negative bias voltage, which will improve the intensity of the bombardment of ions present in the plasma [25]. Bias sputtering is based on the principle that when the bias voltage is applied to the substrate it will result in high energy ion bombardments which in turn result in flux and energy variation of deposited species [24]. The applying of bias voltage in the process almost now a common practice in most of the sputtering process such as DC, RF, reactive, magnetron and so on. The common advantages of using bias sputtering process is the betterment of film properties such as film density, adhesion, step coverage, optical reflectivity and modification in properties such as film hardness, stress (residual), dielectric film electrical properties, also reduction in properties such as etch rate of silicon-nitride films, resistivity of metallic films, film morphology is reformed which implies fine grain microstructure is identified rather than columnar microstructure. The resultant film structure after bias sputtering is generally fine isotropic grain microstructure as the porosity and interfacial voids is being eliminated and thus surface roughening is achieved as expected to improve adhesion of deposited thin film. [1; 24; 26; 27] One of the most important feature of bias sputtering is the sputter etching which will promote surface cleanliness and adhesion of thin film deposited [1; 10; 24].Consider a magnetron sputtering process, in which bias operation can be done by magnetic or electrical means. In this process, two magnetrons are used and it is biased electrically to the ground by giving positive potential to anode. By this setup one of the magnetron will be the source of positive ions and neutral ions. From the following Figure 12, it is observed that the three sets of experiments can be done to understand the importance of bias sputtering such as 1) opposing magnet 2) no magnet and 3) aiding magnet. The energy flux value to the substrate, electrical probe data, resistivity of films are obtained by plotting temperature versus time curve graph in Figure 13 as given by Fraser.et.al [10]. The obtained deposited film of thickness is around 500 nm (nanometer) and it is achieved in 15 minutes (mins) of deposition and it is the same for the entire different configuration which means thin film growth continues starting from neutral particle flux. The resistivity and current value of the film increased in the no magnet setup. However, the energy flux value is very high in aiding magnet setup. [10]

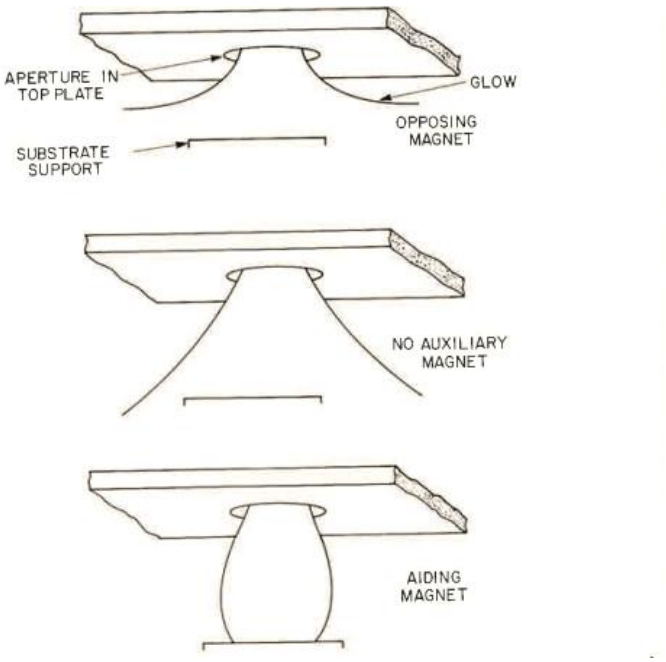

Figure 12. Schematic representation of the influence of magnetron in bias sputtering process with respect to three different setup such as 1) Opposing magnet 2) No auxiliary magnet 3) Aiding magnet [10].

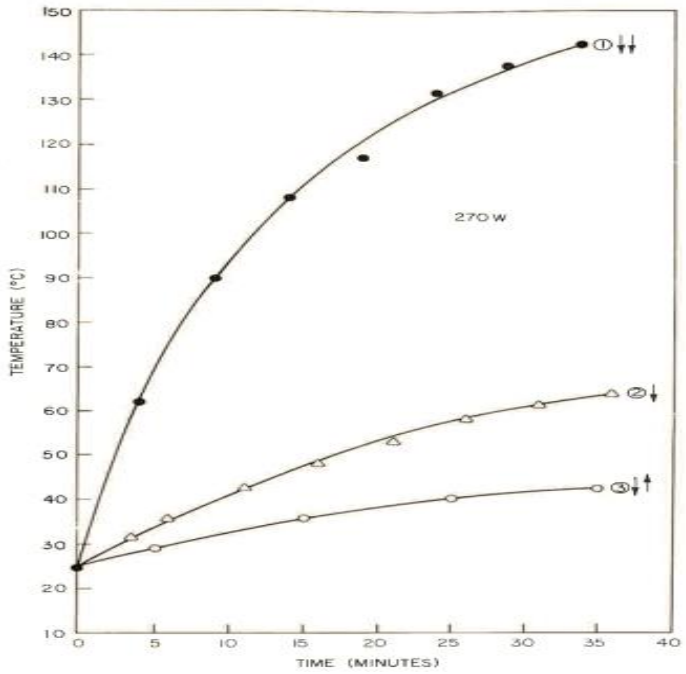

Figure 13. The graph between temperature and deposition time with respect to the above mentioned three different setups of magnets in bias sputtering process is represented [10].

In Bias sputtering, the thin growing film is bombarded mostly with ions and neutrals of low-energy distribution, in some cases the discharge ions also strike the substrate due to the presence of anode dark space near the substrate. When there is low energy bombardment of ions or neutrals, there might be resputtering of thin film along the growing surface. During this the sorbed gases will be incorporated into the growing film at atomic level. These result in various significant changes such as higher adatoms movement, impurity/contamination removal, high temperature rates of interdiffusion, improvement in nucleation and renucleation. In practical, the gas atom fraction is directly proportional to the square of the bias voltage (Vь). [1; 24; 26; 27]

2.6 Sputter etching and cleaning

Sputter etching is normally done by sputtering gas such as argon in sputtering chamber. Plasma etching is general term used to categorize different etching phenomenon such as 1) sputter etching 2) accelerated ion-assisted 3) chemical etching 4) reactive-ion etching and 5) ion-enhanced etching [24]. This plasma etching generally means surface atom removal from substrate or even cathode (in some cases), with plasma acting as a medium for etching the surface [24]. This kind of etching or surface atomic removal is generally done to remove contaminants/impurities from surface and creating surface roughness. The sputter etching mechanism is generally used to improve the efficiency of adhesion strength. At relatively low pressure range, the plasma generated has very high energies and it strike the surface of the material. The bonding forces of the material and the microstructure plays an important role in determining the etching of the material. So to conclude basically any type of material can be sputter etched at same rates.[24]

Sputter cleaning is generally applied to the surface, where clean surface is required for sputter deposition in a suitable vacuum environment. When sputter cleaning is done the adhesion strength and thin film microstructure is improved to larger extent due to the sputtered atoms high ejection rate [28]. One of the most important benefits of sputter cleaning is that it directly correlates to the adhesion property of thin films. According to Tabor, the Van der Waals interaction between surface layer also influence the adhesion property of thin film coating [29]. The other advantages would be substrate grain size is reduced, texture modification and top layer of contaminated substrate surface is removed. The drawbacks of using sputter cleaning are also surface contaminations as backscattered atoms produced from the sputtering process. The other disadvantages would be influence of residual water vapor from the sputtering chamber due to recontamination. [30; 31]

In principle, the sputtering gas such as argon is used to sputter clean the substrate surface, in which by ion bombardment the surface layer impurities are removed. The energetic argon (Ar^+) ions strike the substrate surfaces which in turn influence the

coating growth. The surface atoms and plasmons is the main reason for the formation of metallic bonds between coating and substrate surface. [30] As discussed previously, the several processes which might occur during sputter cleaning are backscattering of atoms, redeposition of target material, removal of surface material, modification to the crystallographic substrate surface, ion implantation and so on [30-32]. Figure 14, represents the typical illustration of how sputter etching is done with argon plasma in a closed environment.

The sputter cleaning is also regarded as cleaning with ions or glow discharge cleaning, as the plasma produced will be glowing around the target or cathode region. The setup is such that sputtering chamber is kept at low pressure range of $<10^{-3}$ mbar (millibar) and the sputtering gas is supplied to produce plasma. The produced plasma will remove the surface impurities and even native oxide layer depending upon the ion bombardment. However, noble gas will not react chemically with the substrate surface upon ion bombardment during sputter cleaning, the argon ions might get implantation on the surface. This problem of ion implantation on substrate surface can be reduced by various other chemical treatments such as baking. According to Hoyt.et.al, and Mathewson.A.G, along with argon gas up to 5 to 10% oxygen is used for better carbon removal from substrate surface [33; 34]. As carbon tend to form various gaseous compounds such as carbon monoxide (CO), carbon dioxide (CO_2) which then will be vented along with the sputtering gas [33; 34]. Thus the ratio of sputtering ions used in sputter cleaning process is reduced by the inclusion of oxygen gas in the mixture [33-36].

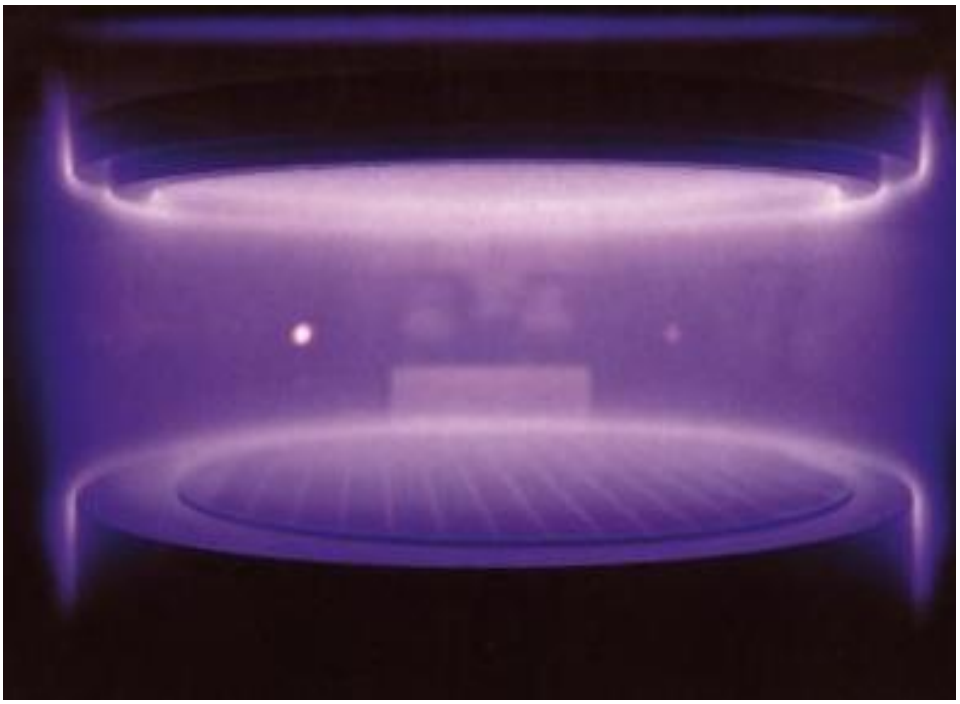

Figure 14. Typical representation of sputter etch cleaning using argon plasma is shown in this Figure for better understanding. [37]

2.7 Thin film coating formation

The vapor-deposited thin film coating grain structures is characterized using structure-zone diagrams (SZD) or structure-zone models (SZMs). These SZD/SZMs make us try to understand the relationship between the variables used in various deposition techniques and the growth mechanisms of thin films. The general growth mechanism would be the incident atoms from vapor condensation will become an adatom which then diffuse over the substrate surface till the desired level of coating thickness is achieved. The diffusion of the adatoms over the substrate is dependent on melting point of condensate (T_M). The diffusion mechanism is divided into four types of processes which are as follows i) shadowing, ii) surface diffusion iii) bulk diffusion and iv) desorption. The substrate temperature (Ts) is other important factor which has influence over the diffusion process and the influence of different types of diffusion mechanism means the morphology of the thin film structure will be affected consequently. The ratio of T_S/T_M is represented as the normalized growth temperature function which is used to characterize the growth zones observed in film structures. In 1969, Movchan and Demchisin proposed the first ever SZD based on the microstructure observed from various coatings of Titanium, nickel, alumina, zirconia and tungsten deposited by evaporation techniques. In their detailed analysis from various coatings and observations from other researchers, Movchan and Demchisin came to the conclusion that the growth of thin films can be categorized into three different zones such as Zone 1, Zone 2, and Zone 3 which is as represented in Figure 15. In 1974 Thornton

formulated SZD by including sputtering gas pressure as a new variable axis for cylindrical-post magnetron sputtering deposition of micrometer thick coatings. The coating used for the study comprises of titanium, iron, copper, chromium, aluminum and molybdenum coatings. The microstructure of the sputtered thin films is influenced by the sputtering pressure (P). When 'P' is increased it will result in zone -1 structure (wide open boundaries), while decreasing P resulted in densification of thin films. Thornton included a new zone named as 'zone T' in his SZD which clearly explains the transition from zone 1 to zone 2 structure. The zone structures present in the thin film is briefed as follows. The zone 1 structure comprised of more columns which are isolated in nature, several cone like regions which are inverted in nature and separated by void boundaries which are very wide in nature (in nanometer range) and it is formed due to shadowing effects. Zone T comprises of fibrous grains which are poorly built, but present in arrays which are dense in nature. Thus zone T is considered as zone of transition between zone 1 and 2. The zone 2 comprises of columnar grains which are isolated by compact intercrystalline boundaries, generally this zone has soft matte appearance. Zone 2 is formed as a result of controlled surface diffusion growth. The zone 3 microstructure prevails due to the dominant bulk diffusion mechanism. The microstructure of zone 3 is composed of smooth surface grains which are equiaxed in nature.[1; 2; 24; 51]. Figure 15 gives the overall combined schematic representation of SZD.

Grovernor et al, in 1984 had further modified previous SZDs according to the observations from TEM of various evaporated thin films of nickel, platinum, aluminum, cobalt, tungsten and chromium. According to this model in zone-1 tapered columns is observed and is comprised of comparatively equiaxed small grains bundles, while zone 2 composed of bimodal distribution of small grain substructure. In the same year, Messier et.al, also proposed a SZD based on interpretation obtained from the combination of several microscopy techniques such as transmission electron microscopy (TEM), scanning electron microscopy (SEM) and field-ion microscopy (FIM), this SZD is used to explain mainly about RF sputtered films. In this model proposed by Messier et al, pressure is replaced by bias voltage (Vs). It is found out that the influence of Vs is inversely proportional to that of pressure (P).

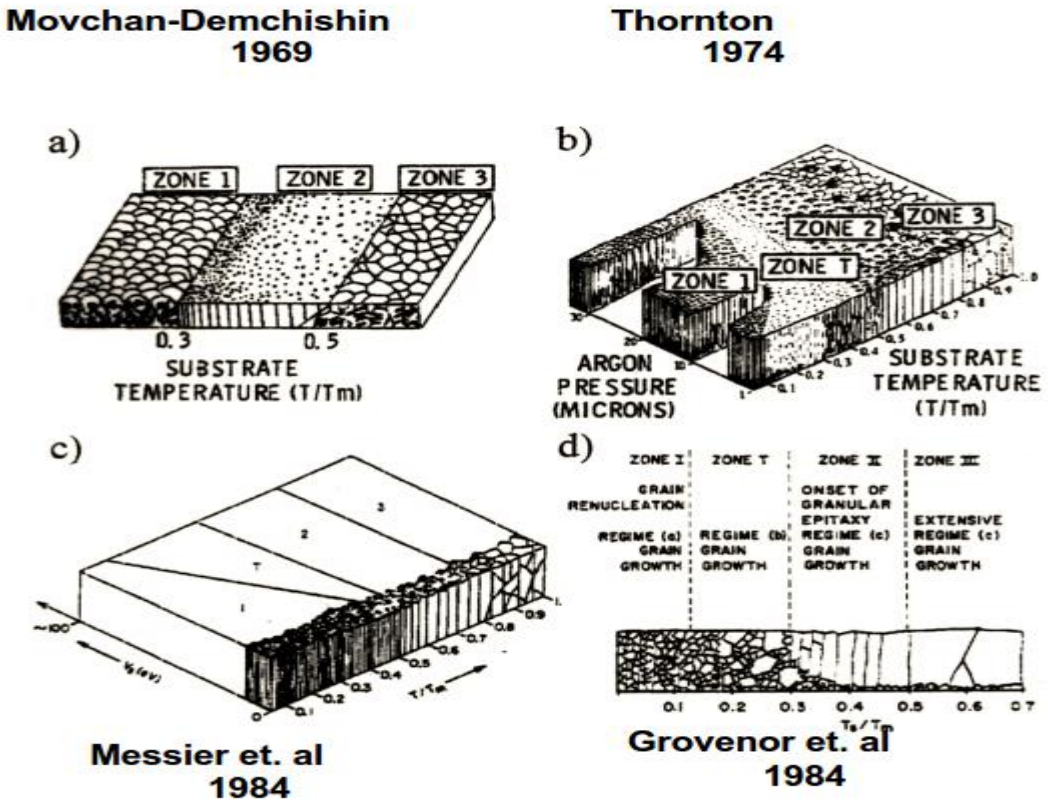

Figure 15. Schematic representation of development of Structure Zone diagrams (SZD) by researchers namely Movchan-Demchishin, Thornton, Messier et.al, Grovernor et.al over the years is presented in this Figure. [51]

2.8 Substrate temperature influence on thin film coating

One of the most important process variables in any deposition process is substrate temperature. The ability to control substrate temperature will have major influence on deposition rate, microstructure and properties of the coating generated. The most significant point with respect to substrate temperature is that it has direct correlation with the resultant microstructure obtained [38]. For instance, if the substrate is at room temperature then the resultant microstructure will be in accordance with substrate used for the deposition. According to Structure Zone Model (SZM) proposed by Thornton, the mobility of surface atoms increases when there is increase in substrate temperature, which leads to the formation of Zone T (transition zone). With increase in temperature during deposition leads to the formation of following zones namely zone 1, zone T, zone 2 and zone 3. This point is clearly depicted in the below Figure 16, which shows the transition of grain size in thin films with substrate temperature as important functional parameter. So in general during sputtering process, the chemical reaction on the substrate surface and the surface atom mobility can be influenced by the substrate temperature. One of the advantages of using high temperature substrate for thin film coating is that residual stress produced in the coating is minimized. In sputtering

deposition process, gas incorporation in the deposited film is one of the disadvantages and this can be lowered when higher substrate temperatures are used.[1; 39] when considering the applications of semiconductors in the commercial market, the influence of substrate temperature plays a very vital part as the physical properties of thin film is modified [40]. Consider the plasma enhanced CVD process, temperature sensitive materials can be deposited using this process as the required reactions is accompanied at lower temperatures. In microwave plasma deposition process, even at room or low temperature, better thin film quality can be achieved. Now it is clear that the substrate temperature influences greatly the growth rate of thin film deposited. In CVD process single crystal growth of thin films is achieved when there is high substrate temperature along with low gas super saturation. When depositing diamond like carbon, temperature of the substrate needs to be less than 300 ˚C (Celsius) as to avoid softening of thin films. At high substrate temperature the critical nucleus size is increased furthermore the barrier to hinder nucleation might also present. In some cases, at higher temperature the defects such as twins and low-angle grain boundaries were removed using annealing. One unique method to improve quality of thin films is by using very high substrate temperature to desorb contaminants from the surface and then precede deposition with immediate low substrate temperature [24]. It is also known fact that during deposition of thin films, equiaxed grain will be formed when the substrate temperature is high and low substrate temperature leads to amorphous or fine grained grain size [41]. [9; 24]

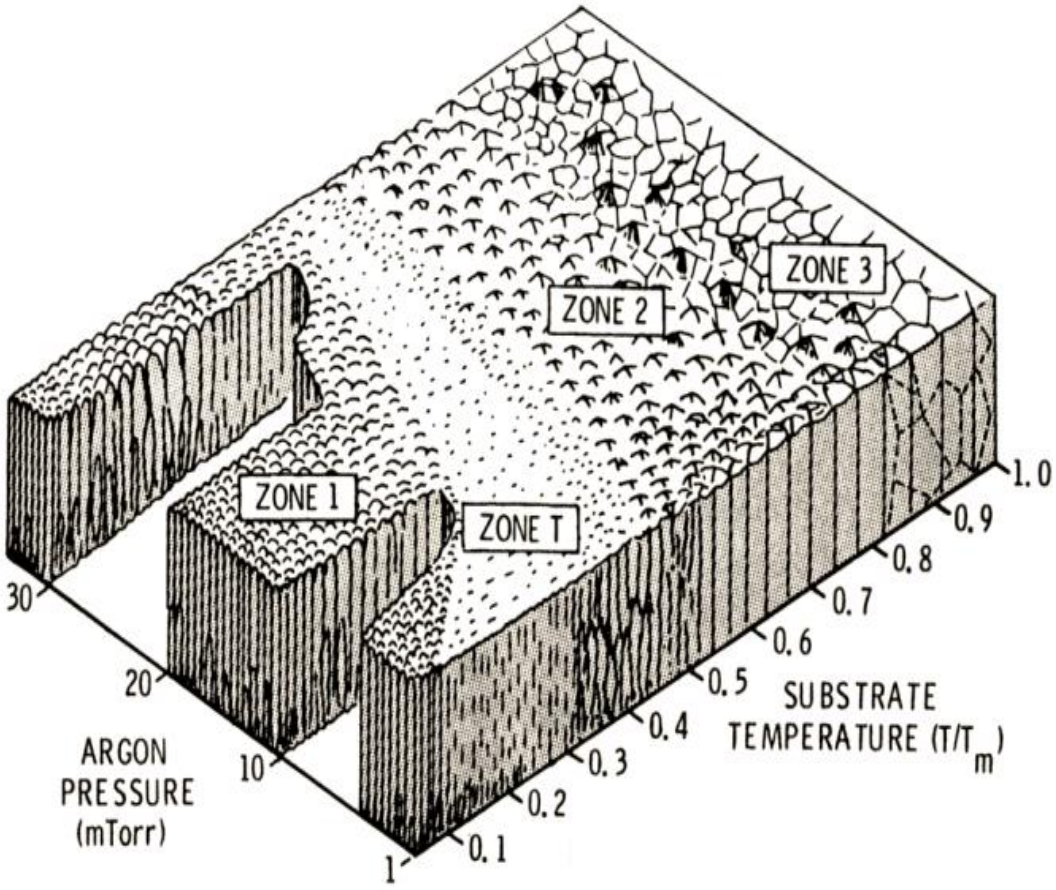

Figure 16. Schematic representation of cross-section images of Structure Zone model proposed by Thornton, which demonstrates the transition of grain size (Zone T) in thin films along with other zone structures. [24]

2.8.1 Substrate heating methods

The substrate heating procedure can be accomplished by different process. The most important methods which can be used effectively to heat the substrates is briefly explained in this section. The substrate heating by plasma during sputtering is firstly considered. As plasma consists of ions and atoms which are highly energetic in nature, when these ions or sputtered atoms comes in contact with the substrate surface it increases the temperature of the substrate. So the rise in temperature of substrate during sputtering is governed by the following parameters such as heat capacity of substrate, density of substrate material used, high rate of deposition, thickness of substrate. The substrate holder presents in the sputtering chamber holds responsible for loss of heat by conduction to some degree. [24] In some cases to achieve better coating and reduce thermal stress in thin film coating, the substrate heating is reduced [1; 39]. As in very high temperature of substrate the quality of coating deteriorates to considerable extent [1; 39]. The typical example of substrate heating using heating elements is shown in following Figure 17.

The DC and RF diode sputtering use irradiation of electrons to heat the substrates present in the chamber. The heating of substrate inside the chamber is achieved by radiant heater of different size and shape, in some cases provisions have been made for this substrate heating and biasing [1; 9]. However, with the introduction of magnetrons in the sputtering process in the past decades, avoids the rise in temperature of substrate by electron bombardment. When substrate heating is lowered, then magnetron sputtering process can be used to deposit decorative coating on automobiles and exterior trim. The reason why the ions increase the substrate heating is that ions are being neutralized before they impact the substrate surface. So these neutral ions are not controlled by the electric field present over the surface of the target. Thus, increasing the flux of the ions present over the substrate and thereby contributing to substrate heating. [1; 9; 10; 39] The other noteworthy methods which can be used efficiently to increase the substrate heating are laser-driven etching, substrate heating by infrared waves, evaporation, resistance heating, laser heating, microwave plasma substrate heating and any ionic bombardment process [42-44]. [9]

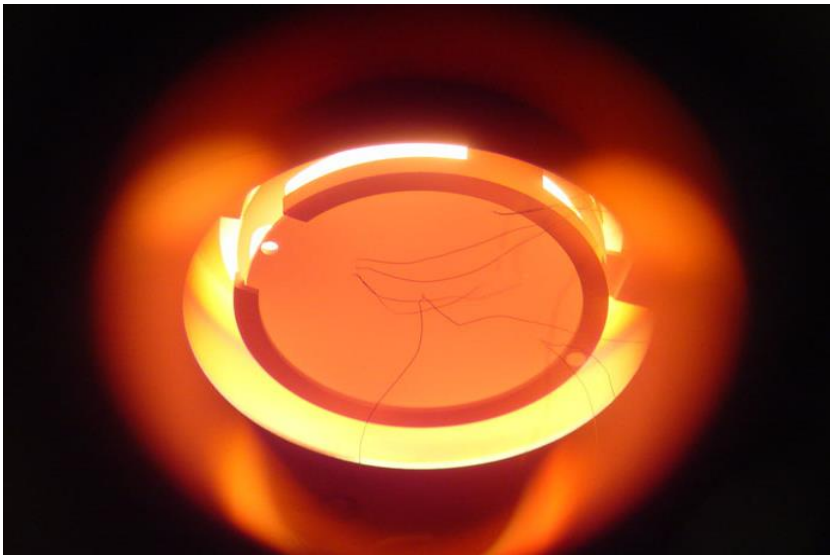

Figure 17. General representation of substrate heating elements which used to heat the substrate used in the sputtering process, in this image the Inconel disc (substrate) is heated to higher temperature with the assistance of red-hot heating element surrounding it. [45]

2.8.2 Influence of substrate temperature on film properties

High temperature of substrate is not always beneficial for certain applications such as microelectronics, flat-panel displays, semiconductor industry and solar cells.[24] As the substrate temperature is increased for titanium dioxide (TiO_2) films, the refractive index is improved [40; 41]. According to I. B. Mbarek et al., at room temperature the coating deposited over any substrate has more porosity in it and as there is increase in substrate temperature the adatom mobility is increased and crystallinity is improved [40]. With

higher substrate temperature, stoichiometric composition of thin film is improved progressively [46]. The grain structure is modified to greater extent because of elevated temperature observed in substrate as grain of small size becomes more rounded [40]. The roughness of thin film with higher substrate temperature might increase or decrease depending on the nature of the substrate element used [40]. Research article by Kaya, S., et al concluded that when substrate temperature is modified, it resulted in alteration in surface roughness value, conductivity and orientation of grain boundary [41]. With increasing substrate temperature, the optical band gap increases gradually till some range and then start decrease with further increase in substrate temperature [47]. In general, the band edge luminescence of deposited films is increased as the substrate temperature is increased and this is because of the reduction of strain in films and improvement of crystallinity of films deposited [47]. The results from Y.H. Kim et al., revealed that transmission is improved when there is increase in substrate temperature, however which will lead to drop in absorption coefficient value [48]. X.-Y. Li et al., suggest that compressive strain generated during thin film deposition is decreased rapidly due to rise in substrate temperature [47]. The growth rate of deposited grains and adatom mobility is increased with respect to rise in substrate temperature [47]. This increase in adatom mobility decreases the surface roughness property of deposited films [47]. When the sputtering power is combined with increasing sputtering temperature, a major improvement is thin film composition and crystal structure is also observed by Kaya, S., et al [41]. The crystallinity of the thin films is improved by increasing substrate temperature [38; 41; 49]. In general to achieve better crystallinity in sputtering process, the deposited atoms is expected to have very high energy, this prerequisite is fulfilled by the use of high substrate temperature [40; 41]. As the substrate temperature is increased the stress and strain produced in thin film coating is decreased [41]. The grain growth observed by Kaya, S., et al, in their experiments is that at elevated substrate temperature, it resulted in elliptical grains while under low substrate temperature the columnar grain growth is achieved [41]. According to Zhang, Z., et al, as the substrate temperature is increased then it will result in increase in atomic mobility and decrease in structural defects [49]. The crystallinity is improved along with the fact the larger grains are formed by coalescence smaller grains formed during initial phase of deposition [49]. This particular process increases the surface roughness and porosity of thin films [49]. Moreover, as the substrate temperature increasing in sputtering process the denser films with lower defects is deposited [38; 49]. At very high substrate temperature the mobility of carrier atom is controlled by lattice vibration scattering [49]. The career atom concentration will be increased with increasing substrate temperature and start to decrease gradually at very higher temperature [50]. The resistivity of the thin film decrease initially as the substrate temperature is increased, but when the temperature is increased further then the resistivity is increased [49].

2.9 Structure and properties of sputtered film coatings

In this section, structure and properties of various sputtered thin film coating is analyzed for better understanding of thin film microstructure. For this purpose, different types of thin films deposited by various sputtering process such as RF magnetron, co-sputtering, DC magnetron is taken into consideration. The thin films depositions are generally ranging from single layer to multi-layer coating depending on the required functionality of the coating. The report of thin film multilayer coating on silica substrate is studied by researchers Xu, Z., & Chan, W. H [52]. According to this scientific investigation, post-annealing condition plays an important role in defining the microstructures and properties of thin films deposited by sputtering technique. [52] When increasing the post-annealing temperature from 600 ˚C to 700 ˚C, there is enhancement in dense and columnar microstructure of thin films [52]. These thin films showed extraordinary electric properties such as increase in saturation polarization and decrease in loss tangent [52]. Owing to these excellent properties these thin films are widely used in thermal and optical sensors in microelectronics [52]. Navamathavan, R., et al used RF magnetron sputtering process to deposit thin film transistors (TFTs), in which they used sputtering to deposit zinc oxide (ZnO) on glass substrates [53]. The ZnO thin film is deposited where the substrate temperature is maintained at 300 ˚C [53]. The thickness of thin film deposited is around 200 nm and the structure of the deposited film is columnar microstructure [53]. These TFTs have superior properties such as transparency, very large band gap, large field effect mobility, good electrical properties, better saturation motilities, minimized leak current and on to off current ratios [53]. Al-Hardan, N. H., et al. reported that properties of sputtered zinc oxide (ZnO) thin films in their research work. From their SEM analysis, it is proved that the deposited thin film is of columnar microstructure. The substrate used in this process is silica and the thickness achieved is around 1.20 μm (micrometer) [54]. The properties of ZnO photodetectors thin films prepared by this method is interesting with respect to electronic applications and it is as explained as follows, I-V characteristics shows increase in current up to 3V, the resistance value is decreased and capacitance value is decreased because of increase in photocurrent value and bias voltage, due to illumination of UV, grain boundary resistance is affected [54]. Wang, Q. M., & Kim, K. H. reported the microstructural transformation of multilayer nanocomposite thin film coating by magnetron sputtering process. From their SEM analysis report, it is revealed that columnar microstructure is most predominant structure obtained [55]. For this research work silica is used as target, thickness obtained is around 1.5 to 2 μm and it is also observed that when silica content is increased finer columns present in the thin film microstructure is increased [55]. When bias voltage is kept at high negative potential then thin film microstructure resulted in dense glassy morphology [55]. According to Chen, L.C. and Liu, S.C., the thickness of sputtered indium oxide thin film achieved using magnetron sputtering is approximately 500 nm [56]. In this research work, crystallinity of deposited indium oxide thin film is measured by X-ray diffraction (XRD) technique and the resultant

structure is polycrystalline cubic in nature [56]. The properties of indium oxide thin films deposited by reactive magnetron sputtering are as follows breakdown voltage of 5V, desired specific contact resistance value, p-type conductivity is achieved [56]. The microstructural columnar growth of sputtered thin film coating is controlled by parameters such as substrate bias voltage, gas flow rate into sputtering chamber [57]. This effect of reducing the columnar boundaries in nanocomposite coating is undergone by researchers Pei, Y. T., et al and the results obtained are significant in understanding the microstructural development in sputtered thin films. Pei, Y. T., et al used bias voltage up to 150 V and used acetylene gas with higher carbon content to nullify the effect of columnar microstructure which is undesired in this research work [57]. In this type of nanocomposite coating, the columnar growth of the thin films deposited is directly affected by the structure of the interface developed. [57] As in this case, when bias voltage is increased from 40 to 80 V, columnar growth increases with dense coating [57]. However when the bias voltage is increased to 100 V or 120 V even though columnar structure increases the density of the coating deposited is decreased considerably and becomes porous [57]. When increasing the carbon content in sputtering deposition does not show very promising effect in reducing the columnar microstructure of deposited coating [57]. Conversely, when the stationary substrate is used with 100% carbon content in DC magnetron sputtering process, Pei, Y. T., et al was able to deposit column free nanocomposite coatings [57]. The interesting properties of these multilayer coatings are as follows increased ductility, improvement in fracture toughness and enhanced tribological properties [57]. From this section, it is clearly understood that columnar structure is the most predominant microstructure for sputtered thin films and the results are confirmed by innumerous research articles related to thin film sputtering depositions.

2.9.1 Structure and properties of metallic Titanium coating

Metallizing is one of the most significant features which can be accomplished by sputtering process. These types of metallic coatings can be used in all kind of general applications ranging from functional to decorative coatings. So with respect to this research work, basic understanding of metallic titanium coating is prerequisite. In this part the microstructural evolution of titanium thin film coatings by sputtering process is discussed. Sengstock, Christina, et al. presented in their report on using glancing angle sputter deposition to deposit metallic titanium coating for biomedical applications [58]. From their SEM analysis, the deposited titanium coating is of sharp-edged columnar structure along with dense surface [58]. The substrates used are silicon (Si) -wafer substrate and the thickness of coating is approximately 60-65 nm [58]. The attractive properties of this nanostructure titanium coatings is widely used in biomedical applications such as selective growth of antibacterial effect, drainage systems of urinal duct where infections mostly occur due to E.coli [58]. A. Besnard et al, in their research work related to titanium thin film deposition reported that sputtering will always result

in columnar microstructure irrespective of resulting incidence angle of sputtered atoms [16]. When the incidence angle is zero, the resulting microstructure is dense with indistinct columns and smooth surface [16]. When incidence angle is 85˚, columnar microstructure of the coating is more inclined and the surface is grooved as shown in below Figure 18 [16]. The other interesting fact is that thin films analyzed revealed microstructures which is in correspondence with Thornton's zone model, provided when there is no external source of substrate heating [16]. The properties of these titanium thin films in general are better transmittance, good optical properties and refractive index value [16].

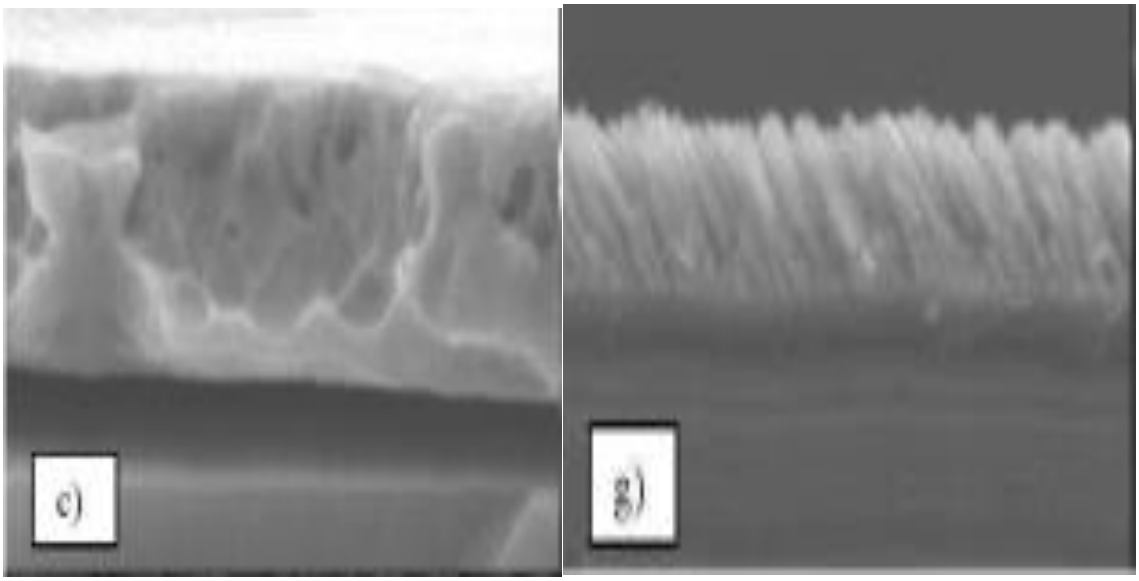

Figure 18. Schematic representation of two different microstructures with respect to deposition incidence angle is shown. The microstructure on left hand side comprises of dense indistinct columns with smooth surface and the deposition occurred at zero degree, whereas the microstructure on right hand side represents inclined columnar grains with coarser surface, as higher incidence angle (85˚) is used for deposition. [16]

With respect to titanium thin film deposition, Chang, Tzong-Sheng, et al, proposed a solution for very-large scale integration applications (VLSI). In their research work, they have taken Si wafers as substrate material and thickness of Ti coating is varied between 10-80 nm to study their effective property of leakage current in VLSI applications [59]. The columnar microstructure of titanium films is predominant and these metallization techniques are widely used in bilayer formation [59]. It is observed that when Ti thickness of film is increased, the resulting properties are increase in junction-leakage current and low junction-depth [59]. In case of VLSI applications the thickness of coating needs to be maintained below 65 nm [59]. Seo, Hyunwoong, et al, suggested that titanium sputter deposition can be used for solar cell applications, predominantly in dye-sensitized solar cells (DSCs) [60]. To compare the effect of Ti (columnar structure) sputter deposition, glass substrates is taken and the thickness is

maintained around 30 nm for solar cell applications [60]. The titanium is deposited over set of samples, one is normally sputtered and the other is acid treated [60]. The SEM and XRD measurement of their research work suggested that the columns present in both set of samples, while there is also notable improvement in current and efficiency value of acid treated sputtered Ti coating [60]. These acid treated samples can be used as one of the effective method for the production of DSCs [60]. In the recent research work concluded by Polyakov, Mikhail N., et al. suggested nanostructured Hafnium-titanium materials can be used to improve the thermal stability of ternary systems [61]. The Si (100) substrate is chosen for this sputtering process while the titanium thin film is deposited around 25-40 nm [61]. From TEM analysis the microstructure of their thin film deposited is characterized. It was reported, that as-deposited sputtered samples revealed columnar nature of grains and the growth of the coating is towards vertical direction [61]. Using this multilayer sputtering technique, the microstructural parameters such as grain size, composition and distribution of element is controlled effectively [61]. The effect of crystallinity is improved to larger extent when titanium is used in any amorphous structures [62]. For instance in chromium-carbide sputtering it results in amorphous structure, but with the introduction of titanium in the sputtering process, the crystallinity is highly improved [62]. The SEM characterization proves the TEM analysis that columnar structure is predominant along with glassy phase microstructure [62]. When titanium content is improved, there is improvement in the columnar microstructure obtained [62]. The properties that are influenced by titanium inclusion are improvement in hardness, toughness and decrease in brittleness of thin films [62].

Metallic titanium is also used in multilayer coating to study the interface effect of Ti thin film over ceramic interface and how the properties such as toughness, crack tip propagation and plasticity is affected [63]. The total film thickness deposited is approximated to be 3 μm in which Ti layers is deposited for 100 nm and the substrate used for this deposition is Si wafers (111) [63]. From their TEM investigation, it is clear that the Ti layer deposited have columnar structure [63]. When crack growth experiments were conducted in multilayer coating of ceramic and metallic Ti coating, it is clearly observed that crack tip propagate through the ceramic layer and then passed through the center of metallic titanium coating [63]. The toughness property of Ti thin film is reduced and ductile fracture is more predominant in case of coating failure [63]. Banerjee, Rajarshi., et al, in their research study related to nanostructured layer found out that engineering property of the structural material is controlled by Ti deposition [64]. Using magnetron sputtering Banerjee, Rajarshi., et al., deposited Ti/Al (aluminum) multilayers over the Si wafer, which is used as substrate material [64]. The nanostructured materials are deposited at around 1- 26 nm depending on different types of Ti/Al multilayers used [64]. The characterization clarified clearly all multilayers deposited at varying thickness exhibited columnar grain morphology and displayed texture of both <0001> hcp (hexagonal close packed) and <111> fcc (face cantered

cubic) [64]. So they were able to formulate the interfacial energy differences for multilayer deposition which is an important parameter for controlling the engineering properties of nanostructured materials [64]. The modification of metallic Ti structures during deposition is of great importance as titanium crystallizes into different forms such as hcp, bcc (body centered cubic), ccp (cubic close packed), hexagonal omega and hexagonal orthorhombic phase [65]. The detailed investigation with respect to the structural modification of Ti is reported by Chakraborty, Jay, et al. According to their investigation, relation between fcc-hcp structural transformations of titanium polycrystalline film is studied for correlation between them [65]. The silicon substrate is used for sputter deposition of Ti films and respective thickness is around 150-700 nm [65]. The cross-sectional SEM micrograph of Ti film of 700 nm indicated clear columnar microstructure present in it [65]. With respect to these thick films (700nm), from XRD analysis it is noticeable that there are new peaks present which matches with the phase transformation of Ti [65]. The two new peaks correspond to fcc and hcp structures [65]. As the thickness of film is increased fcc phase of Ti is decreasing significantly [65]. Surface energy is one of the predominant factors in determining the textural modification of deposited thin films [65]. The following Figure 19 a and b clearly explains the SEM cross-sectional image of columnar microstructure and XRD patterns showing different phases at various lattice parameters correspondingly [65]. From their analysis, it is concluded that fcc Ti phase is stable in thin films of around 140 nm and hcp Ti films can be observed in thicker Ti films of around 700nm [65].

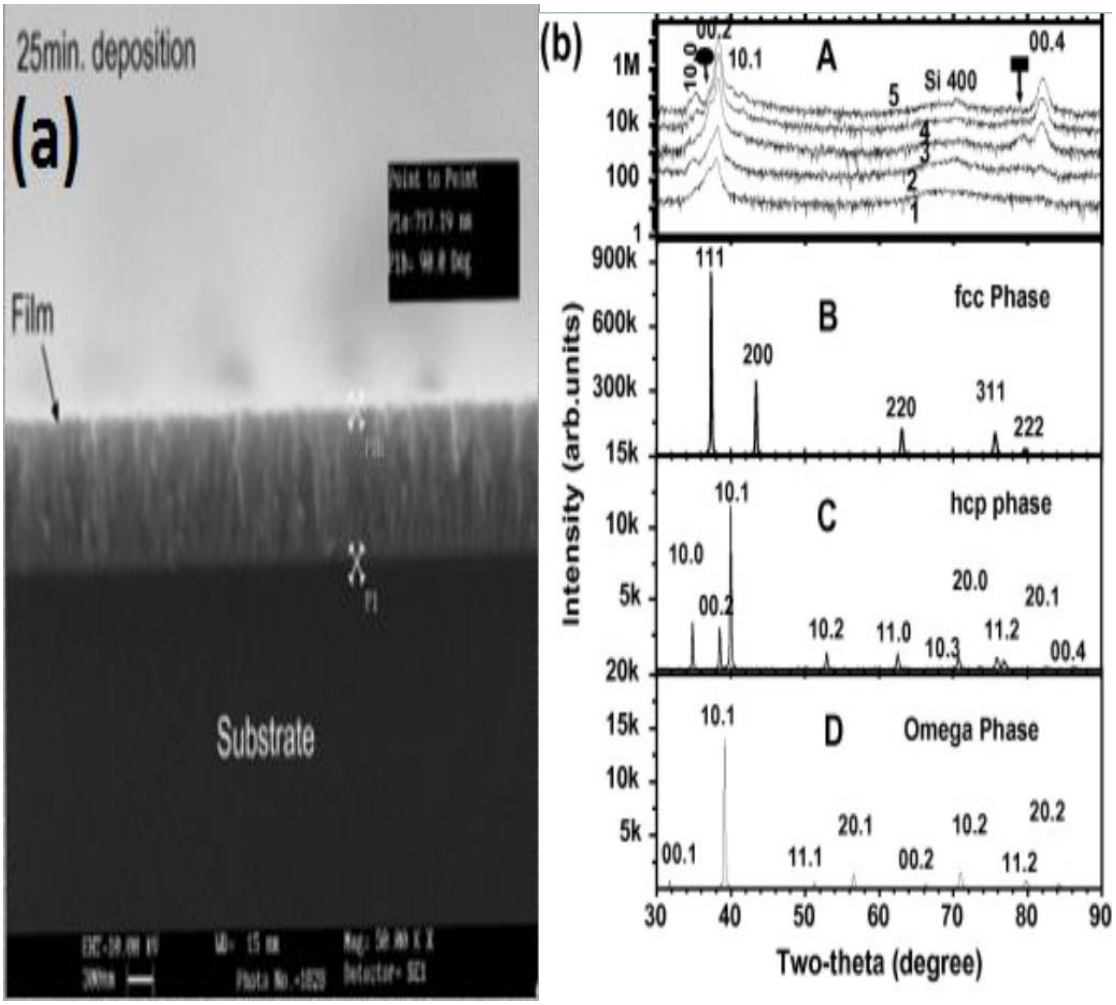

Figure 19 a and b. Typical representation of SEM cross-sectional image of Ti thin film over silicon substrate is shown in Fig 19 (a) and Fig 19 (b) illustrates the resultant XRD patterns which shows several phases at different lattice parameters [65].

2.9.2 Structure and properties of TiN Coating

One of the most important aspects of sputtering deposition is the preparation of alloy compounds for thin film coatings. Titanium nitride is one of the important compounds prepared by sputtering deposition and these nitride films are used in wide range of applications. The TiN deposition is prepared by using nitrogen as the reactive gas and argon as sputtering gas, the composition of thin films can be controlled by different sputtering gas ratios (Ar/ N_2) used. Owing to the importance associated with TiN thin films, it is necessary to understand the structural modification of sputtered thin films. So in this section, investigation about several research findings with respect to TiN microstructural transformations and the resultant properties of thin films is explored. Jeyachandran, Y. L., et al. used nitrogen gas concentration and film thickness as a significant factor in determining the morphological variations observed in TiN films [7]. Two different substrates were in their study 1) silicon 2) glass and thickness deposited

is around 60 - 160 nm [7]. When lower film thickness sample is analyzed, the displayed microstructure is amorphous in nature. The increase in thickness value directly relates to improvement in crystallinity. [7] The TiN phases range from (1 1 1), (2 2 0), (2 0 0) depending on the thickness deposited. The nitrogen gas concentration plays also a very important role in determining the crystal packing and orientation of TiN thin films. [7] When nitrogen gas concentration is around 0.5% the resulting crystal orientation is densely packed, whereas at higher gas concentration, there are cases of bubble precipitation, needle like crystallization and other microstructural abnormalities. [7] In their conclusion, Jeyachandran, Y. L., et al. established that properties such as electrical, optical transmission, stoichiometric composition is enhanced when thickness is increased and nitrogen gas concentration is decreased [7]. When thickness of TiN films is increased, it might result in innumerous defects in the microstructure [66]. In a different research work related to TiN thin film deposition, stainless steel is used as substrate material and thickness deposited is on an average around 1.5 μm [66]. When the nitrogen gas concentration is maintained at low concentration, (hcp) microstructure of Ti is predominant. With further increase in N_2 concentration result in (fcc) TiN phase with preferred golden-yellow color. When the N_2 gas concentration is increased further, resulting crystal orientation is modified to <1 1 1> from <2 2 0>. This TiN film composition when characterized showed columnar microstructure as expected and displayed smooth surface, stoichiometric composition is also established. The above condition holds good when the thickness is less than 1.5 μm and if the thickness is increased further it will result in defects such as peeling, cracking and pinhole defects. [66] The interesting property changes for TiN films deposited are as follows passivation current density decreased with higher thickness, corrosion resistance is improved [66]. When titanium is doped in multilayered nitride films, the crystal orientation is improved which in turn enhances the optical, electrical properties of thin films [67]. The morphological changes of TiN thin films are assessed in an article which is described as follows and its significant impact in aerospace applications. The substrate chosen for this deposition is an aluminum alloy which is used in aerospace and submarines. [68] The parameters of TiN deposition highly influence the morphological properties of deposited material such as fatigue (fretting), S/N curves (stress (S) against the number of cycles to failure (N) or Fatigue), surface hardness, adhesion strength [68]. The TiN cross-section of fractured specimen is used to study the thickness of the sputtered coating. From the following SEM image in Figure 20 shows the TiN coating have columnar structure [69]. The columnar microstructure is more preferred to improve the corrosion resistance of thin films deposited. Improvement of corrosion property is observed in this TiN deposition [69]. The other notable properties which are influenced by TiN coatings are absorption co-efficient, surface roughness and hardness [70]. Janders, M., et al. in their scientific report about microelectrode array analyzed the influence of TiN thin film microstructure and its significance in charger transfer capacity. SEM characterization of these thin films showed the usual columnar structure. [71] The astonishing properties of TiN microelectrode which are widely used in

biomedical applications is as follows high charge transfer ability, increased electrical along with enhanced mechanical properties, decrement in impedance value [71]. In semiconductor applications, TiN thin films are one of important compounds considered widely [72]. The substrate used for deposition is silica (001) and thickness deposited is around 100 nm [72]. The morphological analysis of the deposited film shows mostly fcc crystal orientation. When deposition parameters are varied, corresponding microstructural changes were observed change in grain size, crystal orientation and density. Adatom mobility is one of the important factor in defining the crystal orientation of thin films. The mechanical property of deposited film is influenced by mobility of adatoms. [72] The columnar growth of TiN thin film is majorly dependent on factors such as bias voltage and substrate temperature, which in turn affects the size and spacing of columns deposited [72]. For better mechanical properties in deposited TiN films, (0 0 2) crystal orientation is preferred, along with other parameters such as decrease in density and oxidation resistance [72].

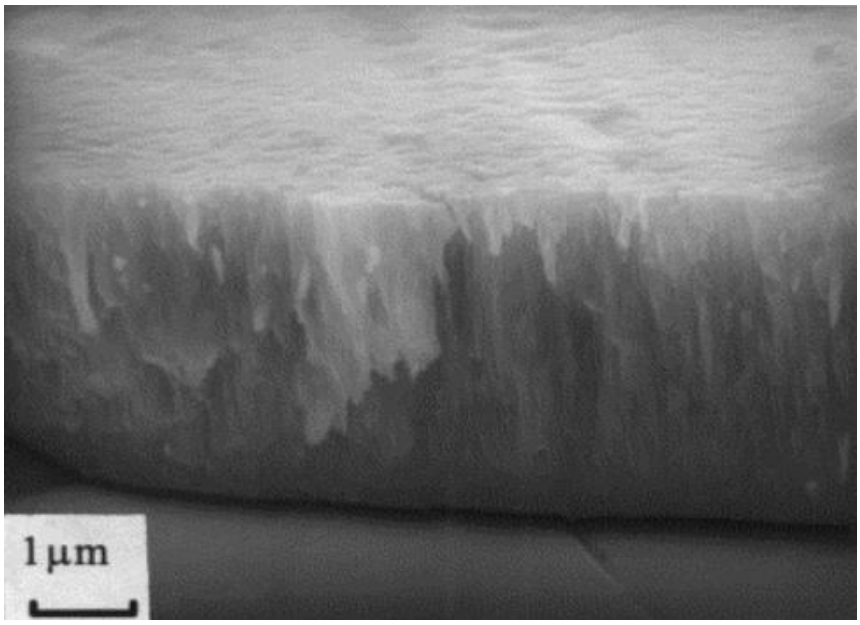

Figure 20. General overview of SEM micrograph images of TiN coating which comprises of well-defined columnar grains with smoother surface morphology [69].

The effect of discharge power of magnetrons is studied in a research work, which have wide influence on final microstructure of thin films deposited [73]. In their research work, glass is used as substrate material and total thickness of thin film deposited is between 1.5-2.0 μm [73]. It is found out that when discharge power is increased, there is densification of the microstructure obtained, with predominant fine grain size present in it. The microstructural change such as decrease in the grain size diameter and surface roughness value is achieved when high magnetron discharge power is used for sputtering process. With this point of view, industrial fabrication of nanostructured coating material with properties such as high hardness, dense structure, and low surface

roughness can be produced distinctly. [73] When the effect of nitrogen gas partial pressure is taken into account, it also influence the final properties if TiN thin films to greater extent. At this point, it is quite obvious that with titanium nitride film formation, resultant microstructure is columnar and it is proved by SEM/TEM characterization. In this research work by R. Wuhrer, W.Y. Yeung, relationship between working distance of sputtering and nitrogen partial pressure is analyzed to find the microstructural impact [74]. The following observations is verified by their SEM analysis, when higher nitrogen partial pressure is used for deposition, grain diameter of around 170-180 nm is attained for different working distance say 65 and 110 mm. [74] In a similar manner, when lower partial pressure is used for deposition, grain size diameter is around 90 nm for both the working distance [74]. However, when medium partial pressure of nitrogen is used, grain size diameter is approximately 100 nm for working distance of 65 mm and grain diameter of 140 nm is attained for working distance of 110 mm [74]. Therefore, thin films obtained in their report displayed nanocolumnar densified microstructure when working distance is reduced [74]. Multilayer coatings of TiN films are taken into account for determining the changes in final microstructure attained [75]. The substrate used in their process is stainless steel with multilayer coating ranging till 3.0 μm [75]. The characterization of deposited films is done before and after indentation and the corresponding microstructural changes are noted for better understanding. The columnar microstructure of TiN multilayer is not affected by the multilayer interface present in the coating. The grain column diameter is increased when the thickness of the coating is increased. The dislocations of TiN crystals are more frequent towards < 1 1 1 > crystallographic directions. The failure in columnar grains along the interface is observed when heavy load is applied and this failure is mainly because of shear sliding force between the columnar grains. [75] When low peaks of loads are applied, then plastic yield failure mode prevails in the microstructure [75]. The properties which were improved during morphological changes are as follows increased absorptance value, high temperature stability, improved oxidation resistance and these coatings are widely used in solar selective coating applications [76]. The mechanical properties of TiN films with respect to fracture properties can be improved by choosing the optimum deposition parameters [77]. The fracture strength of TiN thin film is not influenced by residual stresses present in the film, however fracture toughness of grain boundaries plays an important role in strength properties. The films deposited should have the following final properties such as excellent fracture resistance properties, good adhesion and increased compressive residual stress. The following Figure 21 displays the fracture propagation in TiN films and it displays intergranular fracture and the image displayed is closely resemble to the FESEM images as presented in Figure 41. [77] Kauffmann, Florian, et al. studied in detail about microstructural changes in thin TiN films by introducing silicon content in the coating composition. The single crystal silicon substrate is used to deposit thickness around 2 μm [78]. The silicon content inclusions play an important role in defining the grain structures and crystal orientation of thin films deposited. It is analyzed that when silicon content is low, columnar grains is

observed in films, with further increase in silicon content the microstructure is modified to elongated TiN grains and equiaxed TiN grains. The resulting TiN grains show smaller grain size, improved hardness property and enhanced yield strength. [78]

The optical and photocatalytic properties of TiN are gaining importance as it plays a pivotal role in energy sector applications [79]. In general, sputtered TiN films are very stable at very high temperature, it is also accepted that these nitride films might get oxidized to oxynitride in some cases. The presence of oxynitride degrades both the optical and photocatalytic properties of titanium nitride thin films. So to avoid oxynitride formation over thin films, aluminum layer of 2 nm is deposited as aluminum prevents oxidation of TiN films. However, the above mentioned solution does not hold good for nitride films interface layer. Hence, Okada, Masahisa, et al. studied the methods to improve the mechanical properties of TiN thin films. When film thickness is increased, the refractive index of TiN films is reduced, thus results in improvement in reflectance value which in turn shows improved photocatalytic property. [79] Lin, Z. J., et al, studied the microstructural modification in ternary titanium nitride thin films [80]. These ternary nitrides have unique physical properties such as good thermal shock resistance, high hardness, low density material with increased machinability, wear resistance improved elastic modulus, epitaxially developed grains, high mechanical properties, increased lamellar thickness and biocompatibility. [80] Joelsson, Torbjörn, et al., developed single ternary titanium nitride thin films crystal on magnesium oxide substrates by reactive magnetron sputtering process [81]. These nitride thin films are widely used for protective coatings, microelectronics and cutting tools. The resultant microstructure of ternary nitride films exhibited dense smooth surface coatings. The measured resistivity and young's modulus value of single crystal ternary thin films is much better than the single TiN crystals. [81] With respect to microelectronics applications, TiN is widely used as diffusion barrier, so the effect of microstructural impact is studied for TiN thin films by rapid thermal annealing process [82]. XRD analysis of titanium nitride films after annealing shows that there are no unwanted peaks present in it which is highly advantageous in diffusion barrier applications. The annealing also improved the crystallinity of TiN films, increased resistance and high durability. [82]

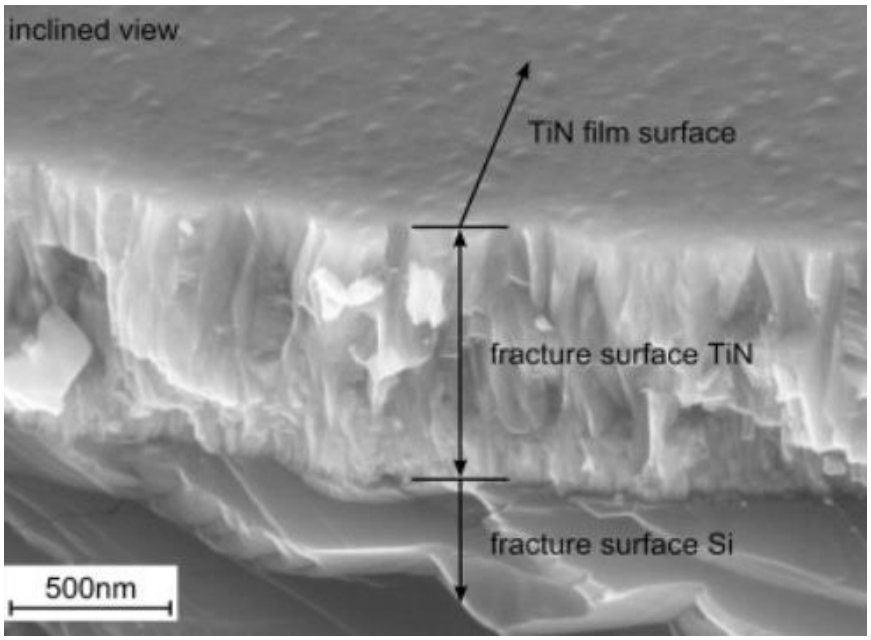

Figure 21. Typical represents the SEM micrograph of fractured TiN grains which exhibits dense, well bonded, indistinct columnar microstructure with rather smooth film surface. The fracture displayed in micrograph is of intergranular in nature. [77]

The adhesion property of TiN thin films gradient multilayers is studied by Chen, Li, et al., and their conclusion is briefed as follows [83]. The multilayers when characterized show columnar microstructures. These thin film multilayer structure is polycrystalline in nature and TiN layers exhibit most stable fcc crystal phase [83]. In XRD analysis, the gradient peak position is moved towards lower angles because of the decrease in lattice constant. The reason for this decrease in lattice parameter is due to the exchange of nitrogen atoms in nitride lattice by other gradient atoms. From their SEM observations, the TiN coatings have bell mouth columnar grain with dense microstructure and whole multilayer coatings shows similar column morphology. In these types of thin film coatings, the interface is the point for energy dissipation and in general coating deformation is avoided. The unique properties of multilayer coatings are increased nano-hardness value and cohesion strength values. [83] The multilayer coatings used for cutting tool applications should exhibit excellent adhesion strength [84]. The failure mechanism observed in thin nitride coatings is predominantly interfacial fracture and it is analyzed by An, T., et al., in their research work. The TiN layer coatings in their report exhibits (1 1 1), (2 0 0) and (2 2 2) crystal orientations. It is concluded in their research, that interfacial fracture is due to interfaces between various thin film layers and crystal orientation. The TiN (1 1 1) thin films show improved fracture toughness and enhanced hardness value than crystal orientation of TiN (2 0 0). [84] Therefore, in general the following factors plays an significant role in determining the microstructure of deposited thin films such as deposition parameters, substrate used, substrate interface with the coatings and crystal orientation of the substrate.

3. AIM

The aim of the thesis work is to study the relationship between depositions parameters used for DC magnetron sputtering process using Nordiko sputtering (NS-2500) equipment. The study is mainly focused to explain the relationship between deposition rates of thin film depositions with respect to sputtering parameters involved. One of the main objective is to study the effect of deposition parameters on microstructures and properties of thin films such as adhesion strength and surface roughness. This research work also deals with investigating the operation of Nordiko sputtering equipment and obtaining relevant experience related to it. The study is also focused on to briefly analyze the effect of substrate heating and etching to understand the morphological changes observed during sputtering depositions. Figure 22 represents the schematic representation of objectives of this research work.

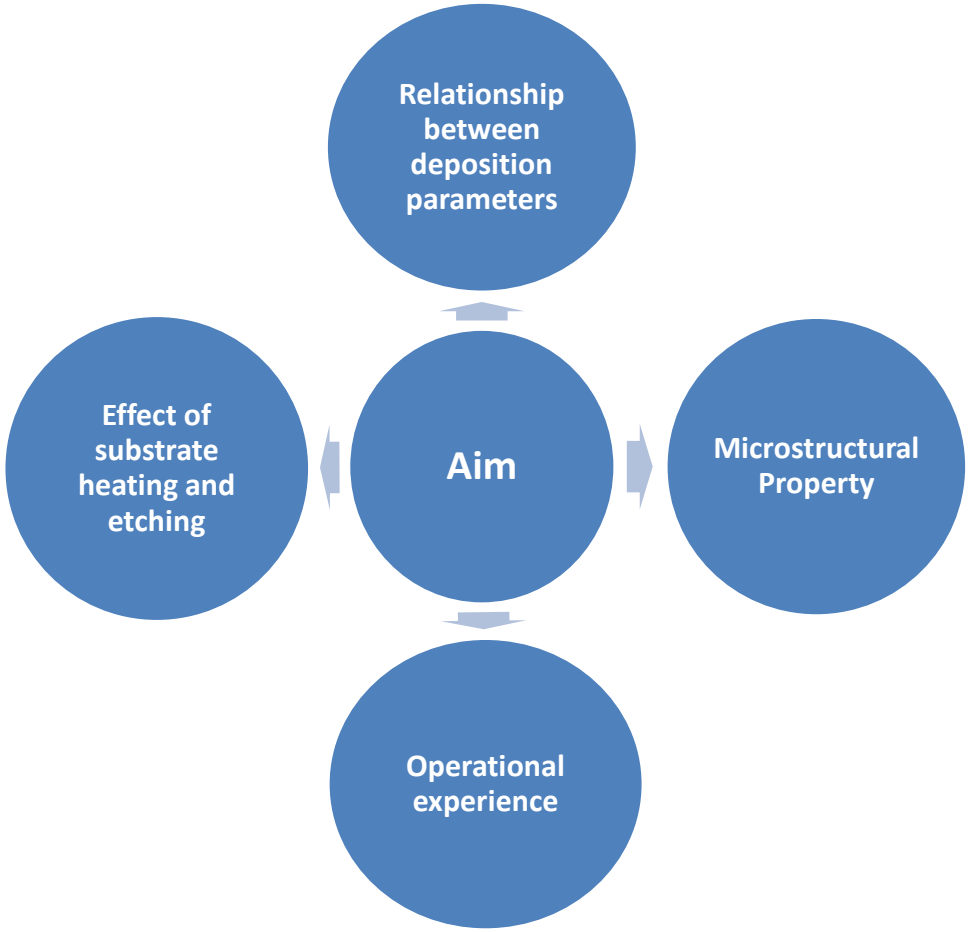

Figure 22. Schematic representation of objectives of this thesis study.

4. EXPERIMENTAL TECHNIQUES

The experimental section is mainly divided into subsequent sections such as materials, equipment, sputter deposition experiments and characterization. The material section gives us a clear idea of different type of substrates and target materials used in the research work and their significant properties, the details related to target and substrate materials is explicated in following section. Nordiko NS-2500 sputtering equipment (Nordiko Ltd., UK) had been used in this research work. The distance between target and substrate material is generally kept in the range of 8-10 cm. The detailed description of this equipment is explained later in this chapter. The sputtering equipment comprises of various components such as vacuum system, DC and RF powers and a control unit. The bombardment of ions is achieved by supplying sputtering gas such as argon in the chamber and produces titanium atoms and thereby deposits titanium coatings. For depositing TiN coatings, the same principle applies, but additionally, reactive gas (nitrogen) is supplied to the chamber to produce uniform titanium nitride coatings. [85; 86]

4.1 Information about target and substrate materials

The copper metal has many interesting physical properties such as it conducts both heat and electricity efficiently, ductile material, increased infrared (IR) reflectance, high thermal conductivity, boiling point around 2500 °C and melting point 1083 °C. Copper is widely used in electrical and electronic industry. [87] For DC magnetron sputtering process, stainless steel is one of the widely used metal substrates. [88] The typical applications of stainless steel AISI 316L (American Iron and Steel Institute-low carbon version of the 316 steel alloy) is that it can be used for many industrial equipment in pulp and paper industry, turbine blades, fuel lines, handrail system tube, exhaust of automobile, heat exchangers, aerospace industries, automobile industries and marine applications. [88-90]

The substrates used in this study are 1) copper 2) stainless steel (Novacel) AISI 316L. The copper sheets thickness is in the range of 0.1 to 0.2 (millimeter) mm, while the steel substrate thickness is in between 1.5 to 2 mm. The thin copper sheets which are used for deposition is manufactured by cold-rolling process. The composition of steel used is given as follows iron, nickel 10%, chromium 16%, molybdenum 2%, manganese 2%, carbon 0.35% and minor constituents of sulphur, silicon and phosphorus [91; 92]. The 316L steel is advantageous as it is free from carbide precipitation over the grain boundary as the overall carbon composition is very low [92; 93]. The significant

physical properties of 316L steel grade is as follows 1) high toughness 2) improved creep resistance 3) increased tensile strength and 4) resistance to stress at high temperature. The oxidation of 316L steel grade is low, because of the presence of chromium content, so the steel possess very high corrosion resistance value [94]. The high toughness value of 316L steel is due to its austenitic structure. The corrosion resistance is high in most of the corrosive medium, however in warm chloride and warm sea water, the steel is subjected to pitting, crevice corrosion problems. The oxidation resistance of 316L steel is good even in high temperature range such as 870-925 ˚C. The annealing treatment is carried over from 1010-1120 ˚C to produce strain hardened steel. As the carbon content is low in this steel type, the machining of 316L steel can be done easily. However, when higher work speed is used this steel tends to harden easily, so care needs to be taken as minimum speed rate is allowed during machining. The hot and cold working process can be applied on 316L steel to improve the mechanical properties of the steel, as post-work annealing in both the process improves the corrosion resistance and reduce internal stresses present in steel. The applications of 316L steel used in various types of industries are given as follows, 1) marine and architectural industries 2) implants used in bio-medical industry 3) pharmaceutical and food industry 4) chemical industry and 5) oil and gas industries [92; 93]. Copper is also used as other substrate material in this research work. [95]

4.1.1 Targets

Titanium: Titanium has physical properties which makes it specifically advantageous material over its competitor elements such as aluminum, magnesium and tantalum. Titanium can be combined with alloys can produce better strength and good thermal expansion coefficient values than steel. The most common properties of titanium are it is lightweight in nature, but the strength is high as compared with stainless steel, density is around 4.5 g/cm^3 (gram/cubic centimeter) which is low, corrosion resistance is high when combined with other alloy elements, melting point of titanium is around 1668 °C, titanium is a passive material which shows immunity to various types of mineral acids, non-toxic in nature widely used in medical industry as bio-implants. The application of titanium is in chemical, biomaterial, marine and petro chemical industries. The titanium elemental composition is also used in the manufacturing of formula-one cars and motorcycles which is exclusively used for racing purposes. The titanium metal is being used in components of products such as frames in bicycle, laptops, helmet grills and cookwares. Titanium is also used in the production of pipes which will be used in power plant condensers owing to its higher corrosion resistance [96; 97]. It is also used in jewelry industry owing to it durable nature. Titanium is one of the most used alloying elements and the alloys are also widely used in aerospace applications. [96-99]

4.1.2 Substrates

Substrates used in the work comprise of metallic and non-metallic substrate materials. The metal substrates used are copper sheets and stainless steel sheets. The non-metallic substrate used in this study is glass. The substrates which are used for coating deposition needs to be perfectly placed to achieve better deposition rate. In Nordiko equipment, the substrates are positioned on a component called substrate table or substrate electrode. The table or the electrode consists of six holes equispaced on pitch circle diameter (PCD), which is of three inch in size. The substrate platen is the component used to hold the corresponding substrate for sputter deposition. The distance between the target and the substrate distance is 80 mm. The six holes present in the table are used to mount the substrate platen in it. This table is supplied with 2000 W (watts) heater, which supplies the necessary heat to the substrate table. The substrate electrode (type SE1), is being supplied with 2000 W heater, which is used to reach the table temperature of around 650 ˚C. The high conductivity property of the substrate platen is considered while choosing the material for platen. The platen is made to fit into the jig for better locking mechanism, care needs to be taken while placing and removing the substrate platen from the table. The platen can be modified according to customer requirements for specific applications.

The DC reactive magnetron sputtering process is effectively used over two different substrates such as copper and stainless steel 316L. The details with respect to the substrate material preparation used in this sputtering process is explained in the following section as follows.

i) Copper (Cu):

The copper sheets used in this sputtering experiments were oxygen-free copper (OFC), which have a minimum 99.95 % purity and maximum 0.001 % oxygen content. They were manufactured using cold rolling. The thickness of Cu sheets was 0.2 mm. The sheets have been cut into required dimensions using guillotine cutting machine. The dimensions which are used for this sputtering experiments are as follows 100 mm *200 mm and 200 mm * 200 mm, consequently sample fits the substrate holder and it is being held together closely so that there is not much space between the sample sheets and holder. The substrate in the holder had been cleaned completely with ethanol for removing surface impurities.

ii) Stainless steel (SS):

The steel substrate has been obtained from Novacel limited (316L-carbon steel). The steel substrates of 200 mm * 200 mm dimension fit have been cut using a guillotine cutting machine. The obtained substrate does have sharp edges around the corner which makes it slightly uncomfortable to use in the sputtering process. So to avoid physical

cutting to the operator person, the substrate edges were smoothen using polishing. The substrates have been cleaned with ethanol and proceeded by acetone cleaning for improved cleanliness and surface impurities removal.

4.2 Sputtering equipment

Nordiko NS-2500 sputtering equipment is explained in the following sections, which then followed with this section ending with characterization used for sputtered coating thin film material deposited using Nordiko equipment. The equipment comprises of sputtering module which is similar to Nordiko NM 400, NM 1500 and NM 2000 sputtering equipment. The pumping system of NS-2500 is similar to the pumping system present in N4-700 and N6-1400 sputtering equipment. As discussed earlier, this Nordiko NS-2500 equipment can be used in sputtering deposition of thin films using various modes such as DC magnetron sputtering, RF magnetron sputtering. Typical representation of Nordiko sputtering equipment is shown in Figure 23. The significant advantage of using NS-2500 equipment is that it can be used to sputter clean both the target and the substrate material. The property of sputtered thin film quality is enhanced to larger extent with the use of substrate heating or substrate etching or in cases even both. The vacuum systems of NS-2500 equipment are discussed in detail in the following section. In general, to achieve high vacuum in any systems two types of vacuum pumps are needed, for instance rotary or mechanical pump and high-vacuum or diffusion pump. The vacuum range of about 10^{-3} torr is achieved through the use of mechanical pump. Further improvement in vacuum in the range of 10^{-8} to 10^{-11} torr, diffusion pump is used [100; 101].

Figure 23. Overall representation of Nordiko NS-2500 sputtering equipment used in this research work with RF (Radio-frequency) power supply unit and control units is shown in this Figure.

4.2.1 Vacuum pumping systems

The pumping systems employed in Nordiko NS-2500 instrument to create high vacuum is explained in this section. To achieve good vacuum range is prime importance as it is the main criteria to create plasma/glow discharge in the target material used. So the knowledge behind the process to create vacuum is necessary to understand the basis for sputtering deposition process. The vacuum pumping systems of Nordiko sputtering equipment comprises of following section such as foreline pump (mechanical), diffusion pump, foreline valve, roughing valve, needle valves, throttle plate. The following subsections explains the vacuum pumping system in detail to understand the mechanism behind the vacuum process creation. The mechanical and diffusion pump used in this Nordiko sputtering (NS-2500) equipment is represented in Figure 24.

Figure 24: Typical representation of the mechanical pumps (left) and foreline pump (right) used in this Nordiko sputtering equipment is presented in this Figure.

The mechanical or foreline pump used in NS-2500 equipment is 'E2M40 rotary vacuum pump' which is two stage oil-sealed vacuum pumps, mainly used in laboratory and industrial applications. The mechanism behind this rotary pump is simple, the gas is entered into the chamber is compressed inside the pump, due to this the pressure of compressed air is slightly higher than atmospheric air. In general, the rotary pump can create vacuum up to 10^{-4} torr. The rotary pump comprises of a vacuum chamber which is connected to inlet and outlet valve. When the rotor operates, it traps a large volume of gas at chamber pressure. This process continues until the air present in the chamber is compressed and so the pressure increases. The compressed air is now conveyed through the outlet valve through the oil present in it. The perfect stage for the mechanical pump is to check the foreline pressure of the chamber and it should be 50 milltorr (mtorr). The following Figure 25 represents the typical mechanical pump used in NS-2500 equipment. One of the major drawbacks of using rotary pump is that they pump condensable vapor such as water vapor. These vapors upon compression get converted to liquid and mix with oil present in pump, which is highly detrimental as it might result in corrosion of pump. So to avoid this gas ballast valve is used to introduce little quantity of nitrogen in the chamber to eradicate the possibility of water vapor condensation significantly. The other useful way to avoid this problem is to replace the oil used in pump frequently [100; 101]. [102]

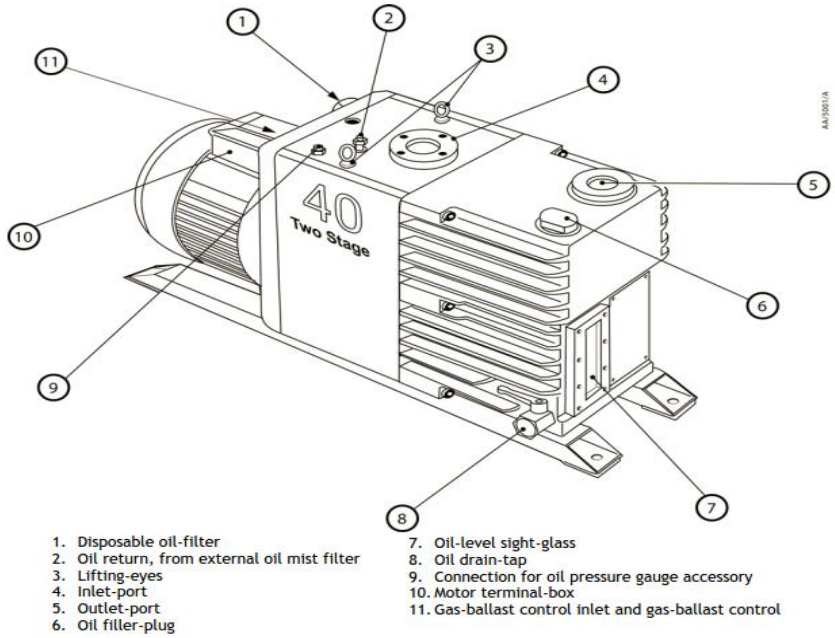

Figure 25. Typical example of rotary vacuum pump and its various components is represented in this Figure. [102]

The diffusion pump or high-vacuum pump used in NS-2500 is Varian diffusion pump. This type of diffusion pump is used to create vacuum up to 10^{-9} torr. The high vacuum pump is made of stainless steel chamber which contains vertically stack pumping cylinder as shown in Figure 26. The assembly of diffusion pump is designed in such a way that the chamber bottom is used to accommodate low vapor pressure oil in it. The electric heater is used to boil the oil present in the bottom of chamber to about 180-250 ˚C. The oil vapor travels up and through the jets, these oil vapors is ejected from the pumping stack as shown in Figure 26 below. When ejected from the jets, the oil vapors acquire high energy and travels up to speed of about 750 mph. These vapor while traveling downwards is collided with the gas molecules present in the pump. The collision of high velocity vapors with the gas molecules is influenced by the following factors such as velocity, density and molecular weight of the oil in use for diffusion pump. The collided gas molecules travel downward towards the outlet along with the high velocity oil jets, to create high vacuum. The cylinder wall is water-cooled as it is circulated with water cooled coils, so that the oil gets condensed and continues the process to create high vacuum. The fore pump is used to remove the condensed atmospheric gases present in the chamber during the vacuum creation process. Thus, by removing molecules from the top portion of the chamber high vacuum is created for the sputtering chamber and over time very high vacuum of about 10^{-9} torr is achieved. This is the maximum vacuum range achieved in Nordiko NS-2500 sputtering equipment. Usually the vacuum range optimally used for sputtering process is around 10-6 mtorr for magnetron sputtering process in NS-2500. [100; 101; 103] There is liquid nitrogen trap (liq.N_2) in diffusion pump which is used to fill the liquid nitrogen once the pump warms up for approximately 10-15 minutes. The liquid nitrogen trap is used to collect

diffusion pump oil so it the water cooled trap is used between pump and nitrogen trap. This liq. N_2 trap is placed in between diffusion pump and high vacuum isolation valve, so that during venting trap is not exposed to air. In NS-2500 sputtering equipment, the size of diffusion pump used is around 4 inch, which ensures high quality vacuum range is accomplished for sputtering process.

As in mechanical pump, it also consists of inlet and outlet valve, both of which are maintained at different temperature. As inlet pressure of the diffusion pump needs to be below 100 mtorr and the outlet pressure is maintained at higher pressure. The compression ratio is very high for this diffusion pump and the outlet pressure might reach about 1 mtorr. In NS-2500, foreline pressure is used to measure the outlet pressure of the diffusion pump and it should not exceed the maximum limit of 50 mtorr under any circumstances.

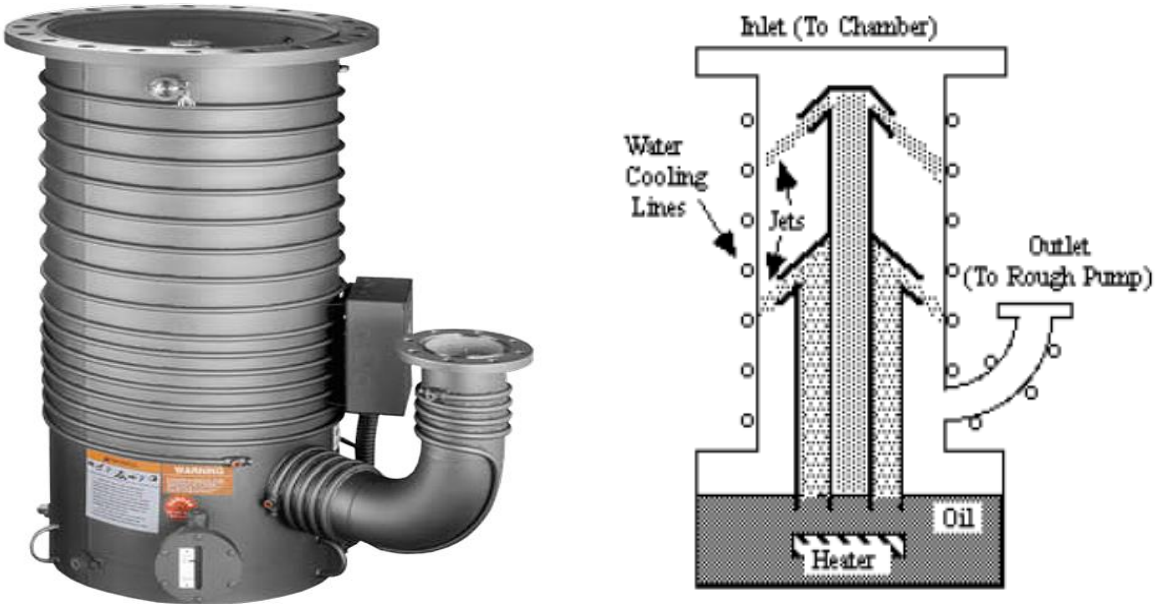

Figure 26. General representation of diffusion pump (left) and its vertically stack pumping cylinder (right) is presented in the above mentioned Figure.[100; 104]

The presence of moisture content/water vapor is unavoidable in the gas chamber at pressure below 10-5 torr, a liquid nitrogen trap is required to counterbalance the effect of water vapor present in the chamber. These traps will be located near to high vacuum isolation valve and diffusion pump, which makes the trap un-exposable to air during venting. This liquid nitrogen trap continuously to accumulate diffusion pump oil, so always water cooled trap is placed right near to it. The pumping stack comprises of 4-6 inches of diffusion pump, chevron baffle, quarter swing isolation valve at a pumping speed of 360 liter/second (l/s). In general, the use of dielectric targets increases the

outgassing rate, which is avoided in this case as dielectric targets are not used in this sputtering experiments. When the substrates are introduced in the chamber, the pressure inside is also increased. The usage of liquid nitrogen can be replaced with the use of 'POLYCOLD' refrigeration unit, which avoids the frequent topping-up implemented in liquid nitrogen trap. The diffusion pump is used in the high vacuum pump owing to its simplicity, reliability and low cost in sputtering systems. [3]

The main use of rotary pump is the ability to maintain the backing pressure of diffusion pump, so that it does not exceed the critical backing pressure which is around 10^{-3} torr. The rotary pump size is not an important factor, as its function is to back the diffusion pump. To maintain a pressure of 0.1 torr, pumping speed of 10^{-3} l/s is required when the gas load is around or less than 10^{-4} torr l/s. So usually the size of the rotary pump pipeline would be 13 mm which is more than enough to achieve the required pressure. Consider this case, in which the pumping speed is 1300 l/s for a six-inch diffusion pump. Thus the maximum gas load that a pump can withstand is 1.3 torr l/s. The rotary pump will pump all the gas that enters the diffusion pump. However, 0.5 torr is the critical backing pressure for 6-inch diffusion pump. Considering a safety margin of around 0.2 torr, pumping speed at the exit is calculated as follows, (1.3/2) l/s. So 6.5 l/s. [3]

The diffusion pump and rotary pump is connected together with ~0.7 of 25 mm diameter pipeline which exhibits the conductance of around 25 l/s. So the speed (Sp) required to calculate the pumping at rotary pump is briefed as shown below, [3]

$$(1/6.5) = (1/25) + (1/Sp) \text{ or}$$

$$Sp = 530 \text{ l min-1, (For 6-inch diffusion pump)}$$

In Nordiko equipment, the DC 704 is the diffusion oil used, which is helpful in rugged and tough applications [105]. The level of oil needs to be checked at specific interims. When the diffusion pump is not performing properly or if poor performance is observed, in general it must be because of the following reasons

1) The level of oil needs to be top up for better performance.
2) If there is any open circuit or if the heater is failed, then it will affect the performance of diffusion pump, so replace heater. After that make sure that heater should be checked when it is being operated
3) If there is contamination or impurities in oil / jet, then the jet assembly needs to be cleaned, re-assembled finally clean oil is filled for better performance. [3]

In Nordiko NS-2500 sputtering equipment, there are three different valves present in the system namely foreline, roughing and high-vacuum valve (Hi-Vac). The diffusion pump operation is critically dependent on the foreline pressure value. The foreline is basically the vacuum line which is used to connect mechanical pump to diffusion pump. The

permissible pressure value for foreline valve is around 50 mtorr. The main reason behind the foreline pressure to maintain in the specified range is for the diffusion pump to function normally else pumping operation is not operational. If the foreline pressure value is exceeded, then the system is checked for outgassing or leaks. The pressure value of foreline valve is measured using thermocouple gauge 1 (TC1), if the pressure value is exceeding 200 mtorr, which gives the indication that the oil might be forced back to the system which might be really harmful for the diffusion pump and the sputtering system. The rise in foreline pressure is rapid after diffusion pump is switched on, at this point it needs to be shut down immediately till the pressure value drops to 50 mtorr. It is advised to warm up the diffusion pump for about thirty minutes, before proceeding with the vacuum generation in the chamber. [106-109]

The diffusion pump which had been warmed up, when comes in contact with atmospheric pressure, might end in diffusion oil decomposition and it will also result in critical damage to both equipment and quality of end product. So to avoid this, a bypass line is employed between diffusion pump and chamber. This bypass line is used to evacuate the chamber pressure to rough vacuum from atmospheric pressure, hence it is called roughing valve or roughing line. When both rouging valve and foreline valves are open at the same time, rapid rise in foreline pressure is noted and consequentially diffusion pump oil is forced back into the chamber and clean environment in the sputter chamber is ruined. So the roughing procedure is carried over by opening the roughing valve, the other two valves are closed specifically foreline and Hi-vac valve. By doing this, the isolation is achieved between diffusion pump, baffle and the cold trap. The roughing valve is closed once the required roughing pressure of around 100 mtorr is obtained. The thermocouple gauge is now switched back to thermocouple gauge 2 (TC2) and foreline valve is opened followed by the opening of hi-vacuum valve. The other interesting and important component of sputtering equipment is cold trap and baffle. The cold trap is present above the diffusion pump, in which liq. N_2 is filled to reduce pressure of the diffusion system. The principle behind this mechanism is as follows, liq. N_2 freezes out the condensable vapors when comes in contact with the surface. These condensable vapors are mostly oil vapors and water vapor, the trap also helps in preventing the oil vapor from back streaming into the chamber. The baffle is used to contain the oil vapor which have been not been condensed by diffusion pump. This type of oil vapor is usually very small in quantity, yet it possesses very serious damage to the system. The baffle is generally situated in between diffusion pump and cold trap. Thus in conclusion, the cold trap is used to prevent back streaming of oil vapor into the system, and baffle is used to condense the small quantity of oil vapor which is not contained by the cold trap. The general overview of typical vacuum system with different types of valves present in sputtering system is revealed in Figure 27. The foreline value used in the Nordiko sputtering equipment is represented in Figure 28. [106-109]

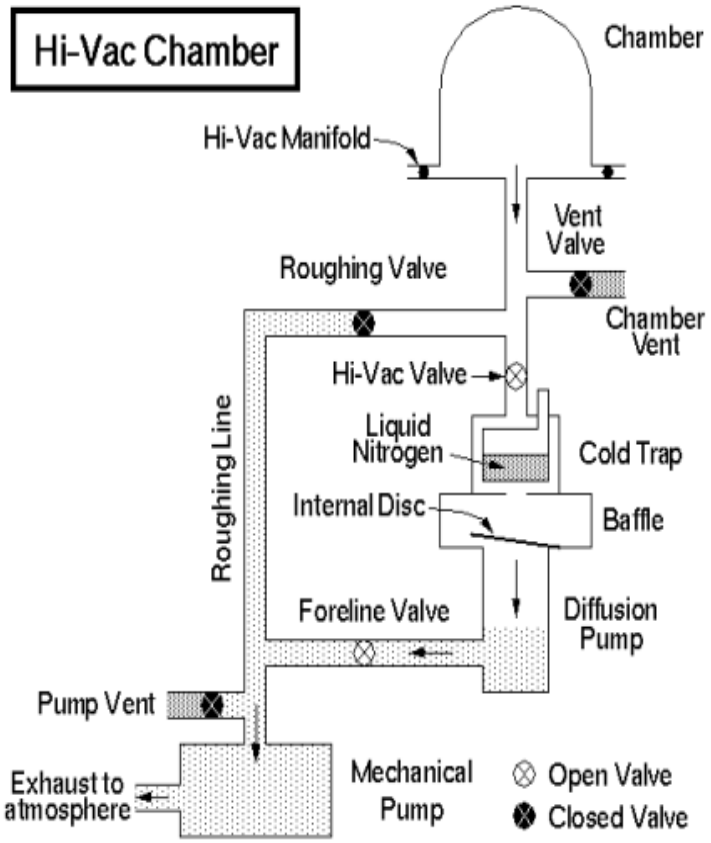

Figure 27. General overview of typical vacuum systems present in the sputtering system is represented in this Figure. The different components in the vacuum system are roughing valve, foreline valve, cold trap is also illustrated schematically for better understanding. [108]

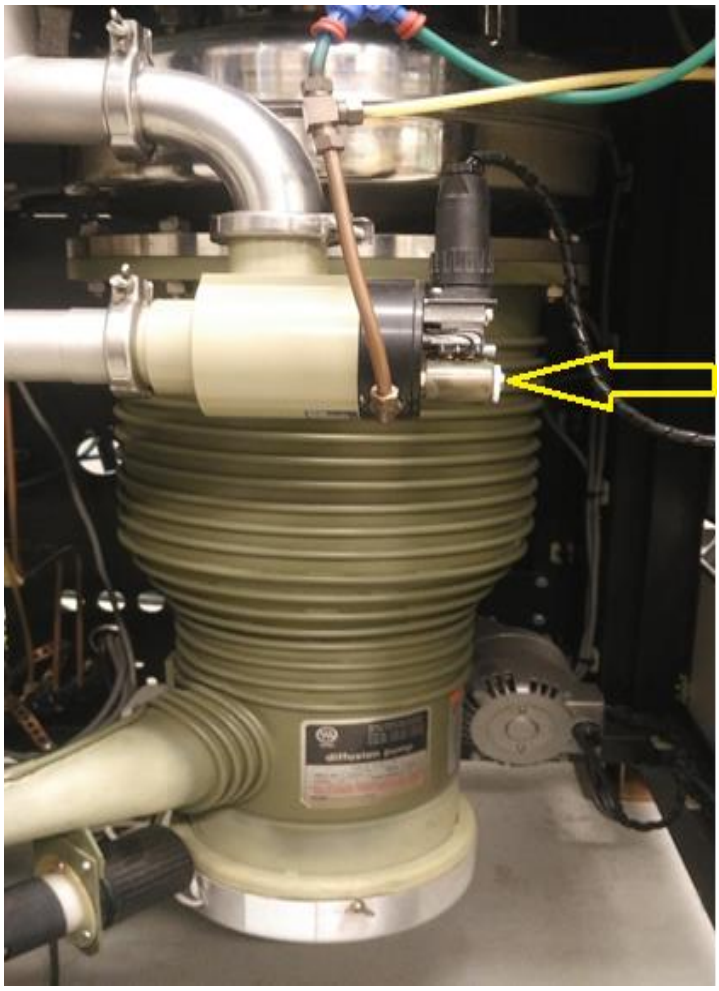

Figure 28: Foreline valve present in Nordiko NS-2500 equipment is represented in this Figure with an arrow towards it.

The pirani gauge is used to measure the pressure change in the sputtering system due to heat loss. The head of the gauge is sensitive as it has very high temperature co-efficient of resistance so the change in pressure is measured easily. The principle behind this is when there is pressure modification in system, which basically means increase or decrease of gas molecules present in the system. So there will be change in the gas conductivity which is measured by the pirani gauge. The increase or decrease in thermal conductivity of gas infers that there is heat loss of filament and it varies with the pressure modification. Thus variation in system pressure means there is modification of resistance of the filament and this value is usually measure in terms of millibar. [109]

In Nordiko sputtering equipment, the Edwards 505 penning gauge is used. The main use of penning gas is that it measures the pressure of the gas used in the sputtering chamber. This measurement of pressure is highly critical as pressure is one of the major parameters which define the final properties of deposited thin films. The penning gauge is basically a cold cathode ionization gauge which comprises of anode and cathode present in it. Using resistors, anode and cathode is subjected to high potential

difference. A permanent magnet is used at right angles of the electrodes to apply magnetic field, so it will result in improvement in the ionization current produced. The mechanism behind this process is as follows when the cathode emits electron, the applied magnetic field deflects the electrons and makes the electron to go on a helical path to reach the anode. By this the emitted electrons takes a longer path, so chances of gas molecule collision are greater than usual. The ionization is further increased, when there is inclusion of secondary electron in the process. In the end, equilibrium is reached when the electrons reach the anode and this mechanism is used to measure the pressure present in the sputtering chamber. [109]

The throttle plate is one of the important factors in raising the pressure in the chamber. The pumping speed of the pumping stack is being reduced when the throttle plate is closed and the pressure is increased because of closing of throttle plate. In the bottom portion of the throttle plate there are two screw positions and these nuts are used to control the degree of restriction. When the foreline pressure is in between 100 to 200 mtorr, then the adjustment in throttle plate is done (closing the throttle plate), thus the chamber pressure of 15-20 mtorr is achieved. This chamber pressure is necessary to achieve RF glow discharge. If the condition specifies there is no use of RF glow discharge and the sputtering can be carried at below 10mtorr, at this point the throttle plate can be open during the sputtering. The throttle plate is closed to achieve very high pressure (15-20 mtorr), without changing the needle valve present in the control unit of the chamber. If the needle valve is adjusted to shut off the flow of gas, then it might result in valve damage. The throttle plate is operated by the pneumatic actuator. [3]

The pressure measurement in the chamber is most important due to the following reasons, as during roughing out the change from rough pumping to fine pumping is carried out between 0.2 to 0.1 torr. For these measurements in Nordiko equipment, HASTINGS thermocouple gauge is used. The rotary pump is used for roughing out while rough to fine pumping is carried out by diffusion pump. The pressure in the chamber is measured using high good scale sensitivity thermocouple gauge such as HASTINGS EVT-5, and the pressure is generally varying between 1 to 20 mtorr. The chamber pumping down before sputtering is measured using penning meter, as the pressure at this point will be 10^{-5} to 10^{-6} torr. The backing line pressure is measured using thermocouple gauge, so that it does not cross the critical limit. Usually the backing and the roughing gauge valve is controlled by the single unit.

For sputtering process, one of the necessary pre-condition which needs to be satisfied is the ability of the sputtering equipment to achieve necessary vacuum. The vacuum obtained is sufficient enough to proceed with the sputtering process. This pumping arrangement is essential to achieve the following tasks i) to achieve low pressure in the chamber between 10^{-6} to 10^{-5} torr, so that the unwanted gases from the chamber is being removed to considerable level, ii) the vacuum chamber is being maintained in the

pressure range of around 10^{-3} to 10^{-2} torr, during the sputtering gas and reactive gas is fed into the chamber. When the system is being pump down the outgassing rate is the most important factor which needs to be considered. During this state, outgassing is being done from the chamber walls, targets, substrates and of course removing the residual gas from the chamber. The outgassing rate (Q) is affected if there are any leaks in the chamber and the rate is determined from pressure (p) and pumping speed (S) of the chamber. The outgassing rate is being measured in terms of litre per second (l/s)

$$Q= pS$$

For reducing the outgassing rate, stainless steel (SS) chamber is preferred as the glass chamber increases the outgassing rate considerably to $6*10^{-4}$ and $6*10^{-5}$ torr l/s. The use of dielectric target always increases the outgassing rate, however metal targets outgas at very lower rate. In this experiments, with respect to sputtering equipment only metal targets such as titanium are used. When chamber is allowed to maintain at atmospheric pressure, downtime of pumping is reduced to considerable extent. Then the chamber is vented from vacuum with atmosphere. If in case, the moisture content is high in the air used to vent the chamber, this will further increase the pump down time. The argon gas is being fed into the chamber till the acceptable range 5 to 17 mtorr.

The gas used for sputtering deposition is one of the significant factors in controlling the nature and microstructure of the deposited coatings. There are different types of gases used for sputtering deposition such as argon, nitrogen and oxygen. In normal sputtering process, in general only noble gases such as argon are used for generating plasma. In the case of reactive sputtering, along with argon gas, reactive gases such as nitrogen, oxygen is used to deposit thin films of varying alloy composition such zinc oxide (ZnO), titanium oxynitride, aluminum nitride (AlN), tantalum oxide (Ta_2O_5) and so on. The Nordiko NS-2500 sputtering equipment is enclosed with provisions to incorporate different types of gases used in the sputtering deposition. The argon gas is used as sputtering gas to generate plasma of required intensity and nitrogen is used as reactive gas to produce compound nitride plasma composition. These gases are supplied from gas cylinders of 99 % quality and both argon and nitrogen cylinder is kept at pressure of 0, 4 bar. The pressure is kept constant during the sputtering process and altering the pressure of gas cylinder has tremendous negative impact on the thin film deposited.

Once the high vacuum range of around 10^{-6} mtorr is achieved in the sputtering chamber, it implies the chamber is suited for sputtering deposition. The penning High voltage (H.V) gauge is switched off, and gas inlet valve of argon and nitrogen is open to fill up the chamber with the required gas mixture. It is best advised to first open the gas inlet valve of argon gas and the pressure of the chamber can reach value up to 5 mtorr. The chamber pressure can even rise to 20 mtorr, but reactive gas mixture composition become negligible when the chamber pressure is very high. One way to make sure that the chamber pressure to not exceed 10 mtorr is that to keep foreline pressure always

below 200 mtorr. The other disadvantage of exceeding the pressure range is that the diffusion pump operation will underperform or even stop. So, after 5 mtorr chamber pressure is achieved, the current is applied to generate plasma. The 'H.T. on' (High tension control switch ON) switch is pressed on, and the intensity of the current applied is increased by rotating the power output in clockwise direction. There are certain limitations in operating the power output button and the current applied as the power level should not exceed above 2 kW (kilowatts) for targets used in the sputtering equipment. If the power level is exceeded, then it will result in termination of plasma immediately. After the required power level is applied, the argon ions strike the target to generate plasma which is blue in color. The plasma is allowed to accrue under the substrate shield to increase its properties before depositing on the substrate material. For reactive sputtering process, the second gas inlet valve for nitrogen gas is open and the chamber pressure should not exceed 8 mtorr in sputtering deposition. So which implies less than 3 mtorr of reactive nitrogen gas is allowed in the total gas composition mixture. This level of nitrogen gas is allowed for reactive sputter deposition as very high gas composition might result in the resulting coating material to be dark-grey in color. The dark color of nitride coating implies sub-stoichiometric composition is achieved in sputtering process. The color of the plasma changes to violet from blue, when nitrogen gas of required range is allowed in the chamber. The level or amount of gas composition allowed in the sputter chamber is controlled by the needle valve present in the control cabinet.

The needle valve is basically a micrometer adjustment, which helps in controlling the throughput of gas in the chamber. When needle valve is open, the foreline pressure increases and this pressure value is measured using TC2 gauge. So as discussed before, the foreline pressure should not surpass the critical value. If the needle valve is used to close completely, to stop the gas flow in chamber then it will result in permanent damage done to the gas valve. So care needs to be taken while adjusting the needle valve controller. The adjustment of gas flow through needle valve is always done incrementally to avoid any damage done to the valve as such. The main advantages of using needle valve are that fine adjustment of chamber pressure is accomplished easily. The chamber pressure cannot be improved, only by allowing increasing gas flow rate. So throttle plate is used to partially close the pumping port to achieve higher chamber pressure. The throttle plate is used to maintain or adjust the chamber pressure between 15 to 20 mtorr without any adjustment in needle valve. So the throttle plate is opened to achieve chamber pressure below 10 mtorr and when the plate is open again the pressure will rise back to be in between 15 and 20 mtorr. During this mechanism of throttle plate open and close, the needle valve setting is kept constant. The closing of throttle plate can be used to strike the discharge to initiate the plasma generation at low pressure range. The throttle plate is operated by pneumatic actuator and the actuator is controlled by variable restrictors. These are the necessary pre-conditions essential to generate plasma of required composition. Once all the conditions are predefined, the substrate to

be coated with thin film is placed over the sputter target and the sputtering process occurs. The duration of sputtering deposition is varied from 3 minutes to 30 minutes to demonstrate the various microstructural property changes of sputtered thin film of titanium and titanium nitride compositions.

4.2.2 Sputter sources and power supply

The targets used in the sputtering equipment is the main source of sputtering atoms which are ignited by the factors power, vacuum level applied in the respective system. In this Nordiko equipment, the targets used are 1) Titanium 2) Copper 3) Nickel chromium alloy. Of these three, the sputtering experiments were conducted with titanium targets to study the effect of deposition variation with respect to various other parameters. The titanium target used in the experiments is grade one quality, which means a purity of 99.8 %. The dimension of titanium target is given as follows 200 mm *100 mm (8" * 4" inches) and thickness is around 6 mm (1/4" inches). The titanium target has been used in planar magnetron setup of Nordiko sputtering equipment. The target needs to be mounted properly in a position where sufficient cooling is achieved over the target contact surface. When there is no proper cooling then the target will be heated at the point where there is no contact with cooling surface, which will affect the properties of the deposited material drastically. The improper cooling also leads to target material to crack as the power produced during ion bombardment is around 15 Watt per square centimeter (Wcm^{-2}). The point at which the target surface is in contact with the water cooled electrode can be considered as heat sinks. The point which is not in contact with cooling surface might be very hot, which result in huge temperature variation along the target surface, thus resulting in thermally induced cracking. In this sputtering experiments, the targets are clamped to the copper or stainless steel backing plate which is screwed to the water cooled electrode. The bonding is usually done by silver loaded epoxy resin or cyanoacrylate adhesive. The targets should be chosen in such as way it can be operated at suitable power levels such as 3 to 10 Wcm^{-2} based on the target size used in the process, otherwise electrical breakdown is achieved at very high voltages. The power supplied should not exceed 1.5 kilowatts (KW) or 2 KW in most of sputtering experiments. When the current is supplied to initiate the ion bombardment from the target sources, the sputtering process begins at 1 A current provided there is good vacuum range in the equipment. The current value can also be increased to comparatively higher range such as 2 and 3 A, but the respective voltage value should not exceed 500 V in any situation. If the power value is increased beyond 1.5 KW, then the power applied is reduced gradually as explained below. [3]

$$Power = I*V$$

Where I = current value in Amperes (A)

V = voltage (Volts)

For instance, with respect to copper targets, when current is applied at 1 A, the resultant voltage value is around 460 - 470 V, so the subsequent power value is around 470V, which is good for sputtering deposition time around 10 minutes.

Power = 1 A* 470 V

Power = 470 W.

If the power is increased to 3 A, the respective voltage is approximated to be 500 – 510 V, now the resultant power value is around or above 1.5 KW as explained below, and so in this case the power value is reduced to 2 A or 1 A depends on the voltage value obtained.

Power = 3 A* 500 V

Power = 1500 W or 1.5 KW.

4.2.3 Control unit

The valves present in the chamber such as roughing, foreline, hi-vacuum, vent and so on is mainly controlled by push buttons present in the control unit and these buttons will illuminate upon switched on. In this section, operations of the control units are analyzed and their function with respect to the sputtering equipment is studied. The push button for roughing or foreline valve is switched on, the respective button illuminates and it switches the electromagnetic valves by supplying the electrical current supply. The electromagnetic air valve is placed inside the vacuum valves and it is integrated with the system. The vacuum valves are open when there supply of air through electromagnetic valve and the valve is closed when the electrical supply is stopped, in the meantime it also vents. The valve also shuts down when there is drop in air pressure and fall in pressure at this point is due to air supply failure. Thus all these push buttons, switches are interlocked to each other.

The function of hi-vacuum valve is to create very high vacuum in the chamber and it is being operated by the ‘hi-vacuum’ push button in the control unit. When this push button is switched on, the electromagnetic 5/3 air valve is actuated and takes control over the supply of air to the pneumatic actuator. When the power is switched off or removed from the valve, then the hi-vacuum valve is closed. The hi-vacuum valve fixes itself in the last position when the electrical power is removed, which results in the air-supply failure. A brief introduction is given about how the vent valve and the respective push button operate to actually vent the chamber. This push button of vent switch on the electrical supply to electromagnetic vent valve, when the power is switched of the vent

valve closes. This means there will be no more venting of the chamber. One of the most important to be noted is that, all these valves operate when rotary pump is functioning or operating during that point. There is certain point which needs to be considered while operating the valve push button in the unit. The roughing and foreline valve cannot be opened at the same time, because power switching of the valves by the buttons is being interlocked. This above condition holds well for hi-vacuum/roughing and vent valve cannot be open at the same time, owing to the interlock condition. In addition to this condition, the hi-vacuum valve and vent valve cannot be opened (both in separate scenario) without the foreline valve is open. The following Figure 29 represents the control units used in Nordiko NS-2500 equipment in TUT.

Figure 29: Control unit of Nordiko NS-2500 sputtering equipment, which acts as a main operating mode of functioning the sputtering equipment efficiently with power supply units and also controlling the vacuum created in sputtering system.

4.2.4 Practical Operation of NS-2500 sputtering system

The user guide is used for operating the Nordiko NS-2500 sputtering equipment efficiently. It provides step by step brief guidelines to be followed for effective operation of sputtering system. The different terminology used in this sputtering process is explained previously as detailed explanation regarding the pumps, gauge is already provided for better understanding of this section. The following guide is divided into several sections for clear instructions.

System start up from cold

1) The Nordiko sputtering equipment is comprised of vacuum pumps and different gauges. So the first step would be to switch on the sputtering mains, followed by opening the cooling water inlet valve and pressurized air valve. The cooling water needs to be checked for proper circulation, as in case of improper cooling of target material, it might result in target burnout or plasma arcing (both cases result in plasma termination).
2) Main power switch from the control unit is ON
3) Mechanical pump is switched on, followed by opening the 'foreline' valve, other valve such as roughing and hi-vacuum is closed.
4) Using thermocouple gauge TC2 the pressure of the foreline valve is measured and it is highly recommended to use the system further when the foreline pressure value drops below or around 50 mtorr. If the system runs fine till this stage, then it implies that there is no leak or outgassing from the system. However, if the foreline pressure is above 50 mtorr, please check for leaks present in the system or in other case fix the outgassing from the cold trap
5) At this stage diffusion pump is switched on, the pump needs to run for about 10-15 minutes, so that it is warmed up from cold state. Once this condition is satisfied, liquid nitrogen of about 4-6 litres is filled in the pump using a provision for cold trap. The sputtering system will be ready for pumping after 20 minutes. This is highly critical, as failing to satisfy any of these conditions will result in severe damage done to the system. For instance, rapid rise in foreline pressure, foreline pressure does not drop below 50 mtorr. [3]

Pumping and Vacuum generation

1) Check the vent valve is closed, if not close it immediately.
2) The time period allowed for diffusion pump to warm up, can be used to place the suitable substrate material used in the sputtering system for thin film deposition. The pre-requisite for substrate preparation and cleaning should have been completed before this process to ensure cleanliness in the process.

3) The substrates used in this sputtering system are stainless steel and copper material.
4) Once the system is loaded with substrate materials, the substrate shield is used to cover the space in between substrate and target material. This is very important point of sputtering process, as covering the shield ensures when there is plasma generation it make sure the wanted gas mixtures is already used and does not deposit on the substrate material.
5) The chamber should be sealed for further process, now open the throttle plate, during this process, gas inlet should be closed.
6) From this step, the high vacuum creation for the sputtering process starts. The foreline valve is closed now, followed by opening the roughing valve. The thermocouple gauge will be switched back to TC1, now there is rise in roughing pressure and it might reach the atmospheric pressure value.
7) Wait for approximately three minutes, by this time the roughing pressure value will be dropped below 100 mtorr. It is advised for effective use of sputtering equipment, wait for some more minutes till the roughing pressure reach around 50 mtorr.
8) If the roughing pressure does not reach 100 mtorr within approximately three minutes, then the following steps needs to be followed,
    i) Switch the thermocouple gauge back to TC2
    ii) Check the foreline pressure, if it is more than 100 mtorr, close the roughing valve, open the foreline valve
    iii) After opening the foreline valve, pump the foreline pressure below 50 mtorr
    iv) Continue the same process from point 6 in section 2 to achieve high vacuum in the sputtering system
    v) If there is rapid rise in foreline pressure, then it means the liquid nitrogen trap should be refilled again else, there is leak in either foreline or hi-vacuum valve. Always remember the leaks are detrimental to any process. So it needs to be fixed immediately.
    vi) The other reason for long roughing time than usual is that vacuum chamber is not sealed properly or there might be leaks from the O-rings seals.
9) Now it is assumed that the roughing pressure is below 100 mtorr, now the roughing valve will be closed.
10) Thermocouple gauge will be switched back to TC2. Then the ‘foreline’ valve will be open, followed by opening of ‘hi-vacuum’ valve.
11) The ‘H.V gauge’ is switched on to measure the pressure inside the chamber. In Nordiko sputtering equipment, penning 505 meter is used as ‘H.V gauge’ and it needs to be pulled out. [3]

Procedure for sputtering process

1) The ideal high vacuum created in Nordiko equipment is in the range of 10^{-5} to 10^{-6} mtorr after an hour of pumping or even less if the system is in good operational condition. One this condition is satisfied that is requires pressure range is achieved, the 'H.V. gauge' is switched off. If needed close the 'throttle' valve.
2) The gas inlet valve is open now, first the argon gas inlet valve followed by nitrogen inlet valve
3) Both the gas cylinder is maintained at 0,4 bar so that the gas flow is constant throughout the sputtering process
4) The argon gas needle valve is open slowly so that the sputtering pressure reaches 5mtorr.
5) Once 5 mtorr sputtering pressure is reached, the needle valve of nitrogen is open slowly till it reaches the pressure value of 7 or 8 mtorr, according to the requirement. The nitrogen gas composition needs to be low in all cases, as too much of nitrogen also result in target poisoning.
6) The required sputtering pressure is set up by using needle valve.
7) Now all the pre-requisite for sputtering deposition is satisfied. So the sputtering deposition of titanium and titanium nitride is shown in the next section. [3]

Sputtering deposition for Titanium and Titanium nitride coating

1) H.T On switch is pressed on now, it will immediately result in plasma generation in the chamber, which can be observed from the glass window present in the chamber.
2) The power value can be raised by rotating the power output button in clockwise direction. The rotation should be done gently, as it is very sensitive and the power value will increase dramatically if care is not taken during this step.
3) The current value will be increased upon rotation of power output from 1 to several amperes upon requirement of the process, also the respective changes in the voltage value is observed.
4) Generation of plasma in the sputtering chamber is accomplished, to achieve superior final quality of deposited thin films the plasma is allowed to accumulate for a certain period of time prior to deposition over the substrate material.
5) The shield is moved using the substrate shield button.
6) The time is noted for the required sputter deposition.
7) For example, in titanium depositions only argon gas inlet valve is open, for titanium nitride composition both argon and nitrogen gas inlet valve is open.
8) The important condition to check is during sputter deposition always makes sure that the sputter chamber pressure is always constant. The value should not drop or increase during the sputter deposition, if there is some change in the sputter pressure value then it means there is some issue with respect to gas flow in the chamber

9) There is a switch for rotating the substrate which is called ‘substrate rotation’ switch which can be used to rotate and select the required substrate for sputter deposition
10) Targets used in the sputtering system can be also selected using a knob. So, three different targets such as titanium, nickel chromium alloy and copper can be used for sputtering process.
11) Once the sputtering of required composition is completed. The power button is switched back to its original position in anti-clockwise direction and ‘H.T. Off’ button is switched on to complete the sputter deposition by discontinuing the plasma generation. [3]

Shutting down of sputtering system

1) The throttle plate is open and followed by closing both the ‘gas inlet’ and ‘hi-vacuum’ valve.
2) Open the ‘Vent’ valve and wait for about 20 minutes for the system to open the chamber, before that open the seals of the chamber.
3) Open foreline valve, switch off diffusion pump. Allow the system to run for about 30 minutes.
4) This time period is to make sure that the system is free of risk now, related to air or electrical supply issues.
5) Close the foreline valve
6) Switch off mechanical pump
7) Switch the sputtering main power off, followed by turning off cooling water and pressurized air
8) The main electricity power is finally switched off for complete shut off of the sputtering system. [3]

Periodic inspection of pumps and valves

The components used to measure inside the chamber is calibrated in general for air, if any other gas is used in the process, calibration needs to be done for that particular gas. To effect enhanced sputtering process, the following conditions must be considered

i) The oil used in the rotary and diffusion pump needs to be checked frequently and recommended level is maintained for better performance.
ii) The flow regulators right near to 5/3 air valve is needs to be adjusted for good opening and closing rate of valve. It is usually not more than 2 seconds, else it will forbid the air flow from actuator. The rings of valve ‘O’ should be replaced at frequent intervals to ensure safety of the equipment.
iii) The gauges need to be checked for particular set of calibration according to the gas used in the process, because penning gauge head is also used for measuring sputtering pressure. So the head of the gauge is more prone to contamination of insulator, which might result in very high pressure value

reading in the control unit. One should take extreme care while cleaning the insulator part. [3]

Needle valve and hoist

The gas which is allowed to flow inside the chamber which will be used for sputtering process is fed through needle valve. This needle valve is accompanied with micrometer adjustment with on/off valve, as the gas supply should be at constant pressure. The needle valve helps in regulating the throughput of gas flow in chamber. The rise in foreline (backing) pressure is measured using thermocouple gauge TC2, when the needle valve is open. However, care needs to be taken that the foreline pressure should not exceed 200 mtorr, which represents the critical pressure limit of foreline pressure. It is generally noted that at 200 mtorr, the pressure in the chamber will not exceed 10 mtorr. When you need finer adjustment in the chamber pressure value then needle valve is adjusted slightly to achieve the necessary pressure value for sputtering process. [3]

The hoist is the part which used to separate the steel cylinder chamber from the base of the control unit. This is used when there are some issues in the sputtering process, and the chamber needs to be lifted up from the base of the cylinder. This can be done by keeping the switch to service mode and then vent push button needs to be open, which will show the illuminating button on the hoist switch to glow which means the hoist can be lifted for further analysis. Once the power is completely shut down as per instruction given in the user manual appendix, one can analyze the equipment for issues. [3]

4.3 Sputter deposition experiments

In sputtering experiments, titanium (Ti) and titanium nitride (TiN_{1-x}) coatings is deposited by varying the deposition parameters. The substiochiometric compositions of titanium nitride compositions is denoted by TiN_{1-x}. The significant parameters which are used for controlling the sputtering deposition in this thesis work is given as follows 1) current/power values 2) sputtering total pressure 3) deposition time. So the coating of varying thickness is prepared by controlling the above mentioned parameters.

4.3.1 Sputtering power/current

The power value is increased to study the microstructural changes observed during depositing titanium nitride thin films. The other parameters such as total sputtering pressure, deposition time are kept constant during the experiments. When the current value is increased from 1.1 A to 1.5 A and increased further to 2 A, gradual increase in deposition rate is observed as shown in below graph 1. Increase in current value implies direct increase in power values as 390.5 W, 540 W and 760 W respectively. The constant values of other deposition parameters would be as follows 1) sputtering

pressure - 7 mtorr, 2) deposition time - 10 minutes. The deposition parameters used for titanium nitride film coating with increase in power value is given in Table 1.

Table 1. Deposition parameters used for Titanium nitride sputtering deposition with increase in power value for each samples mentioned below in table and other respective deposition parameters such as sputtering pressure (mtorr) and deposition time (mins) is kept constant.

Sample	Substrate	Total sputtering pressure (mtorr)	Current (A)	Voltage (V)	Power (W)	Coating type	Time (mins)
S024	Stainless steel	7	1.1	355	390.5	TiN	10
S025	Stainless steel	7	1.5	360	540	TiN	10
S026	Stainless steel	7	2	380	760	TiN	10

The deposition rate of titanium coating with copper substrate is analyzed respect to increase in current (power) values as shown below in table 2. The total sputtering pressure of 5 mtorr and deposition time of 10 minutes is kept constant for Ti deposition. When increased the current value from 1 A to 2 A, the power values increased respectively. The deposition parameters used for titanium thin film coating with increase in power value is given in Table 2.

Table 2. Deposition parameters used for Titanium sputtering deposition with increase in power value for each samples mentioned below in table and other respective deposition parameters such as sputtering pressure (mtorr) and deposition time (mins) is kept constant.

Sample	Substrate	Total sputtering pressure (mtorr)	Current (A)	Voltage (V)	Power (W)	Coating type	Time (mins)
S018	Copper	5	1	320	320	Ti	5
S019	Copper	5	2	340	680	Ti	5

4.3.2 Sputtering pressure

The sputtering pressure is increased from 6 to 8 mtorr and other parameters such as power used and deposition time is kept constant. The stainless steel samples S023, S026 and S034 were used for this set of experiments. The common parameters would be all these samples are as follows i) current – 2 A ii) power – 760 W and iii) deposition time – 10 minutes respectively. As the sputtering pressure is increased from 6 to 7 mtorr and to 8 mtorr, the changes observed during deposition are analyzed. The deposition parameters used for titanium nitride film coating with increase in sputtering pressure value is given in Table 3.

Table 3. Deposition parameters used for Titanium nitride sputtering deposition with increase in sputtering pressure from 6 mtorr to 7 mtorr and finally to 8 mtorr for below mentioned samples respectively and other respective deposition parameters such as power (W) and deposition time (mins) is kept constant.

Sample	Substrate	Total sputtering pressure (mtorr)	Current (A)	Voltage (V)	Power (W)	Coating type	Time (mins)
S023	Stainless Steel	6	2	380	760	TiN	10
S026	Stainless Steel	7	2	380	760	TiN	10
S034	Stainless Steel	8	2	380	760	TiN	10

The copper substrate is used for titanium deposition in this set of sputtering experiments. As sputtering pressure is increased from 5 mtorr to 10 mtorr and further increased to 20 mtorr, the changes observed in the thin film coating are investigated. The deposition parameters used for titanium film coating with increase in sputtering pressure value is given in Table 4.

Table 4. Deposition parameters used for Titanium sputtering deposition with increase in sputtering pressure value for each samples mentioned below in table and other respective deposition parameters such as sputtering pressure (mtorr) and deposition time (mins) is kept constant.

Sample	Substrate	Total sputtering pressure (mtorr)	Current (A)	Voltage (V)	Power (W)	Coating type	Time (mins)
S015	Copper	5	2	340	680	Ti	10
S043	Copper	10	2	280	560	Ti	10
S044	Copper	20	2	280	560	Ti	10

4.3.3 Sputtering deposition time

The deposition time plays an important role in finalizing the deposition parameters of any thin film coating. In this set of experiments, time of deposition were chosen as 5, 10 and 30 minutes for the stainless steel samples namely S026, S045 and S032. The other parameters for sputtering deposition is listed in the below table and it is kept constant during this experiments. The deposition parameters used for titanium nitride and titanium thin film coating with increase in deposition time is given in Table 5 and Table 6 respectively.

Table 5. Deposition parameters used for Titanium nitride sputtering deposition with increase in deposition time from 5 minutes to 10 minutes and then increased to 30 minutes for samples respectively, and other respective deposition parameters such as sputtering pressure (mtorr) and power (W) values is kept constant for the entire sputtering process.

Sample	Substrate	Total sputtering pressure (mtorr)	Current (A)	Voltage (V)	Power (W)	Coating type	Time (mins)
S029	Stainless steel	7	2	380	760	TiN	5
S045	Stainless steel	7	2	380	760	TiN	10
S032	Stainless steel	7	2	380	760	TiN	30

Table 6. Deposition parameters used for Titanium sputtering deposition with increase in deposition time from 3 minutes to 5 minutes, which is further increased to 10 minutes and increased to 30 minutes for samples mentioned below respectively, and other respective deposition parameters such as sputtering pressure (mtorr) and power (W) values is kept constant for the entire sputtering process.

Sample	Substrate	Total sputtering pressure (mtorr)	Current (A)	Voltage (V)	Power (W)	Coating type	Time (mins)
S031	Stainless steel	5	2	340	680	Ti	3
S019	Copper	5	2	340	680	Ti	5
S048	Stainless steel	5	2	340	680	Ti	10
S042	Copper	5	2	340	680	Ti	30

4.3.4 Substrate etching using RF sputtering

In this section, the substrates used in the deposition process is etched using RF sputtering process. The etching is done for 10 minutes with 100 W RF power applied to the process. The sputter etched samples specifically S055 and S056 is compared with samples S031 and S038 (the samples S031 and S038 are not sputter etched) to understand the effects of deposition and adhesion phenomenon observed in thin film sputtering deposition. The deposition parameters used for titanium and titanium nitride thin film coating with respect to sputter etching is provided in Table 7 and Table 8 respectively.

Table 7. Deposition parameters used for Titanium sputtering deposition with sputter etching applied to one sample in this case S055, and other deposition parameters such as sputtering pressure (mtorr), deposition time (mins) and power (W) values is kept constant for the entire sputtering process.

Sample	Substrate	Sample etching	Total sputtering pressure (mtorr)	Current (A)	Voltage (V)	Power (W)	Time (mins)
S031	Stainless steel	No	5	2	340	680	3
S055	Stainless steel	Yes	5	2	340	680	3

Table 8. Deposition parameters used for Titanium nitride sputtering deposition with sputter etching applied to one sample, in this case S056 and other deposition parameters such as sputtering pressure (mtorr), deposition time (mins) and power (W) values is kept constant for the sputtering deposition process.

Sample	Substrate	Sample etching	Total sputtering pressure (mtorr)	Current (A)	Voltage (V)	Power (W)	Time (mins)
S038	Stainless steel	No	7	2	380	760	10
S056	Stainless steel	Yes	7	2	380	760	10

4.4 Characterization techniques

This section comprises of different characterization techniques used for analyzing the properties of sputter deposited Ti and TiN_{1-x} coatings. The microstructure of the thin films produced will be analyzed by FESEM (Field Emission Scanning Electron Microscopy) and cross-sectional images of the coatings is acquired for analysis. From these FESEM micrographs, the thickness of the coating and the uniform distribution of Ti and TiN_{1-x} coatings over the substrate is studied in detail. The adhesion strength of the sputtered film is investigated using adhesion p.a.t.t.i experiments. It is relatively inexpensive equipment and one of the main advantages of using this equipment it is portable and results are reliable. Optical profilometer experiments are used to measure the surface topography of the thin film coating. It is also used to define the surface roughness, dimensions, surface images of 2D (2-dimensional) & 3D (3-dimensional) and thickness of the thin film. XRD (X-ray Diffraction) analysis is done to identify the phase structure of the sputtered thin film coatings deposited over the substrate. So XRD studies is also more important in thin film characterization.

4.4.1 FESEM

Field Emission Scanning Electron Microscopy (FESEM) equipment comprises of energy dispersive X-ray spectrometer (EDS), INCAx-act detector, detectors for secondary electron and in-lens secondary electrons, INCA energy 350 analyztor (Oxford instruments, UK). In TUT, Zeiss ULTRAplus ultra high resolution FESEM is being used for SEM measurements and it is manufactured from Carl Zeiss SMT AG, Germany. By using this ultra-series FESEM the microstructural and morphological features of Ti and TiN_{1-x} thin film coatings manufactured in this experiments. As discussed earlier in this report, both Ti and TiN_{1-x} thin film coatings is examined using FESEM, so that the correlation between the deposition rate and thickness of thin films is analyzed. The coated samples which is ready for FESEM is bended for analyzing the cross-section of coating thickness. The bending for copper samples is done manually using force as these substrates are thin in nature. The machine which is used to bend the SS substrate is known as brake. The substrates are bent carefully and in the meantime caution needs to be taken to avoid any damage to the coating or impurities attached to the surface during sample preparation. The reason for using bending machine is the thickness range for steel substrate used is around in between 1.5 to 2 mm. The bended samples are prone to cracking because of the applied force during bending. Once the bent sample is ready to be used, it is being glued to sample holders using carbon glue. The sample holders are studs which are used in the FESEM analysis. The samples are then kept in desiccator for a day, to remove any moisture content present in samples. The samples are then kept in vacuum chamber present in FESEM for analysis. Once the necessary vacuum is achieved, the sample is titled inside the chamber for cross-sectional measurement of coating thickness. Usually the sample is tilted at 45˚ and working distance between the sample and detectors should be around 5 mm. The surface images are magnified at 5000 and cross section image of the sample surface are magnified at 5000, 10000 and 50000. This SEM analysis uses electric field up to 10 KW range, also it uses secondary electron for image analysis. The microstructure and thickness of the thin film coatings is studied using FESEM analysis**.** From the thickness value and deposition time, the deposition rate is determined. [95] A typical example of ULTRAplus FESEM instrument is shown in Figure 30 [110].

Figure 30. Typical overall representation of ULTRAplus FESEM equipment used to analyze the cross-section images of thin films deposited in this sputtering experiments. [110]

4.4.2 Adhesion strength

Adhesion p.a.t.t.i is a type of adhesion tester used to determine the adhesion and bonding strength of deposited thin film coatings. In TUT, for determining the adhesion strength and to test the bond property of thin film coating 'Elcometer 110 Pneumatic Adhesion Tester' is used [111]. This equipment works on the principle where pneumatic force of measured quantity is applied to piston stub, and the stub is already attached to the coating by gluing [112]. The sample which needs to be investigated is glued to stub and it is kept cured for two to three days. Once stubs are attached firmly to the coating, the samples are attached to the pneumatically operated piston. The force is applied through the piston and the pressure value is noted from the equipment. If the coating failure is not observed then the force is increased further by small increment values, till the failure occurs. The corresponding pressure value is noted down and based on that the strength values are analyzed. The measurement is done for three different samples of same coating to achieve quantifiable results. [113] Thus, the adhesion strength of the thin film coatings and bonding strength between the coating and substrate material is determined. Figure 31 displays the general type of Elcometer which is used in this sputtered sample experiments to analyze adhesion strength. [111; 112; 114; 115]

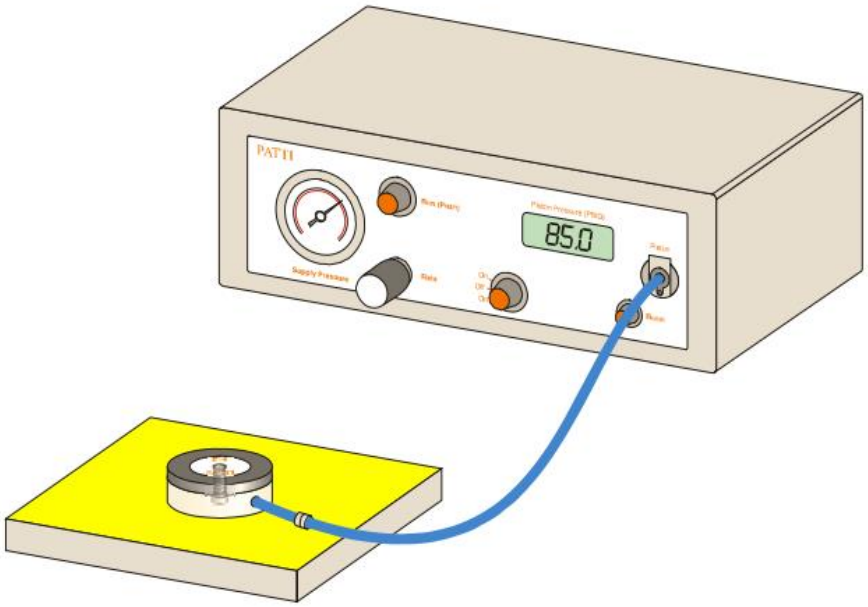

Figure 31. Schematic illustrations of typical Elcometer 110 Pneumatic Adhesion Tester which is used to examine the adhesion strength of the sputtered thin film samples. [115]

4.4.3 Optical profilometer

The investigation of surface topography of thin film coating is accomplished by Alicona InfiniteFocus G5 surface profile 3D optical profilometer at TUT [116]. The measurement made in this optical profilometer is fast, highly flexible and accurate. The image quality obtained is of higher optical resolution with good imaging capacity, results obtained are repeatable and more significantly 3D images can be obtained with real ease. The samples of required dimensions is cut using gluottine machine and is placed in the stage of the equipment. The stage is set such that optimum focus is achieved and there are encoders present in the equipment which makes sure movement of the stage is accurate. The optics can be adjusted according to the measurement requirement. The parameters such as brightness, contrast, light source, polarizer and stage coordinates are set for optimum image quality. Once required parameters are set, the measurement starts and the required optical images are acquired and saved for future analysis in the system database. Figure 32 a, represents the Alicona InfiniteFocus G5 optical profilometer used in TUT to analyze the surface roughness properties of thin film coatings. [116]

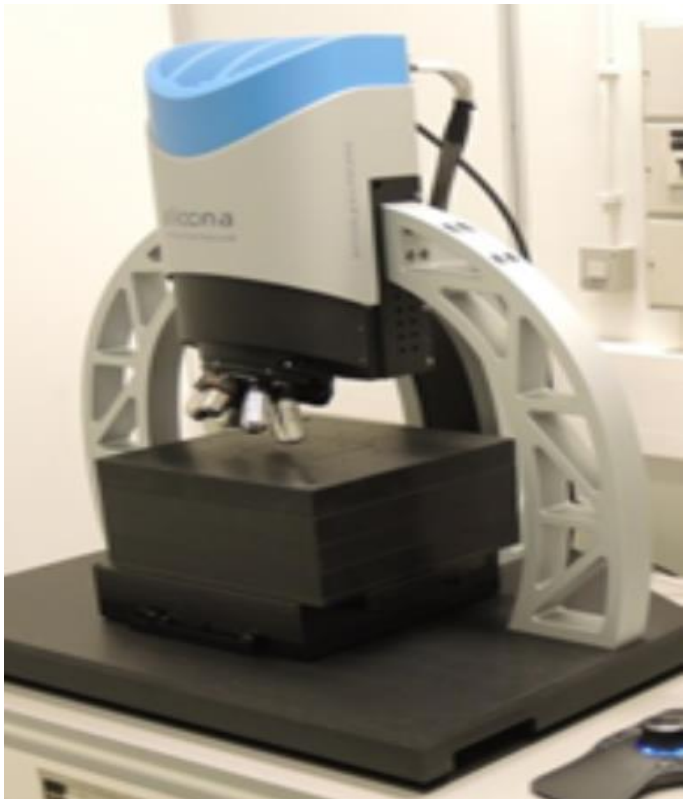

Figure 32 a. Typical representation of Alicona InfiniteFocus G5 3D optical profilometer which is used to measure the surface roughness profile of sputtered thin film coatings in this research work. [116]

4.4.4 X-ray Diffraction analysis

The chemical composition present in our thin films can be identified using 'Panalytical Empyrean Multipurpose Diffractometer' [117]. X-ray diffraction techniques is used to analyze phase identification of a material and can attain information about unit cell dimensions using Bragg's law. The principle is that when X-ray are used for measurement in crystal lattice, the penetrated X-ray travels through the crystal lattice and it gets reflects from the atoms present in lattice and travels back to the surface. The distance travelled by the X-ray and the angle at which the penetration occurs is used to calculated the phase present in the crystal material. The qualitative and quantitative investigation of phase composition is carried out by this XRD [117; 118]. This diffractometer can also be used to measure the stress present in the thin film deposited and texture of the films created [117]. The identification of phases present in films is examined by incidence angle of copper radiation (Cu-Kα). The grazing angle of incidence used is of major importance as dealing with nanometer thin films is highly critical, so the incidence angle is chosen in such a way that it would not affect the phase composition results. The normal range of incidence angle would be 0.2 to 2.0˚. The 2-theta angle used for the XRD investigation is 20-80˚. Panalytical X'Pert High Score Plus software is used for analyzing the phase composition of thin films deposited. The

arrangement of beam from the grazing incidence angle is parallel to incident beam of goebel mirror and in the diffracted beam ‘monochromator and collimator’ is used for data analysis. [95; 117; 118] Figure 32 b, represents the ‘Panalytical Empyrean Multipurpose Diffractometer’ used in the XRD analysis at TUT.

Figure 32 b. General schematic illustration of Panalytical Empyrean Multipurpose Diffractometer equipment, which is used to analyze the XRD pattern of deposited thin films. [117]

5. RESULTS

The results of thin film coatings deposited by DC magnetron sputtering process are discussed in the following sections. In this research work, the deposition parameters influence on the following properties such as crystallinity, adhesion and surface roughness are studied in detail. The section proceeds further by including characterization results of FESEM analysis, adhesion strength, optical profilometer and XRD analysis for investigating the morphological changes observed in thin films deposited by DC magnetron sputtering process.

5.1 Magnetron sputtered titanium coatings

The titanium coatings deposited by magnetron sputtering over copper and stainless steel substrates is analyzed in this section. The microstructures, composition and optical property of thin film titanium coatings are presented in the following subdivision in detail. The modifications observed in thin film coating microstructure are investigated using FESEM analysis. The surface roughness property changes of titanium thin film coatings are studied using optical profilometer measurements. The composition obtained during thin film deposition is analyzed using XRD analysis.

5.1.1 Microstructures

The magnetron sputtered titanium thin film coatings microstructures prepared over different substrates are discussed in this section. The deposition parameters play an important role in determining the final microstructural property of deposited thin films. The crack observed in thin film coating is because of the sample preparation in which the samples are bent to analyze morphological properties of thin films deposited. The significant changes observed during these titanium depositions are noted for interpretations alongside respective micrographs supporting the case. The titanium coatings deposited over copper substrates is taken into consideration for better understanding. The deposition of titanium coatings is done for 10 minutes with increasing the power from 1 to 2 A respectively. From Figures 33 and 34, the respective micrographs represent columnar microstructures which are dense in nature and there is no porosity present in the surface. The sample S012 micrographs is represented in Figure 33 followed by Figure 34 which represents FESEM images of sample S015.

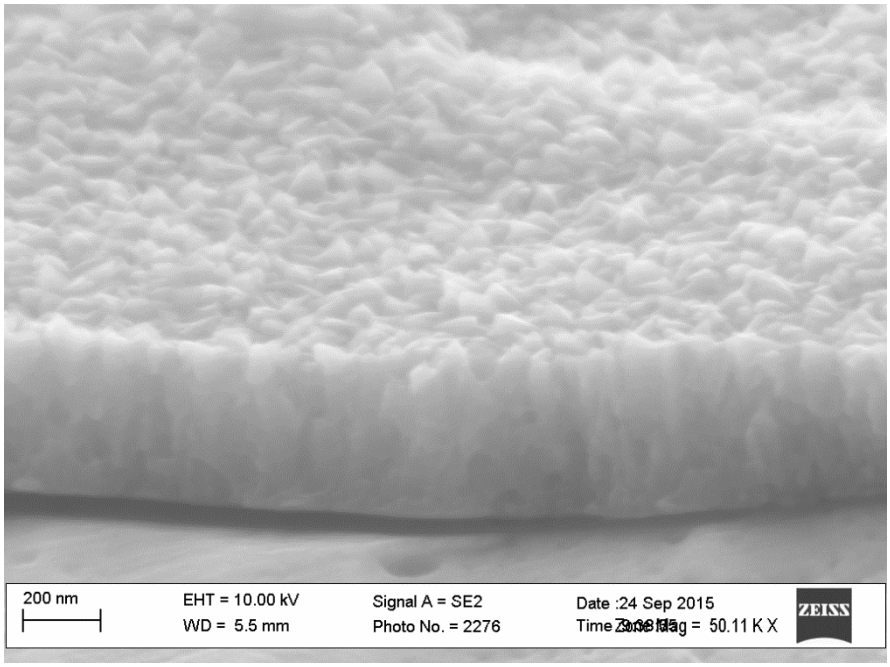

Figure 33. FESEM images of microstructure of sputtered Ti coatings on copper (S012), the coatings exhibited dense, uniform columnar microstructure with coarser surface morphology. The deposition parameters used for this sputtering are as follows current – 1 A, deposition time -10 minutes, sputtering pressure - 5 mtorr.

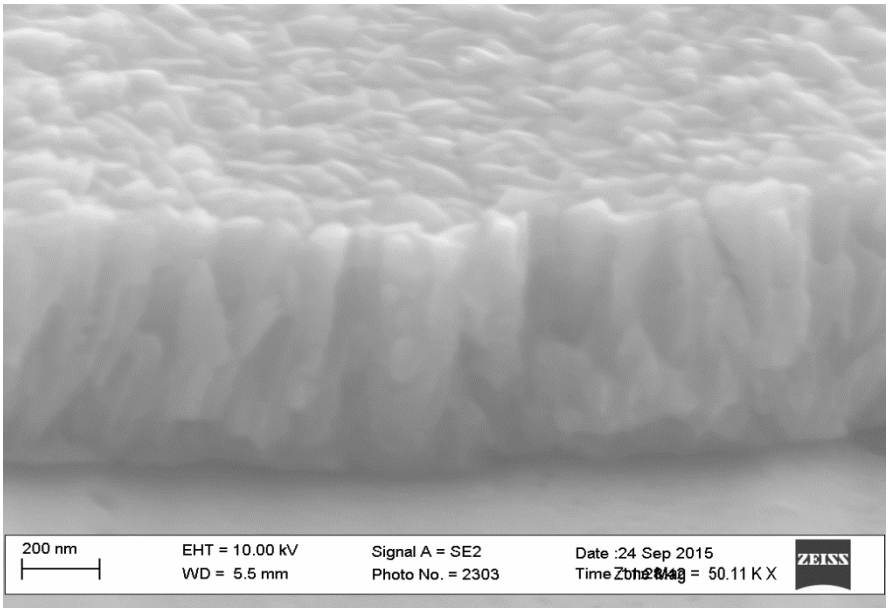

Figure 34. FESEM images of microstructure of sputtered Ti coatings on copper (S015), the coatings exhibited dense, uniform columnar microstructure only slightly exhibiting coarse surface morphology. The deposition parameters used for this sputtering are as follows current – 2 A, deposition time - 10 minutes, sputtering pressure – 5 mtorr.

The deposition time of five minutes is considered and the corresponding changes observed in thin film coatings are analyzed in this section. The fused columnar microstructure is predominant in these samples namely S018 and S019. The power value is increased from 1 to 2 A with constant 1 A as increment value. The microstructures of these thin film coatings are well-bonded structures which are uniform, dense in nature with no porosity present in it. The Figures 35 and 36 presented below represents the copper samples S018 and S019 correspondingly, and the current used for this titanium deposition is 1 and 2 A respectively.

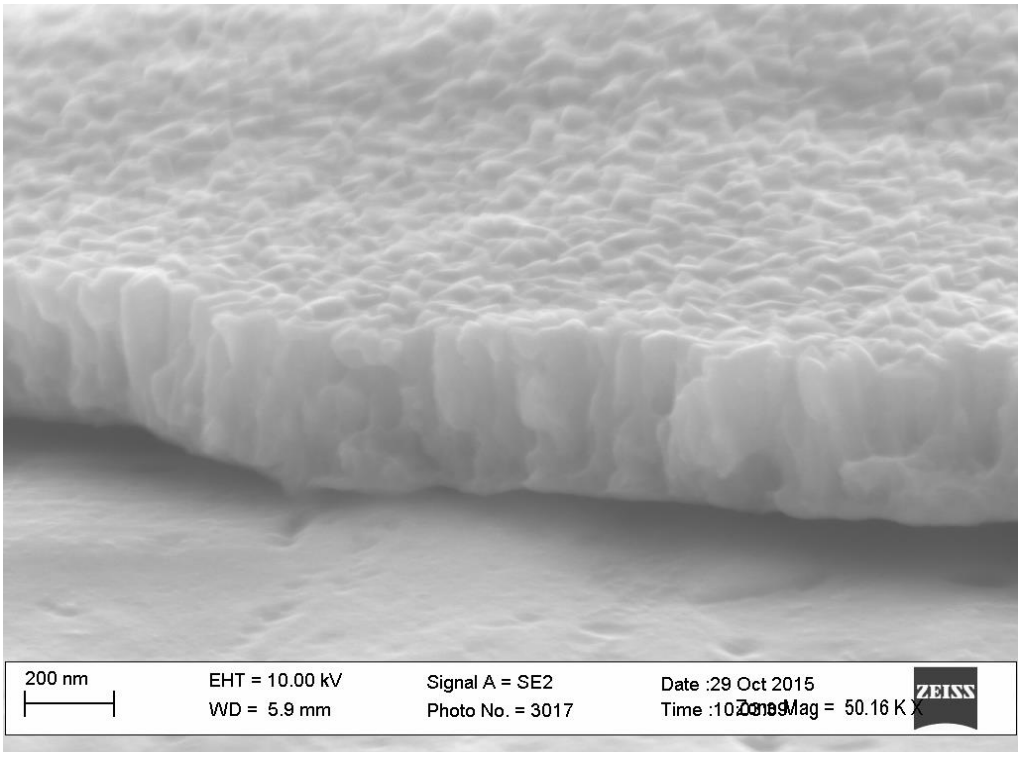

Figure 35. FESEM images of microstructure of sputtered Ti coatings on copper (S018), the coatings exhibited dense, well bonded, non-porous, uniform columnar microstructure with coarser surface morphology. The deposition parameters used for this sputtering are as follows current – 1 A, deposition time – 5 minutes, sputtering pressure – 5 mtorr.

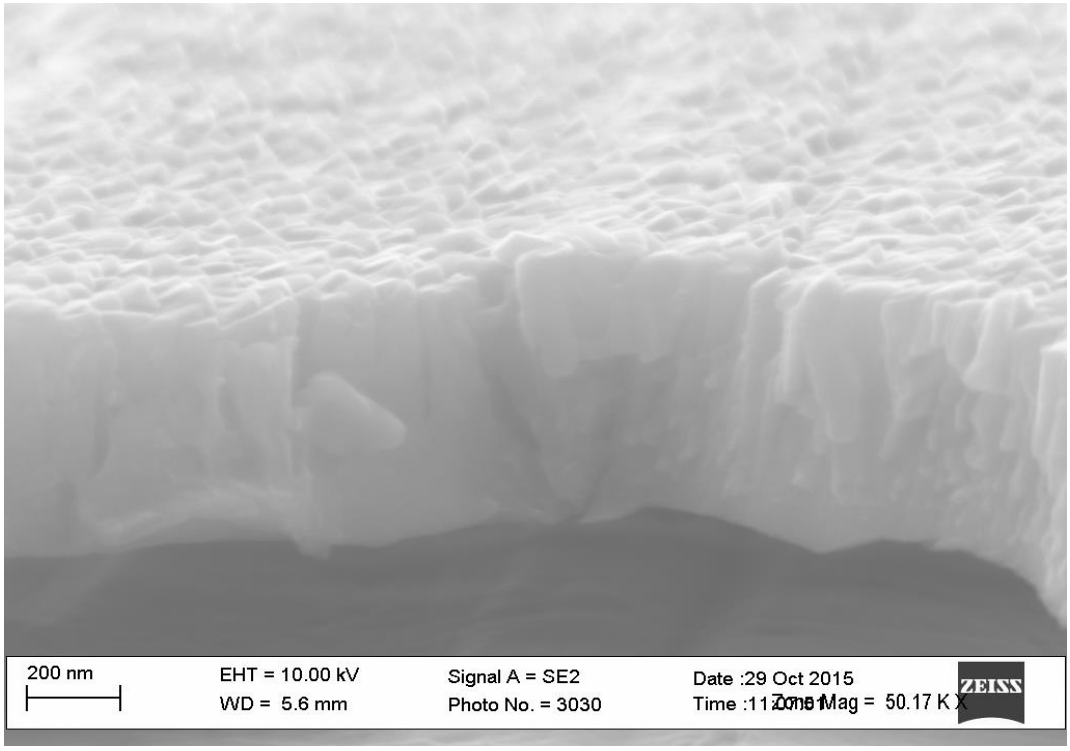

Figure 36. FESEM images of microstructure of sputtered Ti coatings on copper (S019), the coatings exhibited well bonded, nonporous, dense, uniform columnar microstructure with coarser surface morphology. The deposition parameters used for this sputtering are as follows current – 2 A, deposition time - 5 minutes, sputtering pressure – 5 mtorr.

The microstructure changes for the following samples S043 and S044 is analyzed in this section. The titanium thin film coating is deposited over copper substrates with high sputtering pressure is evaluated. The sputtering pressure used for these above mentioned samples are 10 and 20 mtorr respectively. The other important deposition parameters used for this deposition are as follows, deposition time - 10 minutes, current – 2 A. The morphological changes observed in S043 is the columnar grains which are dense in nature, grains are non-uniform, however the surface of the grains are coarser in nature with needle like grains thus representing coarser surface. Figures 37 and 38 represents the cross-sectional micrographs of titanium thin film deposition for samples S043 and S044 respectively. The micrograph from Figure 38 clearly represents the columnar microstructure, which is needle-shaped, flake-like, coarse, thick grains in nature. The columnar growth is non-uniform and the direction of grain growth is random in nature.

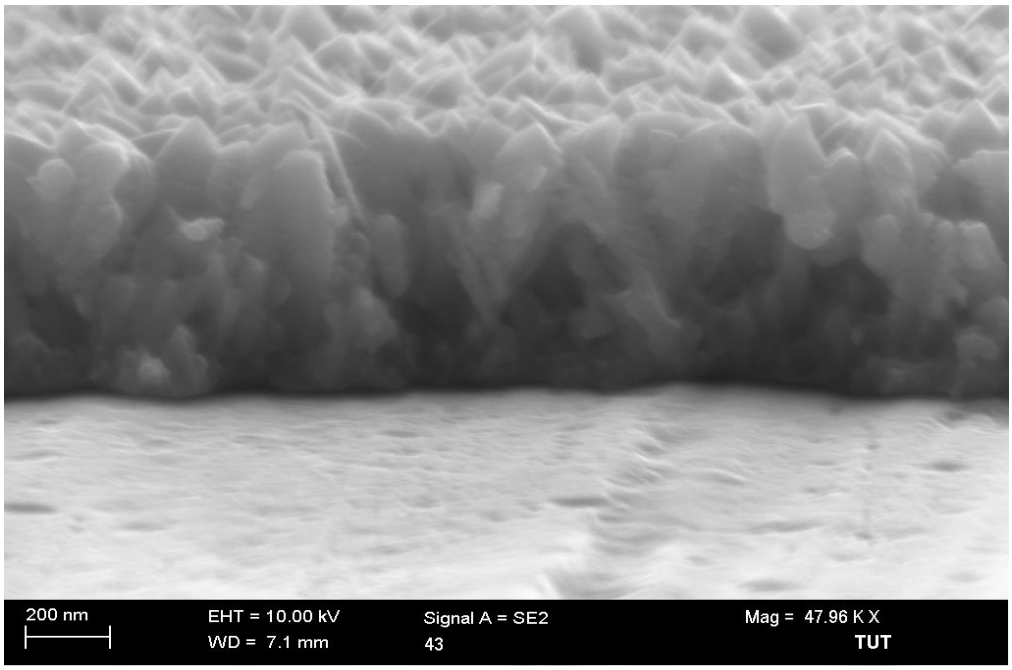

Figure 37. FESEM images of microstructure of sputtered Ti coatings on copper (S043), the coatings exhibited dense, non-uniform columnar microstructure with coarser surface. The deposition parameters used for this sputtering are as follows current - 2 A, deposition time - 10 minutes, sputtering pressure - 10 mtorr.

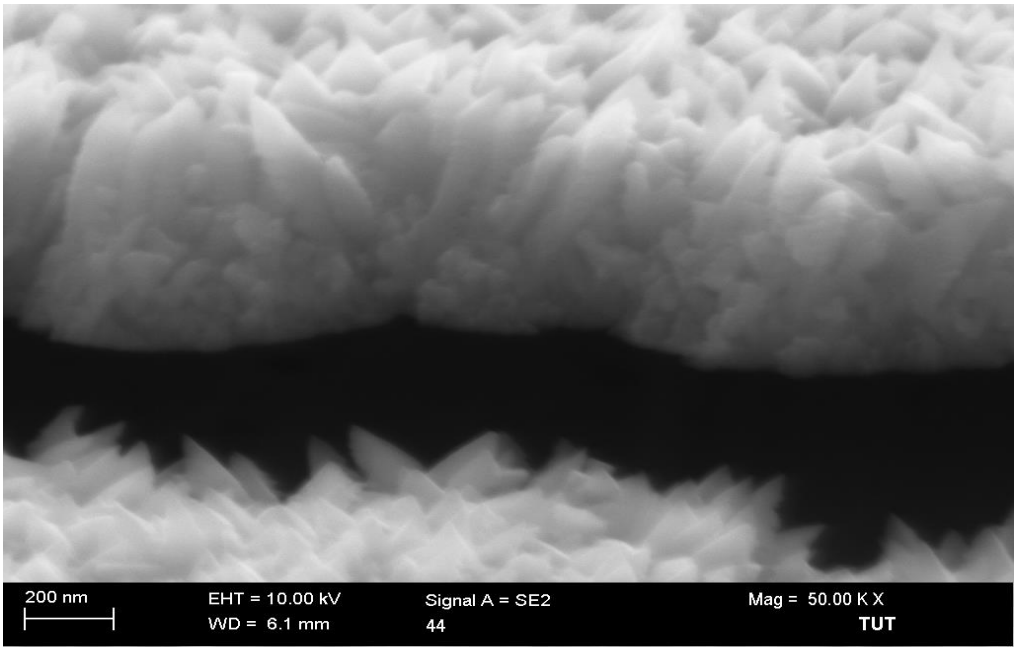

Figure 38. FESEM images of microstructure of sputtered Ti coatings on copper (S044), the coatings exhibited dense, non-uniform, needle like columnar microstructure, grains are randomly oriented with coarser surface morphology. The deposition parameters used for this sputtering are as follows current – 2 A, deposition time - 10 minutes, sputtering pressure – 20 mtorr.

The microstructure of sample S042 is of major importance as the deposition time of 30 minutes is used. The growth of the columnar grains is slightly inclined towards an angle. The other interesting properties of columnar microstructure in this film growth are well-bonded dense microstructure, coarser grain surface and uniform in nature. Figure 39 represents the microstructure of titanium thin film sample S042.

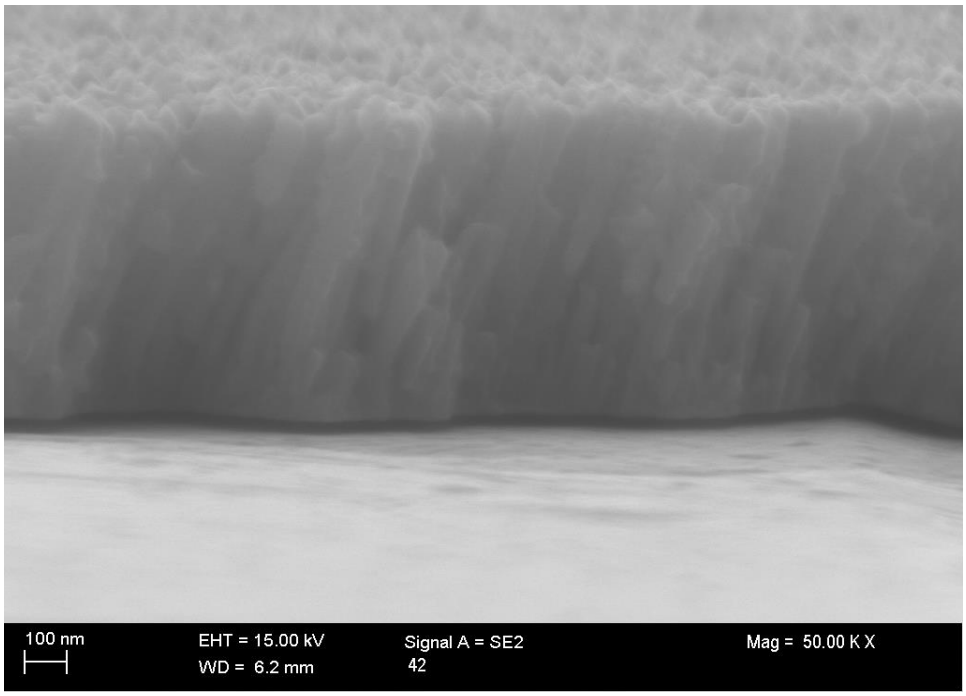

Figure 39. FESEM images of microstructure of sputtered Ti coatings on copper (S042), the coatings exhibited dense, uniform columnar microstructure, slightly inclined columnar grains is observed with coarser surface morphology. The deposition parameters used for this sputtering are as follows current – 2 A, deposition time - 30 minutes, sputtering pressure - 5 mtorr.

The samples S030 and S031 are taken into consideration in this section. These samples use stainless steel as substrate materials and the current is increased from 1 A to 2 A for the sample S030 and S031 respectively. The sample S030 and S031 represents similar thin columnar structures which are dense, fused and uniform in nature. Figure 40 represents the micrographs of S031.

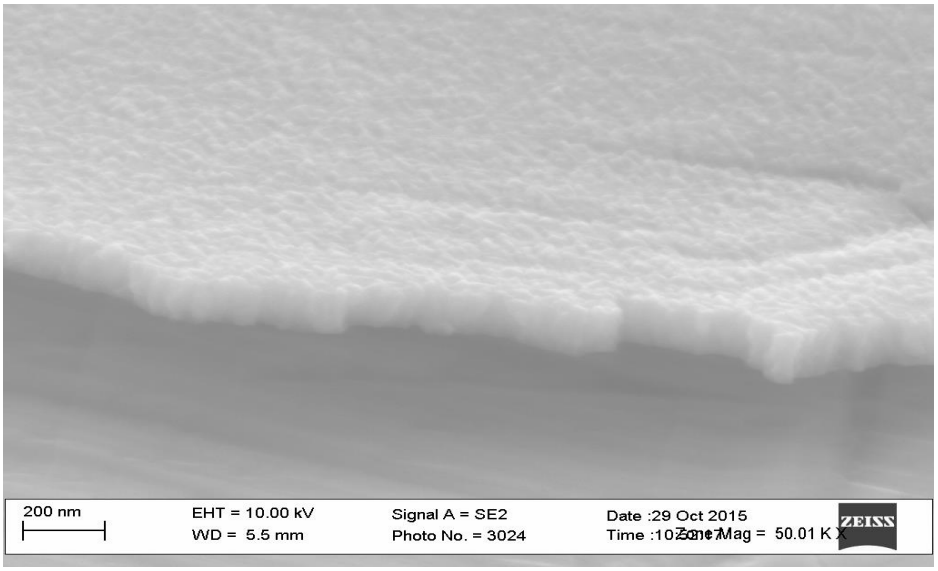

Figure 40. FESEM images of microstructure of sputtered Ti coatings on stainless steel (S031), the coatings exhibited dense, uniform columnar microstructure with relatively smooth surface morphology. The deposition parameters used for this sputtering are as follows current – 2 A, deposition time - 3 minutes, sputtering pressure – 5 mtorr.

The next set of samples which are considered for investigation are S048 and S049. The resultant microstructures of both the samples are similar in nature which is well bonded dense columnar microstructure. Figure 41 represents the FESEM micrographs of sample S048.

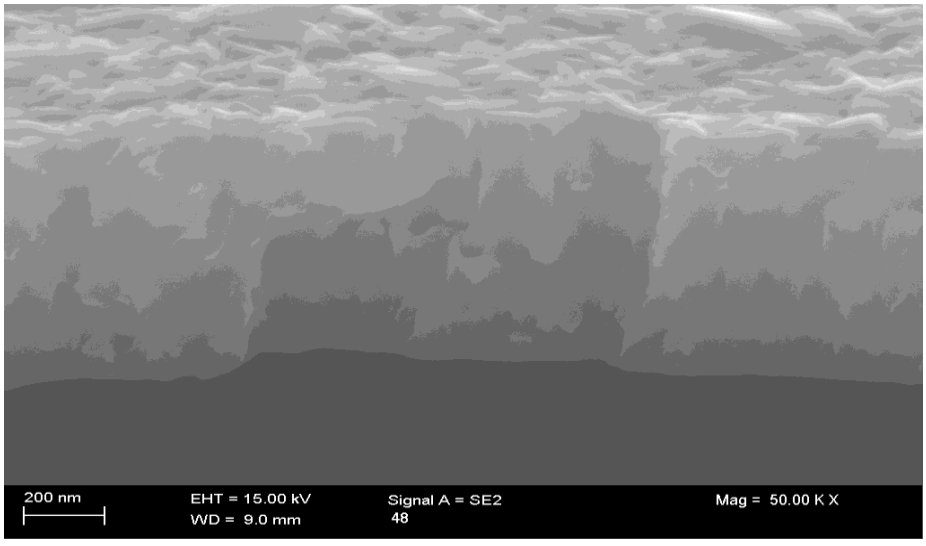

Figure 41. FESEM images of microstructure of sputtered Ti coatings on stainless steel (S048), the coatings exhibited dense, well-bonded, thick, uniform columnar microstructure with slightly smoother surface morphology. The deposition parameters used for this sputtering are as follows current – 2 A, deposition time – 10 minutes, sputtering pressure – 5 mtorr.

The sample S055 is etched with argon plasma and titanium thin film deposited using sputtering process is analyzed using FESEM. The crystal morphology of S055 is fully dense well bonded columnar microstructure as shown in Figure 42.

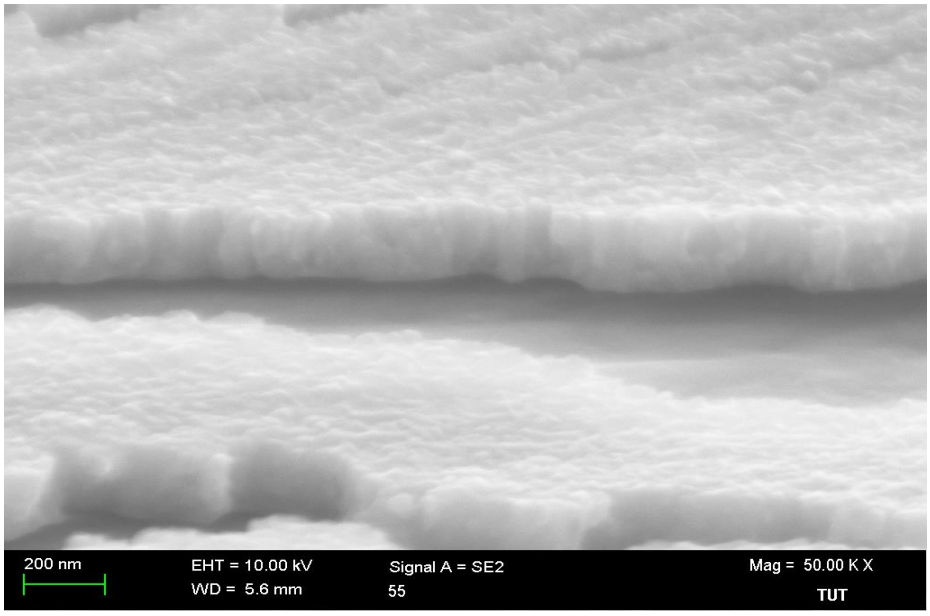

Figure 42. FESEM images of microstructure of sputtered Ti coatings on stainless steel (S012), the coatings exhibited dense, uniform columnar microstructure with smooth surface morphology. The deposition parameters used for this sputtering are as follows current – 2 A, deposition time - 3 minutes, sputtering pressure – 5 mtorr.

The stainless steel substrate is heated for 30 minutes for S039 and titanium thin film is deposited. From FESEM images, it is clear that the well bonded columnar grains are dense and it is uniform. Figure 43 represents the sample S039 with titanium deposition prior to the deposition substrate heating is accomplished. The sputtering experiments data for thin film titanium coatings is summarized in Table 9.

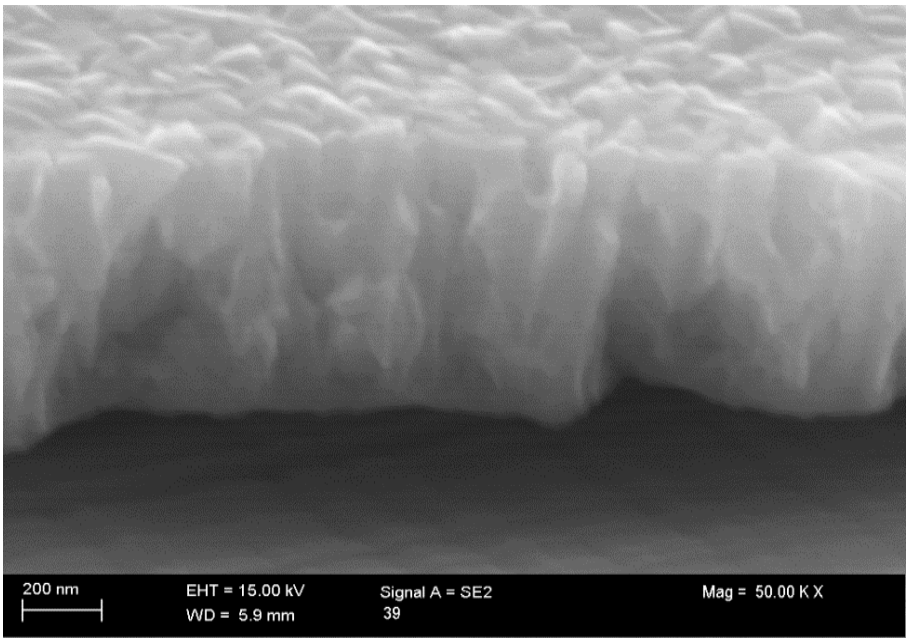

Figure 43. FESEM images of microstructure of sputtered Ti coatings on stainless steel (S039), the coatings exhibited dense, well bonded, uniform columnar microstructure with smooth surface morphology. The deposition parameters used for this sputtering are as follows current – 2 A, deposition time - 10 minutes, sputtering pressure – 5 mtorr.

Table 9. Summarizes the data of sputtering sample used for Titanium sputtering deposition and its respective deposition parameters, resultant thickness value and its corresponding deposition rate value used in section 5.1. The symbols which are used in Table 9 are given as follows current (I), voltage (U) and deposition rate (Dep. rate).

Sample	Substrate	Ar Pressure (mtorr)	I (A)	U (V)	Power (W)	Thickness (nm)	Time (mins)	Dep. rate (nm/min)
S012	Copper	5	1	320	320	440	10	44
S015	Copper	5	2	340	680	730	10	73
S018	Copper	5	1	320	320	375	5	75
S019	Copper	5	2	340	680	600	5	120
S030	Stainless steel	5	1.2	320	384	80	3	27
S031	Stainless steel	5	2	340	680	140	3	47
S042	Copper	5	2	340	680	765	30	26
S043	Copper	10	2	300	600	725	10	73
S044	Copper	20	2	280	560	470	10	47
S048	Stainless steel	5	2	340	680	780	10	78
S049	Stainless steel	5	2	340	680	355	5	71
S055	Stainless steel	5	2	340	680	200	3	67
S039	Stainless steel	5	2	340	680	705	10	71

5.1.2 Phase structure

From XRD analysis of thin film coating the crystallographic orientation of the resultant phase is obtained. The samples which were taken into consideration are S031 (Ti). The substrates which are used for thin film deposition were stainless steel. The data analysis from XRD represents that the crystal system of thin film sputtered titanium coating deposited is hexagonal. The preferred orientation of titanium is observed in the XRD pattern and titanium phase obtained during sputtering deposition is generally α-Ti (alpha-titanium) which is the stable form of titanium. The high intensity of peak is detected at 2θ (theta)= 37.777 degree (˚) and preferred crystal orientation is observed at (0 0 2) crystal plane. The other notable crystal orientation is observed at 2θ = 34.955˚, 69.635˚ and the respective crystal orientation is at following crystal planes (1 0 0) and (1 0 3) [119]. The substrate used in this deposition is stainless steel (316L) and the

peaks observed are due to the austenite (γ-Fe) phase of the stainless steel used. The γ-Fe is observed at 2θ = 43.038˚, 50.375˚, 74.679˚, 90.998˚. The crystal system of the stainless steel used is cubic in nature and the major composition present in steel are iron and nickel, these compositions are matching the resultant XRD pattern as shown in Figure 44 a. The reference pattern used for this titanium XRD analyses is 04-008-4973.

The stainless steel, austenite (γ-Fe) phase is observed in crystal planes (1 1 1) and (2 0 0) as described in various research articles. [120; 121] XRD pattern of sputtered titanium coating sample S031 is illustrated below in Figure 44 a.

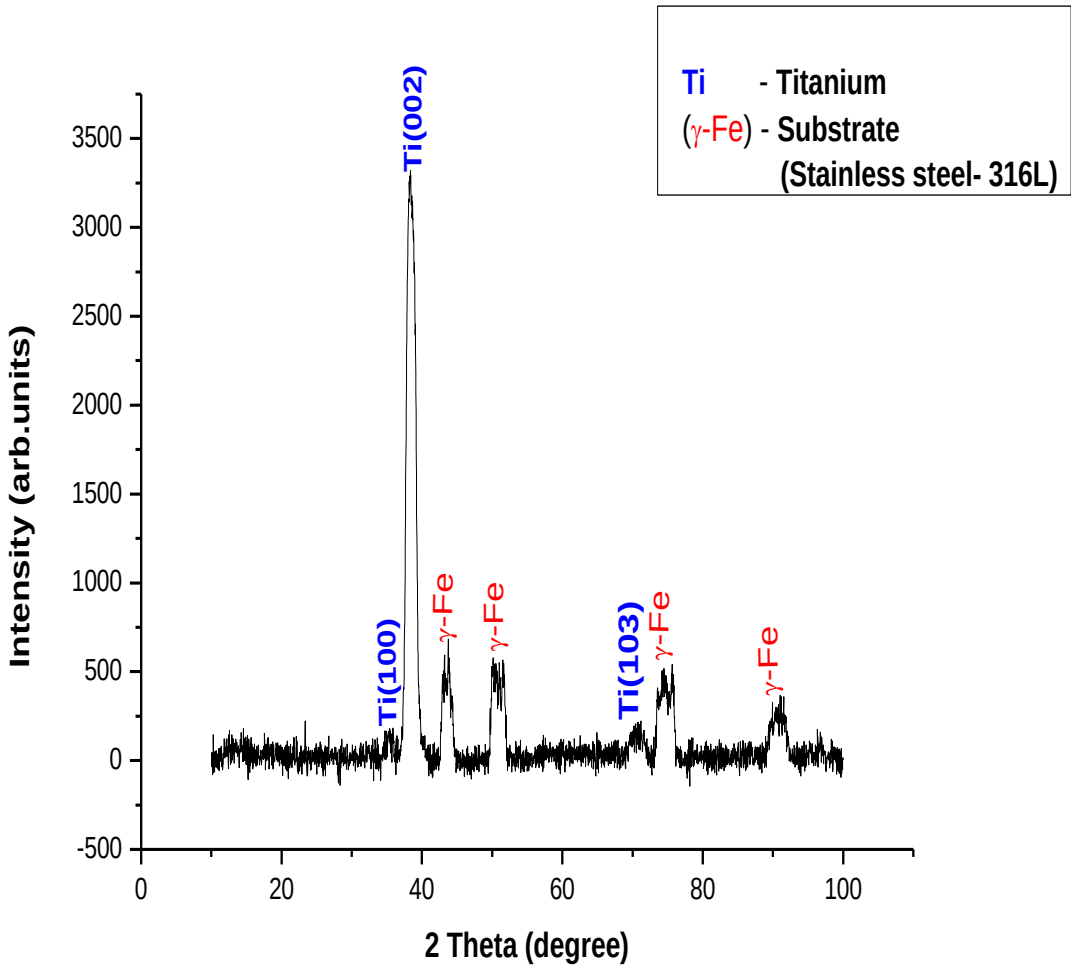

Figure 44 a. XRD pattern of sputtered Titanium coating of S031 which representing different phases of titanium (Ti) and stainless steel substrate (γ-Fe) is shown in this Figure.

The resultant peak from XRD analysis shows that sample S031 typically match with element titanium reference composition. This can be proven by the XRD peak which is in range with the stick pattern as shown in below Figure 44 b. The observed peaks from S031 XRD analysis are denoted in red color, while the peaks from substrate is marked

in blue color and reference titanium peaks is marked in green color. The stick pattern of the XRD analysis is present in Figure 44 b, which will give the clear idea about the XRD pattern for better understanding.

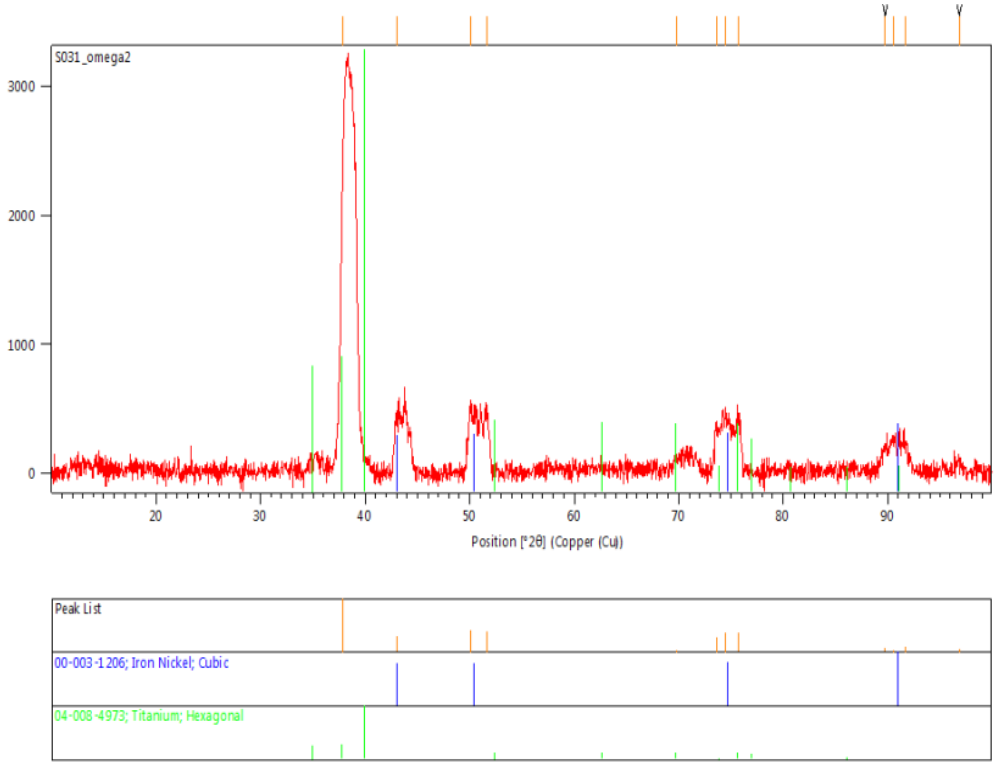

Figure 44 b. XRD pattern of sputtered Titanium S031 which representing peaks matching with the reference stick pattern as shown in this Figure.

5.1.3 Adhesion strength

The adhesion strength of titanium coatings is analyzed in this section. The samples which were considered into consideration for this analysis are S030 and S031. The substrates used for this deposition is stainless steel, the current value is increased from 1.2 A to 2 A to measure the difference in the measured adhesion property. The other deposition parameters such as sputtering pressure 5 mtorr and deposition time - 3 minutes is kept constant during both the deposition. The value of adhesion is measured using adhesion P.A.T.T.I instrument. The measured adhesion value of S030 is 0.8 MPa, while S031 resultant adhesion value is approximately 1.3 MPa. So in comparison, the adhesion strength of sample S031 is relatively better than S030. Figure 45 represents the images of the measured sample which were used for adhesion value measurement for adhesion strength. From the below Figures, it is clearly understood the both thin film coatings are adhered completely to aluminum stub rather than the surface of the sample. The sample S055 is sputter etched by argon plasma and adhesion strength is measured after titanium coating depositions. The resultant adhesion value from measurement represents 3.2 MPa. Figures 46 represents the image of the measured sample which

were used for adhesion value measurement. Table 10 provides the data list of deposition parameters for sputtered titanium coatings with properties such as adhesion strength and surface roughness value.

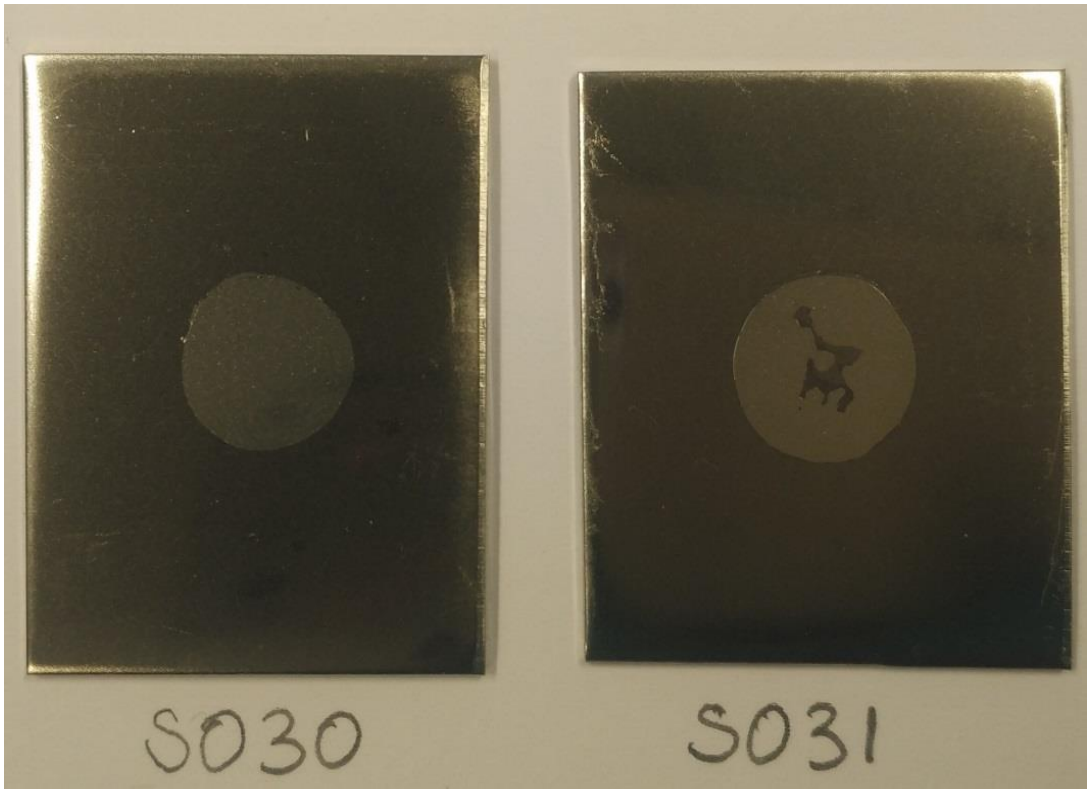

Figure 45. Adhesion tested surface of sputtered titanium coating using adhesion p.a.t.t.i equipment is presented in this Figure. The samples which were used for testing are S030 and S031. The deposition parameters used for S030 are as follows current - 1.2 A, deposition time - 3 minutes, sputtering pressure – 5 mtorr and parameters used for S031 are current – 2 A, deposition time – 3 minutes, sputtering pressure – 5 mtorr.

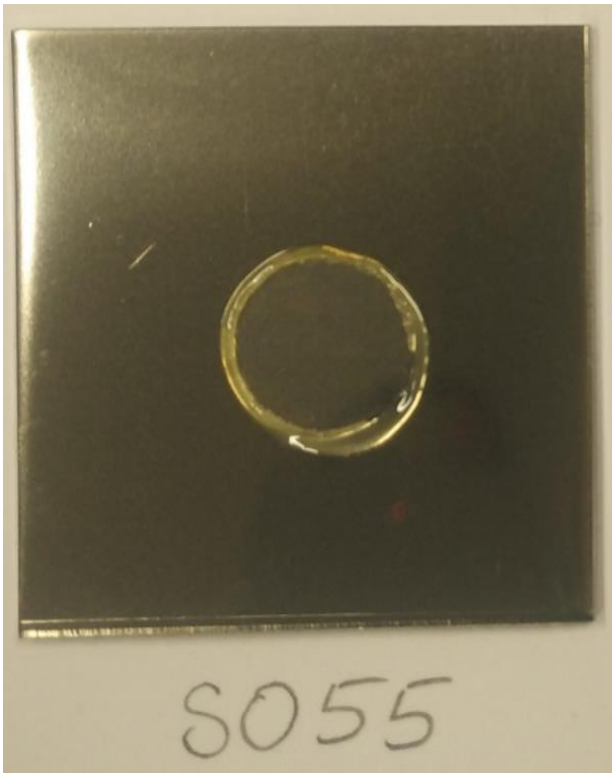

Figure 46. Adhesion tested surface of sputtered titanium coating using adhesion p.a.t.t.i equipment is presented in this Figure. The sample S055 used for adhesion test are sputter etched for 10 minutes with 100W RF power. The deposition parameters used for S055 is given as follows current – 2 A, deposition time - 3 minutes, sputtering pressure – 5 mtorr**.**

Table 10. Provides the data for sputtering sample which are used for Titanium sputtering deposition and its respective deposition parameters and resultant thickness value used in section 5.1.3 – 5.1.4. The following samples S030 and S031 were used to study the surface coating properties such as adhesion strength and surface roughness (Ra).

Sample	**Ar pressure (mtorr)**	**I (A)**	**U (V)**	**Power (W)**	**Time (mins)**	**Thickness (nm)**	**Adhesion strength (MPa)**	**Ra (nm)**
S030	5	1.2	320	384	3	80	0.8	349
S031	5	2	340	680	3	140	1.3	251
S055	5	2	340	680	3	200	3.2	-

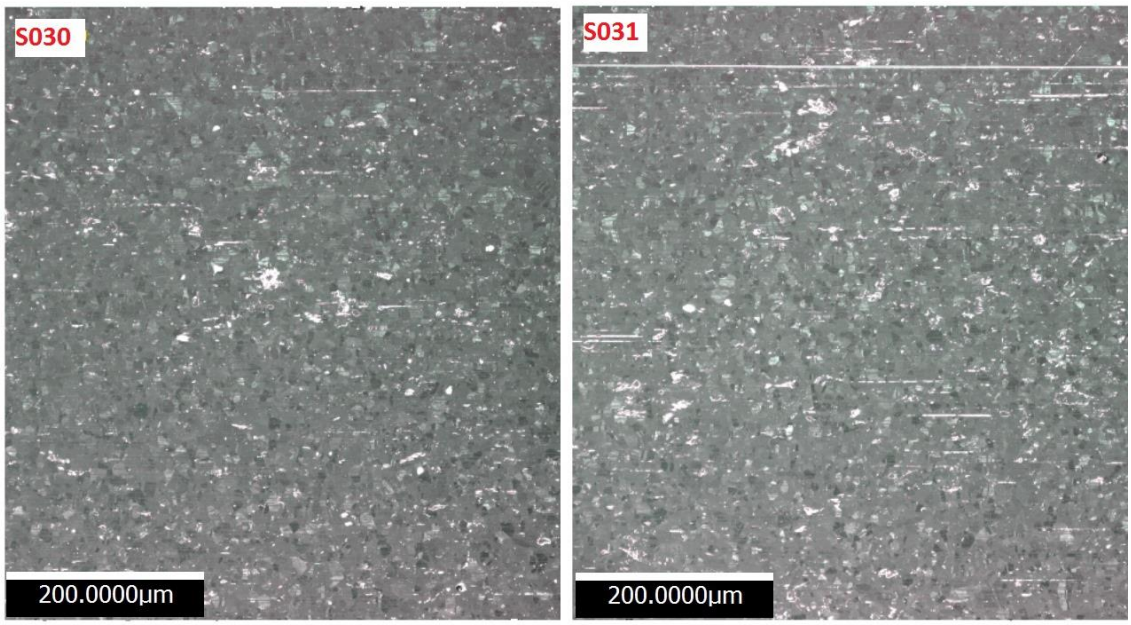

Figure 47. Surface roughness profile of sputtered titanium sample is represented in this Figure and the roughness profile value is accomplished by optical profilometer. The titanium samples which were used for testing are S030 and S031 respectively. The deposition parameters used for S030 are as follows current - 1.2 A, deposition time - 3 minutes, sputtering pressure – 5 mtorr and parameters used for S031 are current - 2 A, deposition time - 3 minutes, sputtering pressure – 5 mtorr.

5.1.4 Surface roughness

The surface roughness of titanium coating is measured using Alicona optical profilometer. The samples S030 and S031 are chosen for better analysis of surface roughness property of deposited titanium coating. The deposition parameters such as sputtering pressure - 5 mtorr, deposition time - 3 minutes is kept constant, however the current value is increased from 1 A to 2 A for samples S030 and S031 respectively. The measured surface roughness value is represented in nm scale. The measured surface roughness value of S030 and S031 are 349 nm and 251 nm respectively. Figure 47 represents the optical profilometer images of the measured sample S030 and S031. The sample name in the Figure is mentioned in the top right corner of the image.

5.2 Magnetron sputtered titanium nitride coatings

The magnetron sputtered titanium nitride thin film coatings is analyzed in detail in the following sections. The substrates explicitly copper and stainless steel were used for the thin film deposition of titanium nitride composition. The microstructural modification of deposited thin film is analyzed using FESEM analysis, adhesion test, optical profilometer and XRD analysis.

5.2.1 Microstructures

The titanium nitride thin film coating microstructure is studied in this division. The samples S013 and S014 is considered for this analysis. The deposition parameters used for these samples are as follows sputtering pressure - 6 mtorr, deposition time – 10 minutes, whereas the current value is increased from 1 A to 2 A respectively for the samples considered. The microstructures observed for both the samples are uniform dense columnar microstructure with coarser grains surface. Figures 48 and 49 represents the cross-sectional micrographs of titanium nitride thin film deposition for samples S013 and S014 respectively. The columnar grains present in the microstructure is dense, well bonded, uniform in nature.

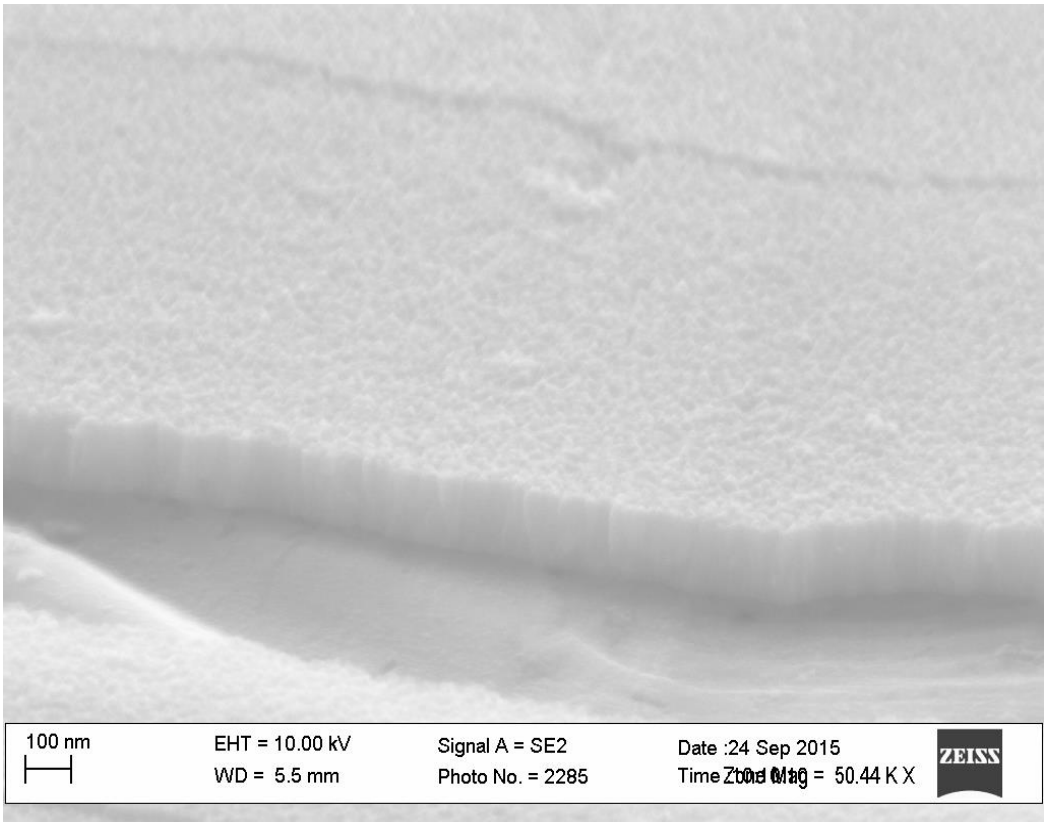

Figure 48. FESEM images representing microstructure of sputtered TiN coatings on copper (S013), the coatings exhibited dense, well bonded, uniform columnar microstructure with smooth surface morphology. The deposition parameters used for this sputtering experiment are as follows current – 1 A, deposition time – 10 minutes, argon sputtering pressure – 5 mtorr, nitrogen sputtering pressure – 1 mtorr.

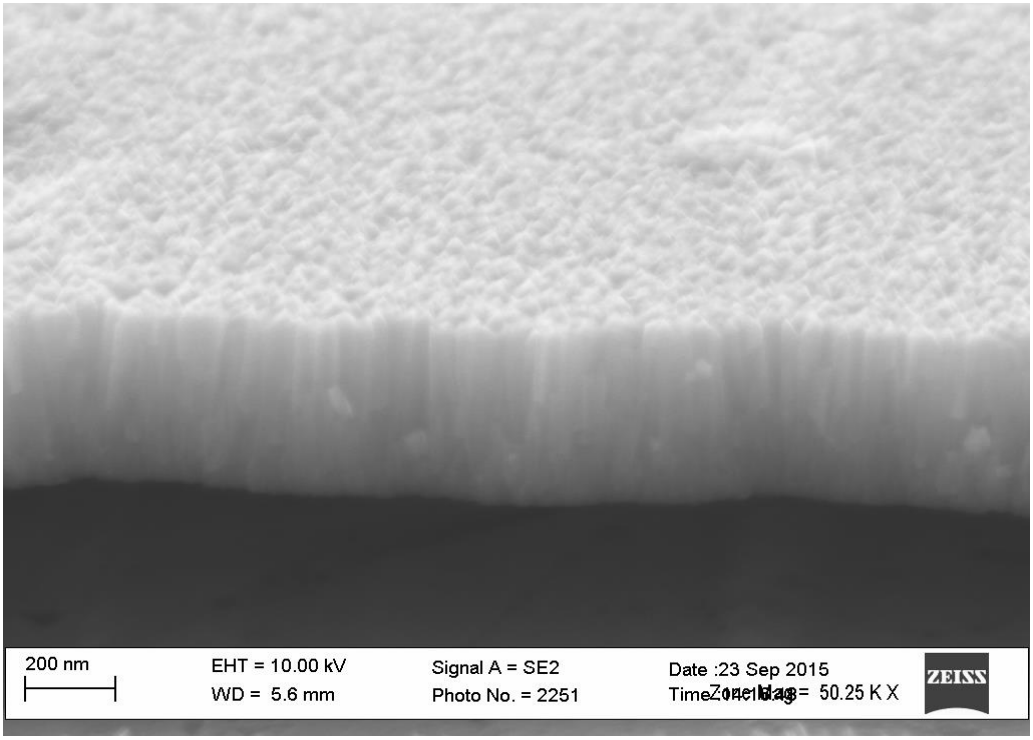

Figure 49. FESEM images representing microstructure of sputtered TiN coatings on copper (S014), the coatings exhibited dense, well bonded, uniform columnar microstructure with sharp edge surface morphology. The deposition parameters used for this sputtering experiments are as follows current – 2 A, deposition time - 10 minutes, argon sputtering pressure – 5 mtorr, nitrogen sputtering pressure – 1 mtorr.

The samples S016 and S017 is observed for microstructural variations by increasing the sputtering pressure to 7 mtorr. The current used for the sputtering deposition is 6 A and 7 A respectively and deposition time used is 10 minutes. From the micrograph observation it is clear that both these samples microstructure is well-bonded columnar structure which are dense in nature. The substrates used for these samples S016 and S017 is copper. The Figure 50 and 51 shown below represents the SEM images for samples S016 and S017 respectively.

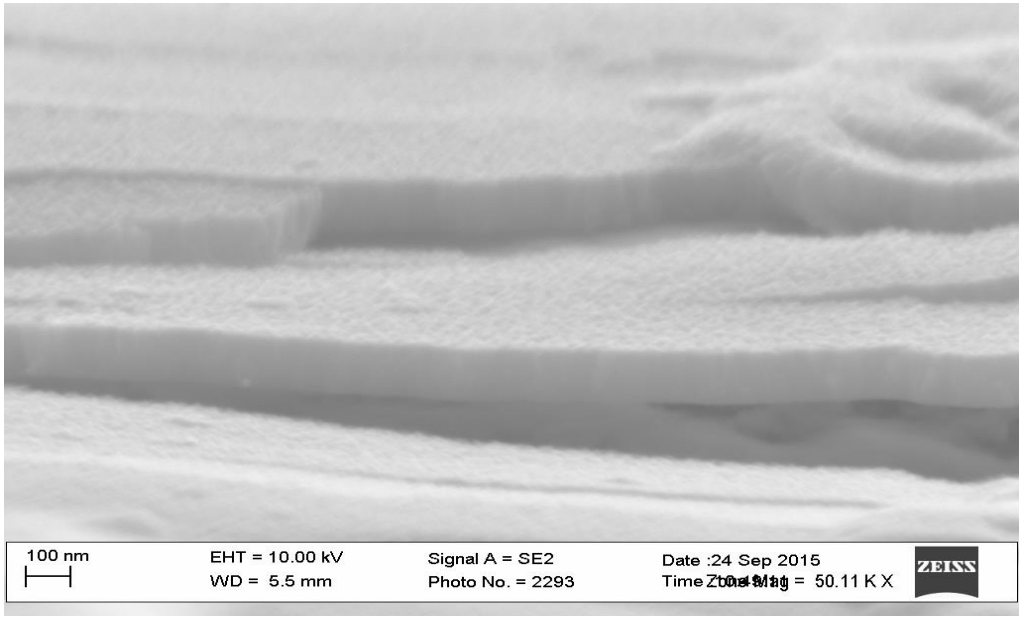

Figure 50. FESEM images representing microstructure of sputtered TiN coatings on copper (S016), the coatings exhibited uniform, thick, columnar grain microstructure with a touch smooth surface morphology. The deposition parameters used for this sputtering experiments are as follows current – 1 A, deposition time - 10 minutes, argon sputtering pressure - 5 mtorr, nitrogen sputtering pressure - 2 mtorr.

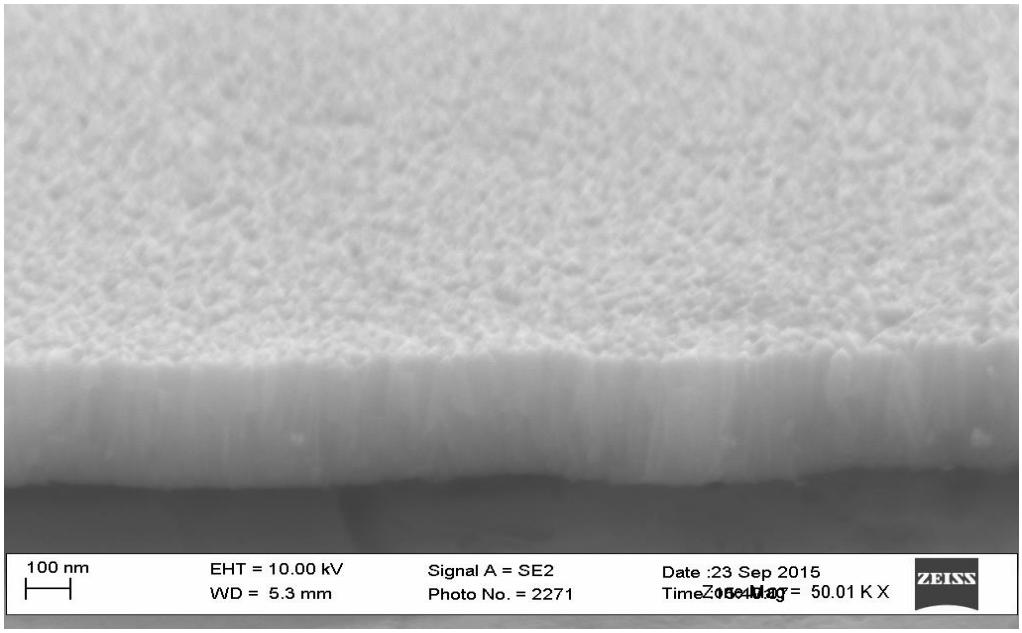

Figure 51. FESEM images representing columnar microstructure of sputtered TiN coatings on copper (S017), the coatings exhibited dense, uniform column grains microstructure with sharper edge surface morphology. The deposition parameters used for this sputtering experiments are as follows current – 2 A, deposition time - 10 minutes, argon sputtering pressure – 5 mtorr, nitrogen sputtering pressure – 2 mtorr.

In this research work, the thin film sputtering deposition of titanium nitride (TiN) is carried over mostly on stainless steel substrates owing to easy access of steel substrate obtained for laboratory works. Consider the samples S023 and S026, the current used for the deposition is 2 A, and deposition time is 10 minutes. For this sputtering deposition of TiN, the sputtering pressure used for these samples are 6 mtorr and 7 mtorr respectively. The micrographs suggest that sample S023 and S026 shows fine grained uniform columnar microstructure. The Figures 52 and 53 represents the micrographs for samples S023 and S026 respectively

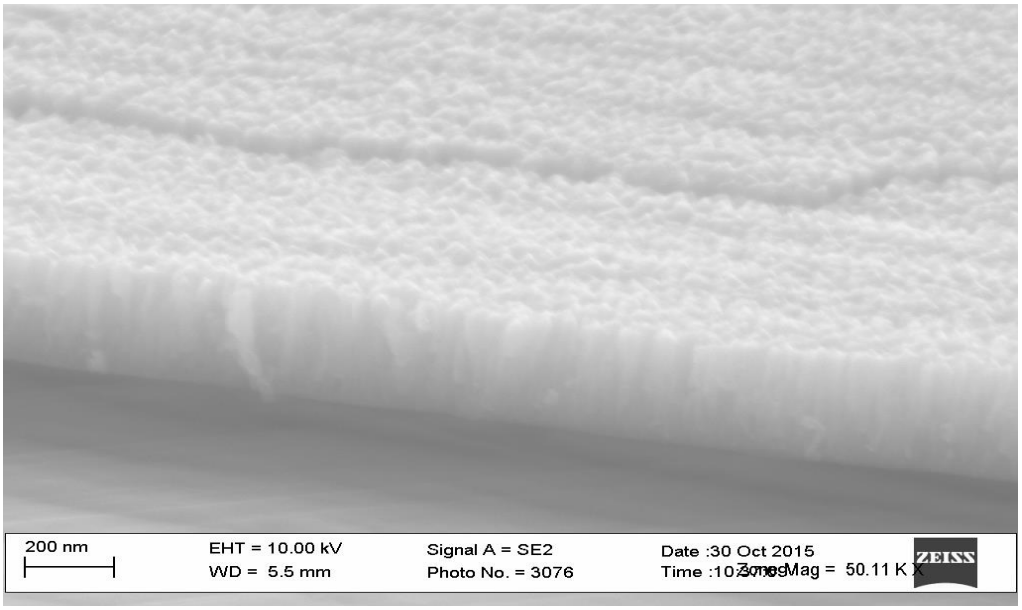

Figure 52. FESEM images representing microstructure of sputtered TiN coatings on stainless steel (S023), the coatings exhibited densely packed uniform columnar grains with sharp edge surface morphology. The deposition parameters used for this sputtering experiments are as follows current – 2 A, deposition time - 10 minutes, argon sputtering pressure – 5 mtorr, nitrogen sputtering pressure – 1 mtorr.

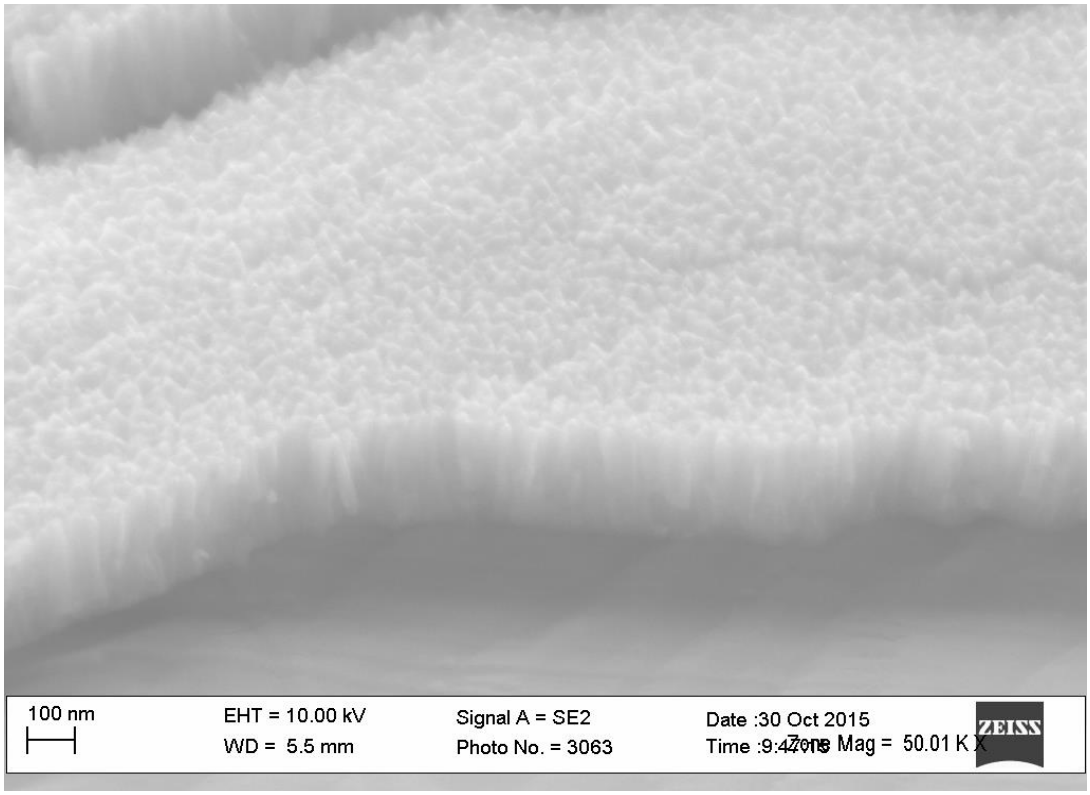

Figure 53. FESEM images representing microstructure of sputtered TiN coatings on stainless steel (S026), the coatings exhibited dense, well bonded, uniform columnar microstructure with sharp edge surface morphology. The deposition parameters used for this sputtering experiments are as follows current - 2A, deposition time - 10 minutes, argon sputtering pressure – 5 mtorr, nitrogen sputtering pressure – 2 mtorr.

The samples S024 and S025 is analyzed for morphological changes through SEM images. From the micrographs it is clear that both the microstructure of sample S024 and S025 is similar in nature. The microstructure is fine columnar grains which are uniform. The deposition parameters used for these sputtering deposition is as follows sputtering pressure - 7 mtorr, deposition time - 10 minutes and current used is 1.1 A and 1.5 A respectively. Figure 54 represents the FESEM images of sample S025 for better understanding.

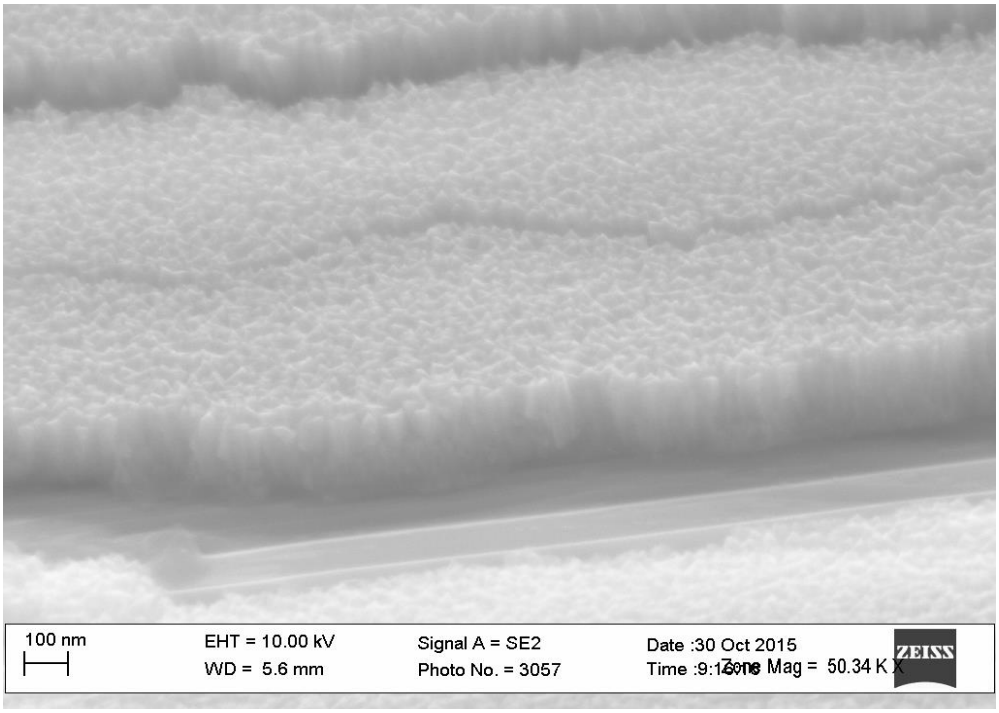

Figure 54. FESEM images representing microstructure of sputtered TiN coatings on stainless steel (S025), the coatings exhibited uniform columnar microstructure with coarse surface morphology. The deposition parameters used for this sputtering experiments are as follows current - 1.5 A, deposition time - 10 minutes, argon sputtering pressure – 5 mtorr, nitrogen sputtering pressure – 2 mtorr.

The deposition parameters play an important role in determining the final microstructure of the deposited thin films. So in this section, the deposition parameters such as current 2 A, sputtering pressure 7 mtorr is kept constant, but the deposition time is increased from 5 minutes to 10 minutes and finally to 30 minutes to observe the morphological changes present in TiN thin film deposition. So to satisfy the above criteria, the following samples S029, S033 and S032 were chosen correspondingly. The substrate used is stainless steel substrate. The resultant micrographs from FESEM suggest that S029 have fine grained uniform columnar microstructure which is further supported by the Figure 55 for better understanding. From S033 FESEM images represented in Figure 56, it is implied that the columnar microstructure is fused but uniform structure is predominantly observed in it. The micrograph of S032 is represented in Figure 57, which represents the principal columnar structure present in it. These columnar microstructure comprises of larger grains and more uniform surface is observed.

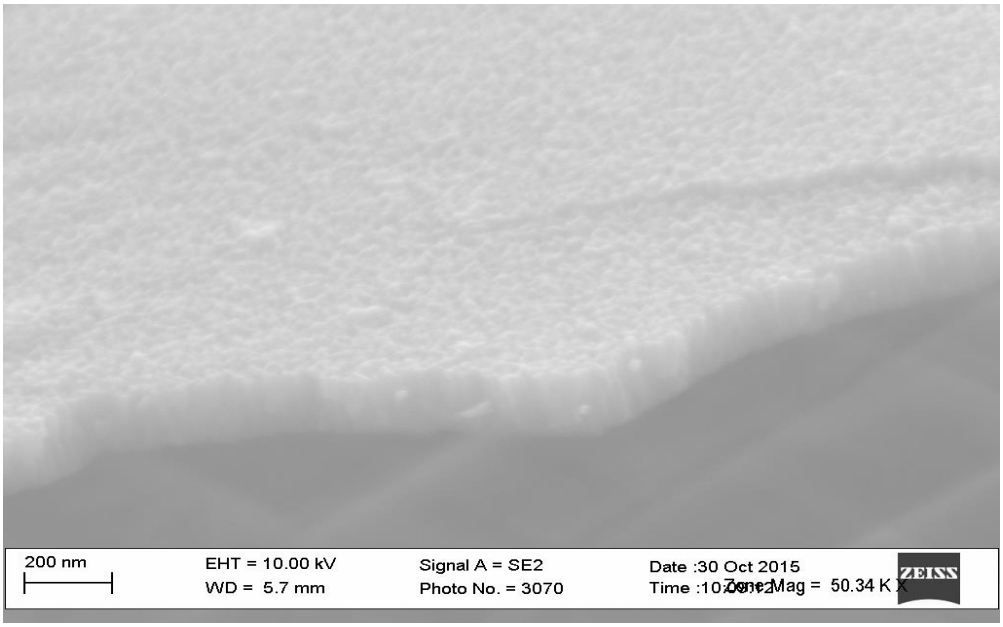

Figure 55. FESEM images representing microstructure of sputtered TiN coatings on stainless steel (S029), the coatings exhibited dense, well bonded, uniform columnar microstructure. The deposition parameters used for this sputtering experiments are as follows current – 2 A, deposition time - 5 minutes, argon sputtering pressure – 5 mtorr and nitrogen sputtering pressure – 2 mtorr.

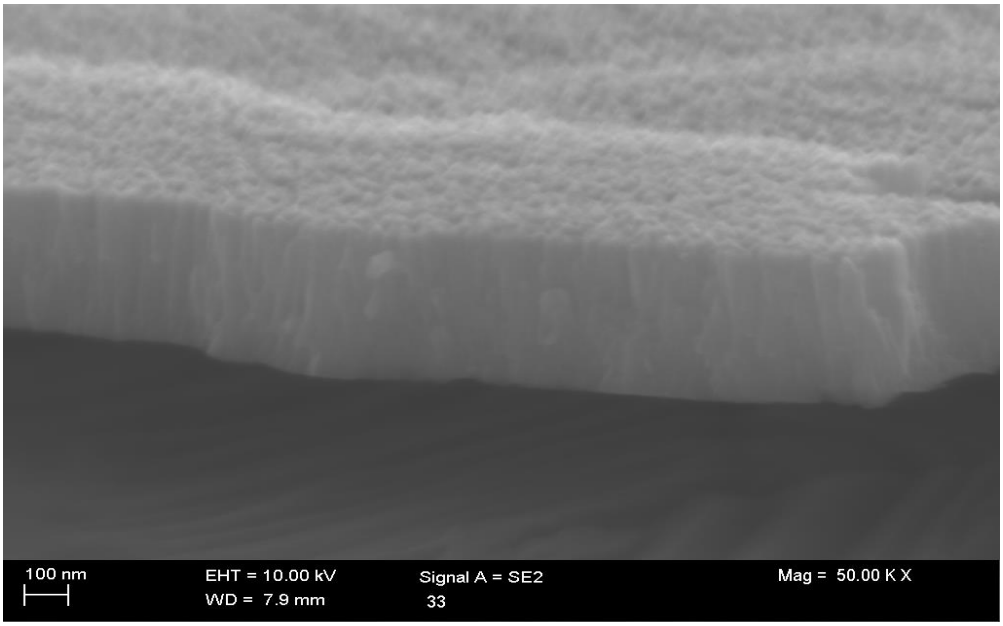

Figure 56. FESEM images representing microstructure of sputtered TiN coatings on stainless steel (S033), the coatings exhibited dense, well bonded, uniform columnar microstructure with smooth surface morphology. The deposition parameters used for this sputtering experiments are as follows current – 2 A, deposition time - 10 minutes, argon sputtering pressure – 5 mtorr and nitrogen sputtering pressure – 2 mtorr.

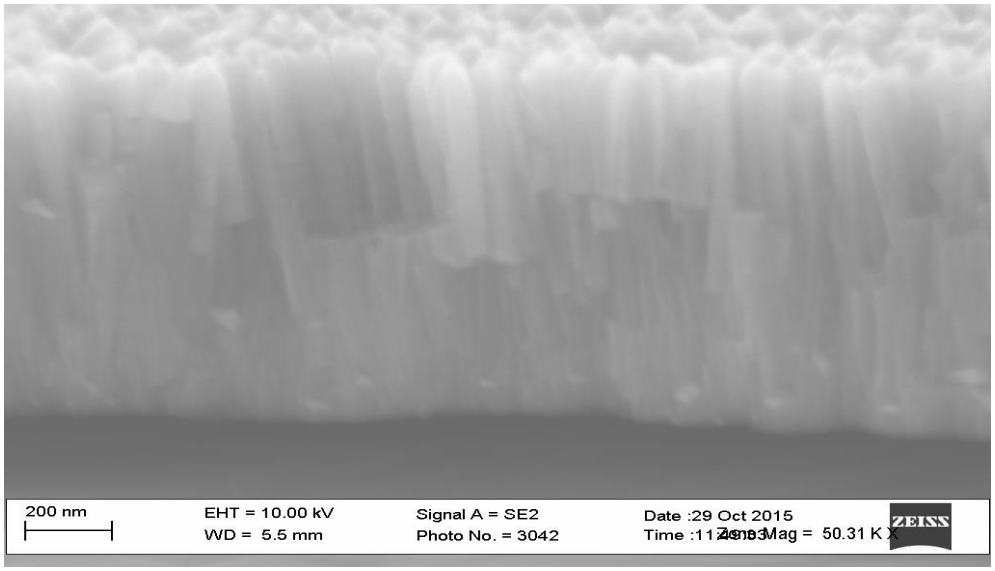

Figure 57. FESEM images representing microstructure of sputtered TiN coatings on stainless steel (S032), the coatings exhibited dense, uniform columnar microstructure with pyramid-like surface morphology. The deposition parameters used for this sputtering experiments are as follows current – 2 A, deposition time – 30 minutes, argon sputtering pressure – 5 mtorr and nitrogen sputtering pressure – 2 mtorr.

The samples S034 and S035 is considered for analysis, in these samples the sputtering pressure is maintained at 8 mtorr and current is applied at 2 A, while the deposition time is changed to 10 and 30 minutes respectively. From the micrographs it is clear that S034 represents well-bonded uniform columnar microstructure as shown in Figure 58, whereas S035 exhibits large columnar grains with coarse surface region and it is represented in Figure 59.

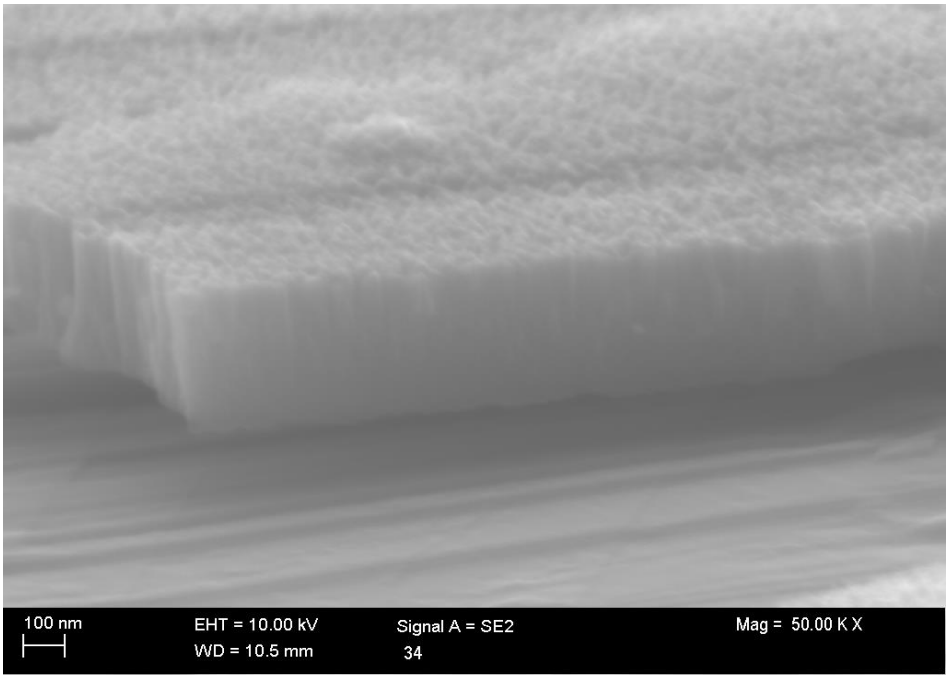

Figure 58. FESEM images representing microstructure of sputtered TiN coatings on stainless steel (S034), the coatings exhibited dense, well bonded, compact, uniform columnar microstructure with smooth surface morphology. The deposition parameters used for this sputtering experiments are as follows current – 2 A, deposition time - 10 minutes, argon sputtering pressure – 5 mtorr and nitrogen sputtering pressure – 3 mtorr.

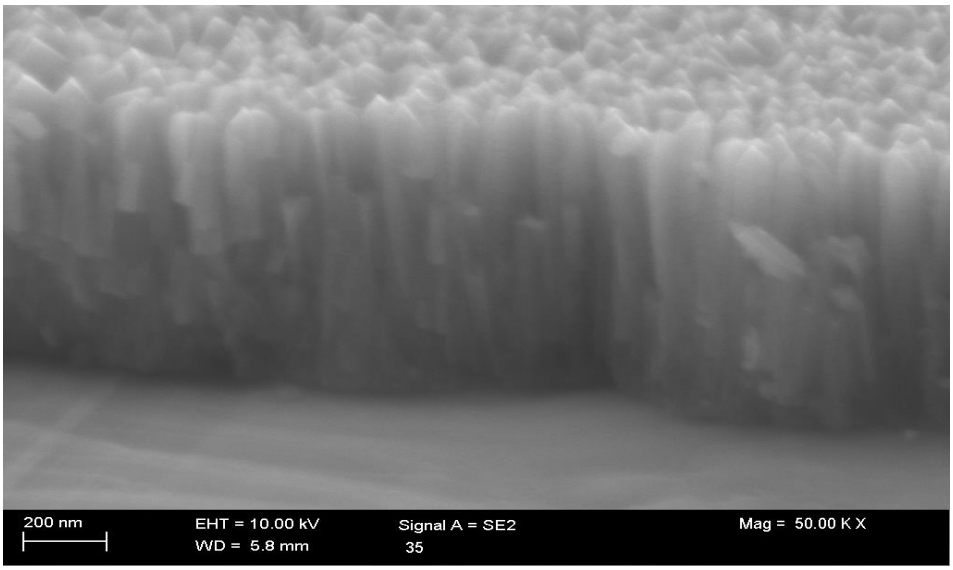

Figure 59. FESEM images representing microstructure of sputtered TiN coatings on stainless steel (S035), the coatings exhibited uniform columnar microstructure with pyramid-like sharp edge surface morphology. The deposition parameters used for this sputtering experiments are as follows current – 2 A, deposition time - 30 minutes, argon sputtering pressure - 5 mtorr and nitrogen sputtering pressure – 3 mtorr.

The sample S056 is etched with argon plasma and then sputter deposited to produce TiN coating which is analyzed using FESEM and the microstructure is predominantly comprising of columnar grains which are dense in nature. Figure 60 represents the FESEM images of sample S056.

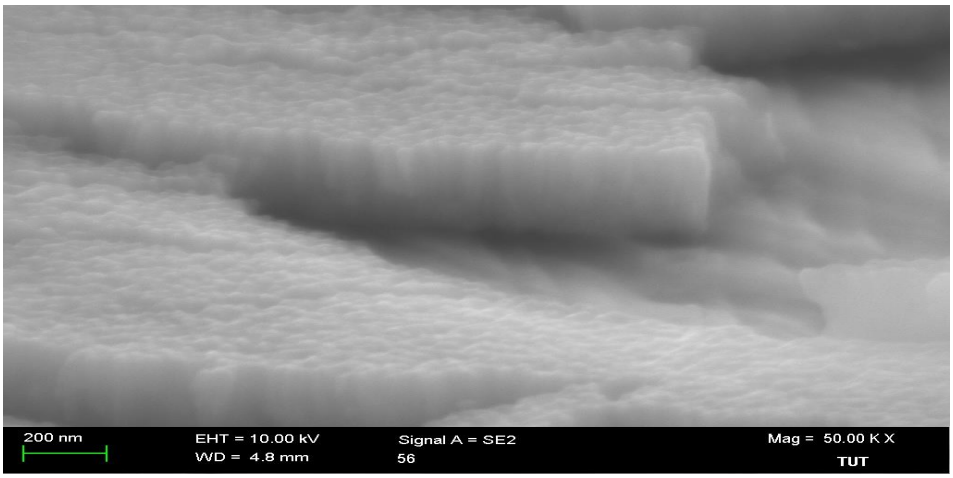

Figure 60. FESEM images representing microstructure of sputtered TiN coatings on stainless steel (S056) the sample is sputter etched using argon plasma for 10 minutes, the coatings exhibited dense, uniform columnar microstructure with relatively smooth surface morphology. The deposition parameters used for this sputtering experiments are as follows current – 2 A, deposition time - 10 minutes, argon sputtering pressure – 5 mtorr, nitrogen sputtering pressure – 2 mtorr.

The S040 and S041 is heated for 30 minutes prior to titanium nitride thin film deposition. From FESEM images, that resultant microstructure is bonded columnar grains which are uniform in nature in both the samples considered. With increase in current value for titanium nitride composition, it is clear that the microstructure represents very dense columnar coarse structure. Figure 61 and 62 represent the micrographs for sample S040 and S041 respectively. Table 11 provides the sample data list for sputtered TiN thin film coatings which were deposited during this thesis work.

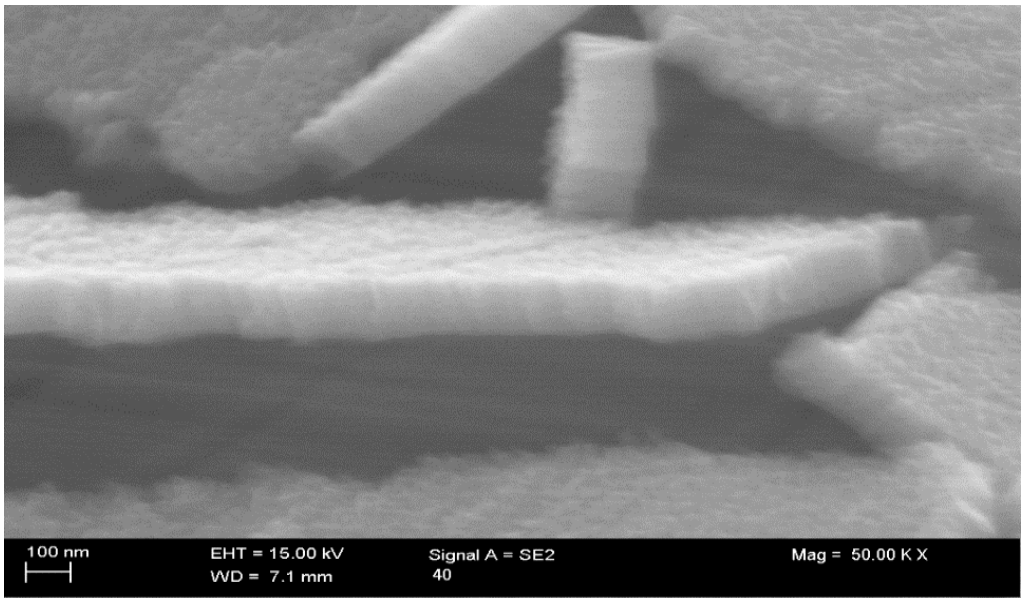

Figure 61. FESEM images representing microstructure of sputtered TiN coatings on stainless steel (S040) sample is heated for 30 minutes in the chamber, the coatings exhibited dense, well bonded, uniform columnar microstructure with sharp edge surface morphology. The deposition parameters used for this sputtering experiments are as follows current – 1 A, deposition time - 10 minutes, argon sputtering pressure – 5 mtorr and nitrogen sputtering pressure - 2 mtorr.

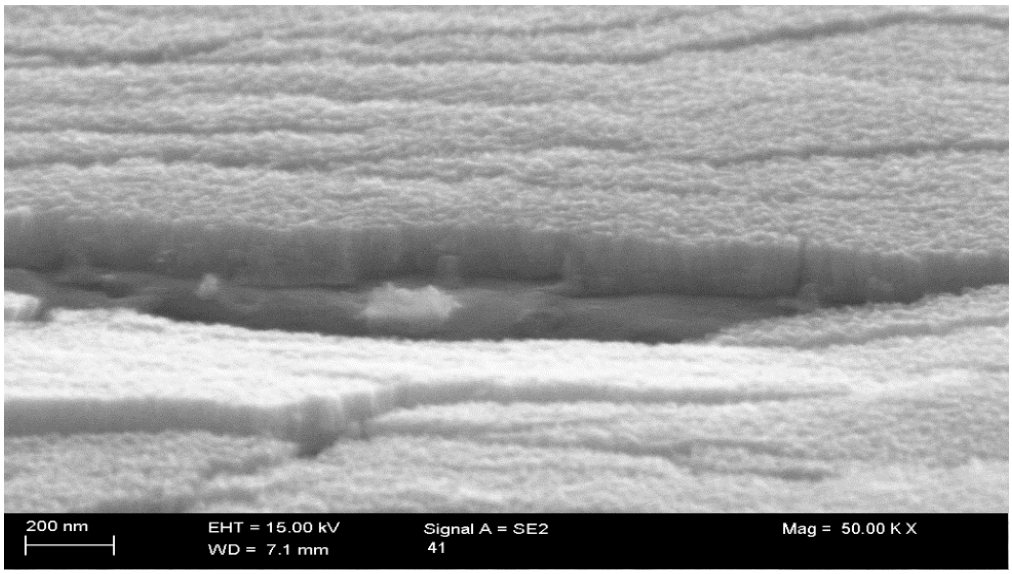

Figure 62. FESEM images representing microstructure of sputtered TiN coatings on stainless steel (S041) sample is heated for 30 minutes in sputtering chamber, the coatings exhibited dense, compact, uniform columnar microstructure with coarser surface morphology. The deposition parameters used for this sputtering experiments are as follows current – 2 A, deposition time - 10 minutes, argon sputtering pressure – 5 mtorr, nitrogen sputtering pressure - 2 mtorr.

Table 11. Summarizes the sample data used for Titanium nitride sputtering deposition and its respective deposition parameters, resultant thickness value and its corresponding deposition rate value used in section 5.2. The symbols which are used in Table 11 are given as follows Argon pressure (Ar. Pr), Nitrogen pressure (N_2. Pr), current (I), voltage (U) and deposition rate (Dep. rate).

Sample	Substrate	Ar. Pr (mtorr)	N_2. Pr (mtorr)	I (A)	U (V)	P (W)	Time (mins)	Thickness (nm)	Dep. rate (nm/min)
S013	Copper	5	1	1	360	360	10	155	16
S014	Copper	5	1	2	380	760	10	405	41
S016	Copper	5	2	1	360	360	10	150	15
S017	Copper	5	2	2	380	760	10	350	35
S023	Stainless steel	5	1	2	380	760	10	315	32
S024	Stainless steel	5	2	1.1	355	390.5	10	140	14
S025	Stainless steel	5	2	1.5	360	540	10	190	19
S026	Stainless steel	5	2	2	380	760	10	240	24
S029	Stainless steel	5	2	2	380	760	5	170	34
S032	Stainless steel	5	2	2	380	760	30	1200	40
S033	Stainless steel	5	2	2	380	760	10	380	38
S034	Stainless steel	5	3	2	380	760	10	325	33
S035	Stainless steel	5	3	2	380	760	30	830	28
S056	Stainless steel	5	2	2	380	760	10	340	34
S040	Stainless steel	5	2	1	360	360	10	160	16
S041	Stainless steel	5	2	2	280	560	10	155	16

5.2.2 Phase structure

The titanium nitride sample S032 is examined using XRD analysis. The compound formed during the sputtering deposition is evaluated as $TiN_{(1-x)}$. As the thickness of titanium nitride composition used in this XRD analysis is around 1.2 µm, low glancing angle is advised for measurement purpose. The crystal system of sputter deposited titanium nitride TiN is cubic in nature, as described in several research articles. [122] The sputtered TiN exhibits preferred crystal orientation at high intensity peaks 2θ = 42.601˚ and the corresponding crystal plane is (2 0 0). However, in the observed XRD spectra the peaks at 2θ = 61.858˚, show very high peaks in the pattern so the crystal

orientation might also be predominant in (2 2 0) crystal plane. The other notable peaks which are observable in the XRD pattern is at 2θ = 36.691˚, 74.125˚and 93.249˚. The reference pattern used for this titanium nitride XRD analyses is 04-004-2917.

The substrate used in this deposition is stainless steel (316L) and it is the same as used in titanium sputtering deposition. The XRD peaks detected from the substrate are matching with the austenite (γ-Fe) phase of the stainless steel used. The stainless steel substrate used in the experiment is cubic in nature and the major composition present in it are iron and nickel which is in match with the attained XRD pattern as shown in Figure 63 a.

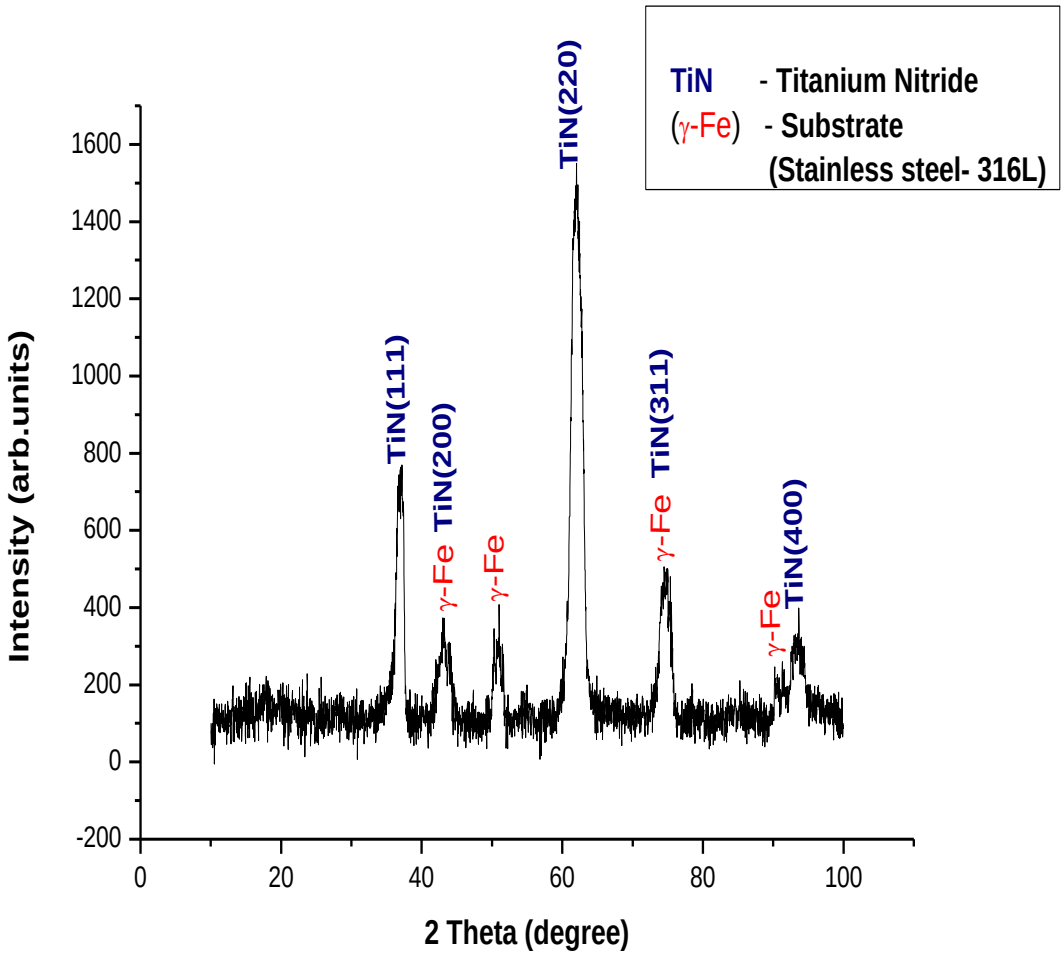

Figure 63 a. XRD pattern of sputtered Titanium nitride thin film coating of S032 which representing different crystal orientation as shown in this Figure.

From XRD analysis of thin film coating the crystallographic orientation of the resultant phase is obtained. The sample which are taken into analysis S032 (TiN). The substrates which are used for thin film deposition were stainless steel. The sample S032 is matched with reference peaks from titanium nitride composition as shown below in Figure 63 b. The obtained XRD peaks from S032 is represented in red color, while the

peaks from substrate is marked in blue color and reference titanium nitride peaks is marked in green color.

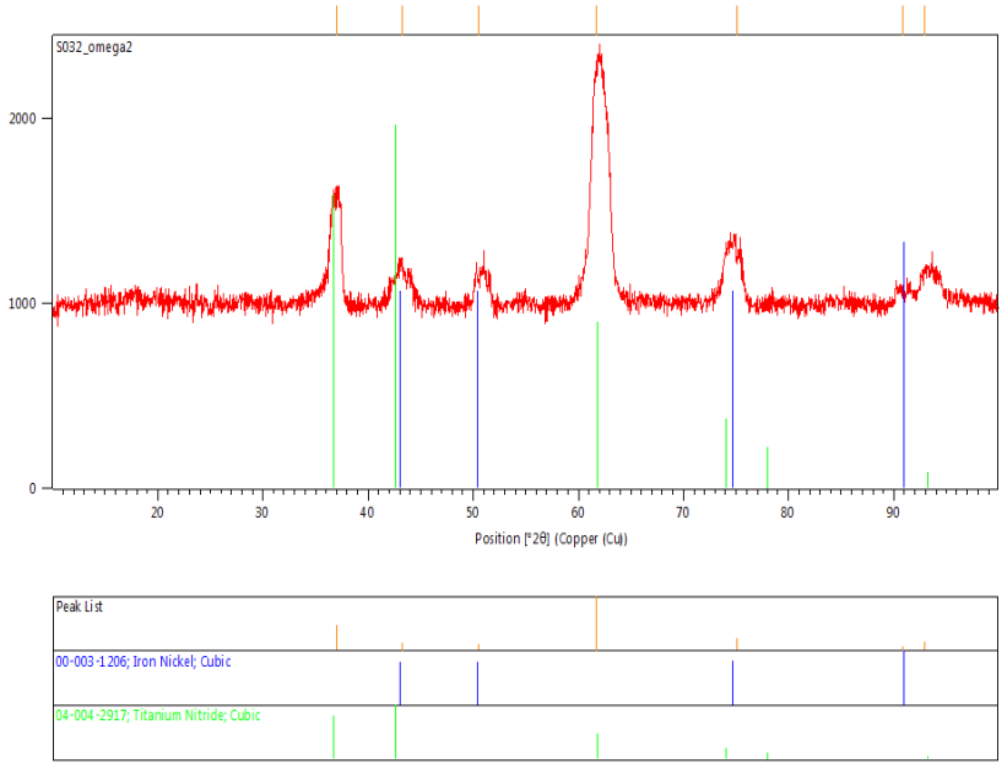

Figure 63 b. XRD pattern of sputtered titanium nitride thin film coating, S032 which representing peaks which are matching with the reference stick pattern as shown in this Figure.

5.2.3 Adhesion strength

The Titanium nitride thin film coating is subjected to adhesion strength measurements to evaluate the adhesion property of the coatings deposited by DC magnetron sputtering process. As mentioned earlier in experimental part, adhesion P.A.T.T.I is used to examine the TiN coated samples. Let us consider samples S023, S026 for investigation, in these sample the deposition parameters such as current 2 A, deposition time 10 minutes is kept constant. The sputtering pressure used is 6 mtorr and 7 mtorr for samples S023 and S026 respectively. From the measurement, the adhesion value of S023 is 4.4 MPa and for S026 is 1.6 MPa. The next set of samples which are evaluated for adhesion test is S024 and S025. For these samples, the deposition parameters such as sputtering pressure - 7 mtorr, deposition time - 10 minutes, with only exception is current value as 1.1 A is used for S024 and 1.5 A for S025 respectively. The resultant value of adhesion strength for S024 is 6.5 MPa and for S025 adhesion strength value is 7 MPa. The final set of samples considered for adhesion strength examination are S029

and S032. In these samples, the sputtering pressure used is 7 mtorr, current - 2 A, while the deposition time used is 5 minutes and 30 minutes respectively. The adhesion value of sample S029 is 1.7 MPa while the adhesion value of S032 is 1.66 MPa. Figures 64, 65, 66 represents the images of the measured sample which were used for adhesion strength measurement. The adhesion strength measurements of titanium nitride coatings with respect to sputter etched by RF sputtering is also studied. The sample S056 is of titanium nitride deposition, and the resulting adhesion strength value is 9 MPa. Figure 67 represents the images of the measured sample S056 which were used for adhesion value measurement.

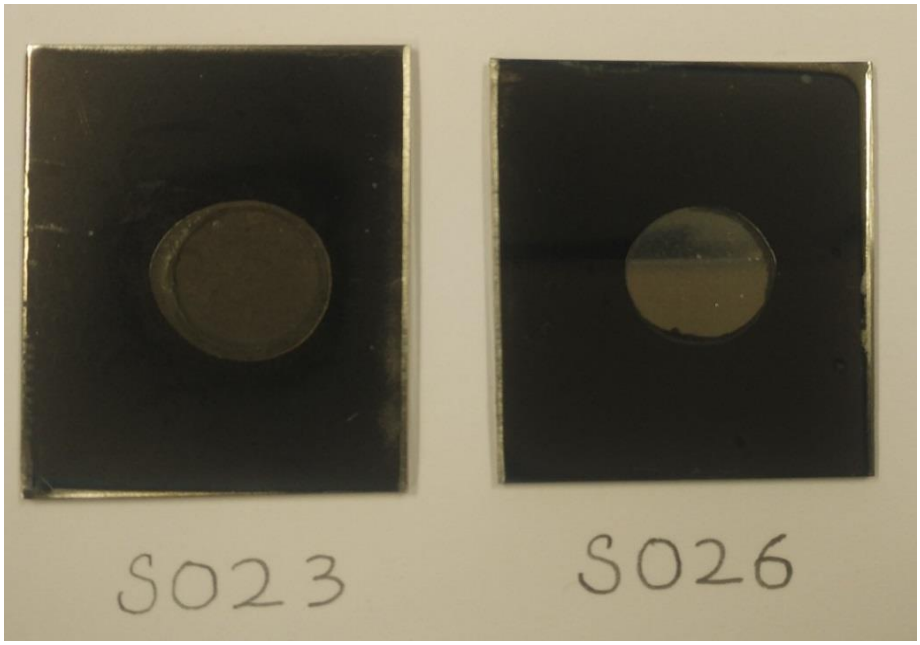

Figure 64. Adhesion tested surface of sputtered titanium nitride coating using adhesion p.a.t.t.i equipment is presented in this Figure. The samples which were used for testing are S023 and S026. The deposition parameters used for S023 are as follows current – 2 A, deposition time - 10 minutes, argon sputtering pressure – 5 mtorr and nitrogen sputtering pressure – 1 mtorr and parameters used for S026 are current – 2 A, deposition time - 3 minutes, argon sputtering pressure – 5 mtorr and nitrogen sputtering pressure – 2 mtorr.

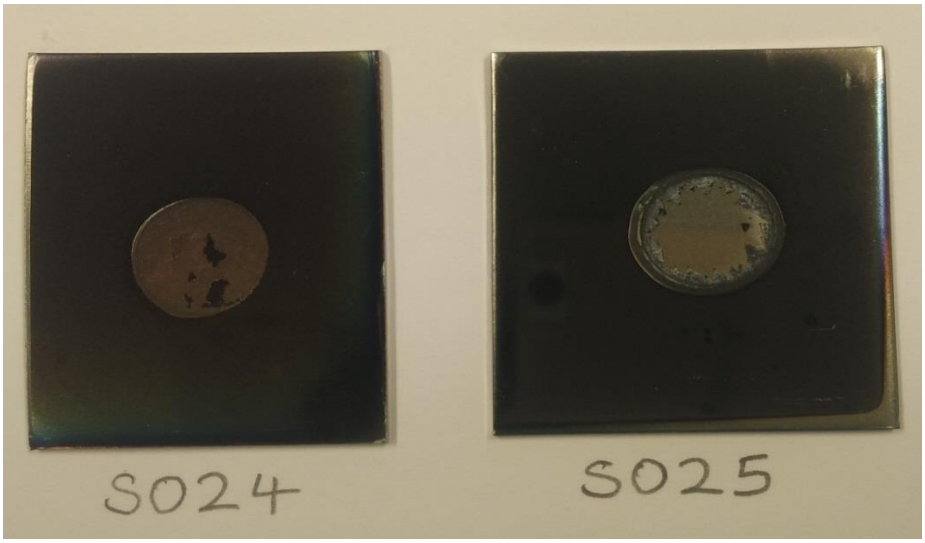

Figure 65. Adhesion tested surface of sputtered titanium nitride coating using adhesion p.a.t.t.i equipment is presented in this Figure. The samples which were used for testing are S024 and S025. The deposition parameters used for S024 are as follows current - 1.1 A, deposition time - 10 minutes, argon sputtering pressure – 5 mtorr and nitrogen sputtering pressure – 2 mtorr and parameters used for S025 are current - 1.5 A, deposition time - 10 minutes, argon sputtering pressure - 5mtorr and nitrogen sputtering pressure – 2 mtorr.

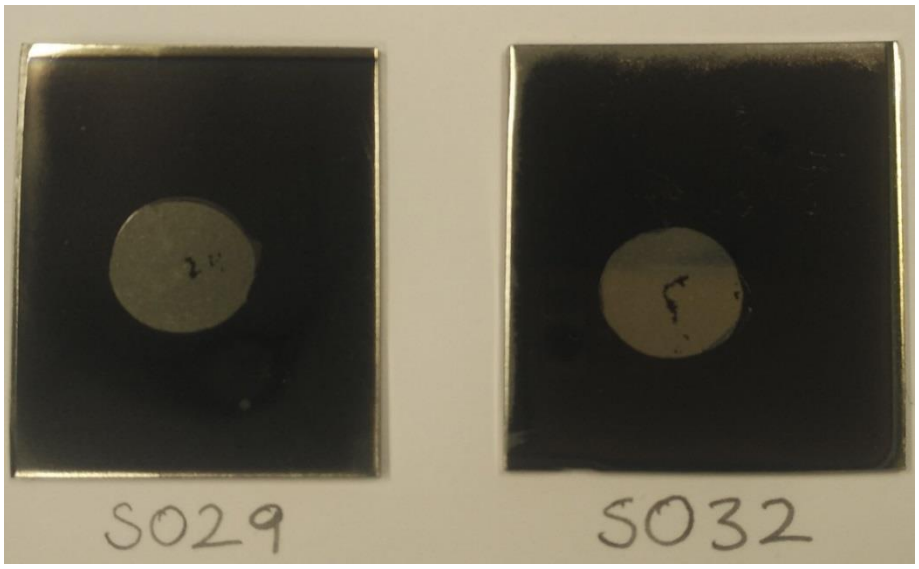

Figure 66. Adhesion tested surface of sputtered titanium nitride coating using adhesion p.a.t.t.i equipment is presented in this Figure. The titanium samples which were used for testing are S029 and S032. The deposition parameters used for S029 are as follows current – 2 A, deposition time - 5 minutes, argon sputtering pressure – 5 mtorr and nitrogen sputtering pressure – 2 mtorr and parameters used for S032 are current – 2 A, deposition time - 30 minutes, argon sputtering pressure – 5 mtorr and nitrogen sputtering pressure – 2 mtorr respectively.

Figure 67. Adhesion tested surface of sputtered titanium nitride coating using adhesion p.a.t.t.i equipment is presented in this Figure. The sample S056 used for adhesion test are sputter etched for 10 minutes with 100W RF power. The deposition parameters used for S056 is given as follows current – 2 A, deposition time - 10 minutes, argon sputtering pressure – 5 mtorr and nitrogen sputtering pressure – 2 mtorr.

5.2.4 Surface roughness

The Alicona optical profilometer is used to analyze the surface roughness value of sputtered titanium nitride coated samples. For this analysis three sets of samples are considered as follows 1) S023, S026 2) S024, S025 and 3) S029, S032. The test results from optical profilometer shows S023 and S026 exhibits roughness value of 251 nm and 243 nm respectively. The second set of samples shows roughness value of around 635 nm and 456 nm respectively. The final set of samples demonstrates roughness value of 306 nm and 180 nm respectively. For these samples, the details about the deposition parameters is explained in the previous section. The sample name in the Figure is stated in the top right corner of the corresponding image respectively. Figures 68, 69 and 70 represents the optical profilometer images of the measured TiN samples. Table 12 provides the data list of deposition parameters for sputtered titanium nitride coatings with properties such as adhesion strength and surface roughness value.

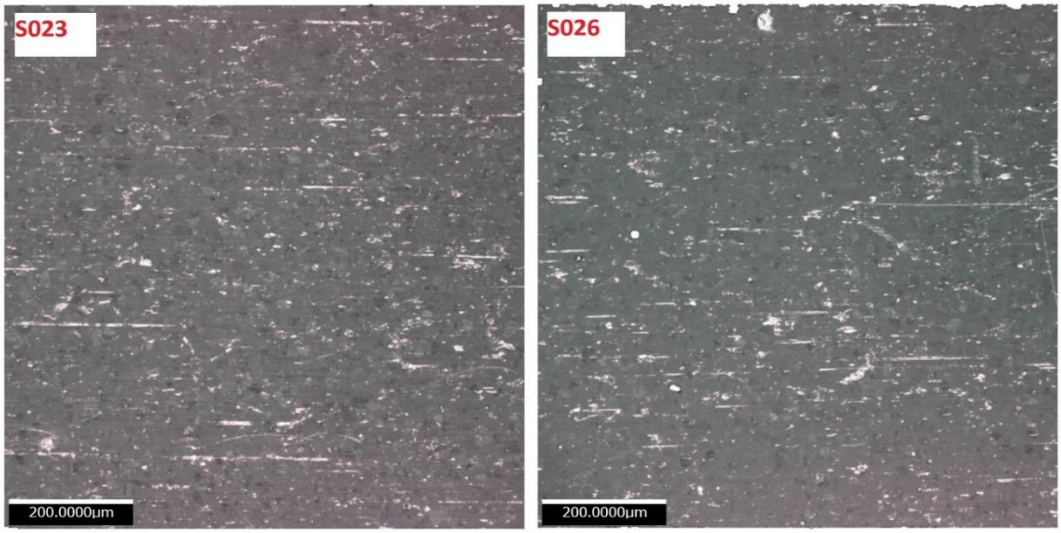

Figure 68. Surface roughness profile of sputtered titanium nitride thin film sample is represented in this Figure and the roughness profile value is accomplished by optical profilometer. The samples which were used for testing are S023 and S026 respectively. The deposition parameters used for S023 are as follows current - 2 A, deposition time - 10 minutes, argon sputtering pressure – 5 mtorr, nitrogen sputtering pressure – 1 mtorr and parameters used for S026 are current - 2A, deposition time - 10 minutes, argon sputtering pressure – 5 mtorr, nitrogen sputtering pressure – 2 mtorr respectively.

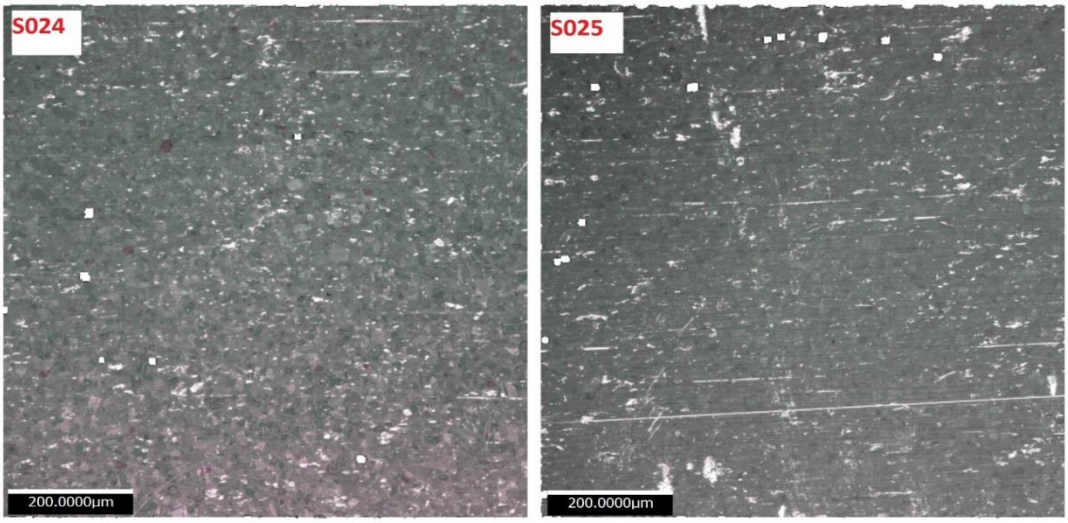

Figure 69. Surface roughness profile of sputtered titanium nitride thin film sample is represented in this Figure and the roughness profile value is accomplished by optical profilometer. The samples which were used for testing are S024 and S025 respectively. The deposition parameters used for S024 are as follows current - 1.1 A, deposition time - 10 minutes, argon sputtering pressure – 5 mtorr, nitrogen sputtering pressure – 1 mtorr and parameters used for S025 are current - 1.5 A, deposition time - 10 minutes, argon sputtering pressure – 5 mtorr and nitrogen sputtering pressure – 2 mtorr respectively.

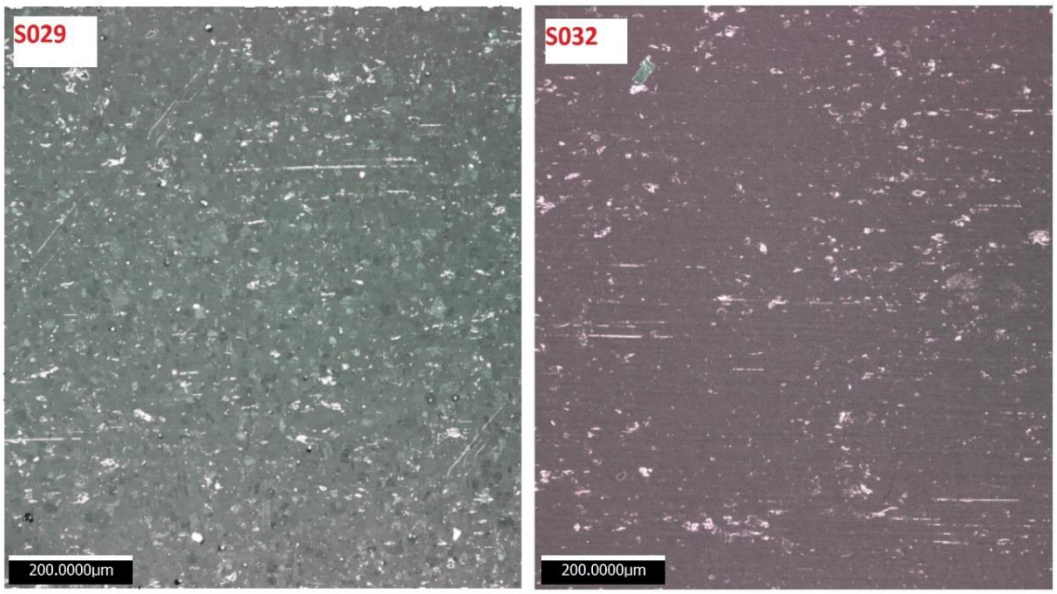

Figure 70. Surface roughness profile of sputtered titanium nitride thin film sample is represented in this Figure and the roughness profile value is accomplished by optical profilometer. The samples which were used for testing are S029 and S032 respectively. The deposition parameters used for S029 are as follows current – 2 A, deposition time - 5 minutes, argon sputtering pressure – 5 mtorr, nitrogen sputtering pressure – 1 mtorr and parameters used for S032 are current – 2 A, deposition time - 30 minutes, argon sputtering pressure – 5 mtorr and nitrogen sputtering pressure – 2 mtorr respectively.

Table 12. Provides the data for sputtering sample which are used for Titanium nitride sputtering deposition and its respective deposition parameters, resultant thickness value and its corresponding deposition rate value used in section 5.2.2 – 5.2.4. The following samples specifically S023, S024, S025, S026, S029, S032 and S056 were studied to analyze the surface coating properties such as adhesion strength and surface roughness. The symbols which are used in Table 12 are given as follows Argon pressure (Ar. Pr), Nitrogen pressure (N_2. Pr), current (I), voltage (U), power(W), deposition rate (Dep. rate) and surface roughness (Ra).

Sample	Ar.Pr (mtorr)	N_2.Pr (mtorr)	I (A)	U (V)	P (W)	T	Thickness (nm)	Dep. Rate (nm/min)	Adhesion strength (MPa)	Ra (nm)
S023	5	1	2	380	760	10	315	32	4.4	251
S024	5	2	1.1	355	390.5	10	140	14	6.5	635
S025	5	2	1.5	360	540	10	190	19	7	456
S026	5	2	2	380	760	10	240	24	1.6	243
S029	5	2	2	380	760	5	170	34	1.7	306
S032	5	2	2	380	760	30	1200	40	1.66	180
S056	5	2	2	380	760	10	340	34	9	-

6. DISCUSSION

The correlation between deposition parameters of deposited thin films in this thesis study is discussed in the following sections. The latter part of the section also discusses about microstructure evolution of Ti and TiN thin film coatings and XRD analysis of as deposited thin film coating. The discussion part deals with specific properties of thin films such as adhesion strength and surface roughness.

6.1 Discussion - Magnetron sputtered titanium coatings

The different types of relationship between deposition parameters of sputtered Ti coating is evaluated in this section. The deposition parameters such as deposition time, sputtering pressure and current/power value is investigated to study the relation between the thickness and deposition rate of titanium thin film coating. The reason for the existing correlation between the deposition parameters is discussed in detail.

6.1.1 Relation between sputtering power and deposition rate

In this section, the relationship between deposition rate and sputtering power for titanium thin film coating by sputter deposition is analyzed. The increase in deposition rate for titanium thin film coating with respect to increase in sputtering power is shown in below Figure 71. So from the Figure 71, it is clearly understood that as the power is increased, the gradual increase in the deposition rate of titanium coating is observed and it is confirmed for various sets of samples. These sample sets were chosen with respect to different deposition time for sputtering process. In the following samples S012 and S015, the deposition rate improved gradually thus confirming the fact that with high sputtering power, the bombardment of argon atoms is increased hence resulting in higher rate of deposition [11; 15; 123].

The sputtering power used for this experiments are ranging from 320 W and 680 W respectively and the corresponding current value used are 1 A and 2 A respectively. The sputtering experiments for titanium deposition is also conducted with 3 A current, slightly higher deposition rate is achieved during the sputtering experiment, however resultant thin film lacked adherence to the substrate surface. Thus, in general relatively lower current/power value is considered for superior coating quality of titanium thin films. The following Figure 71, describes the relationship between the sputtering power and deposition rate of sputtered Ti coatings.

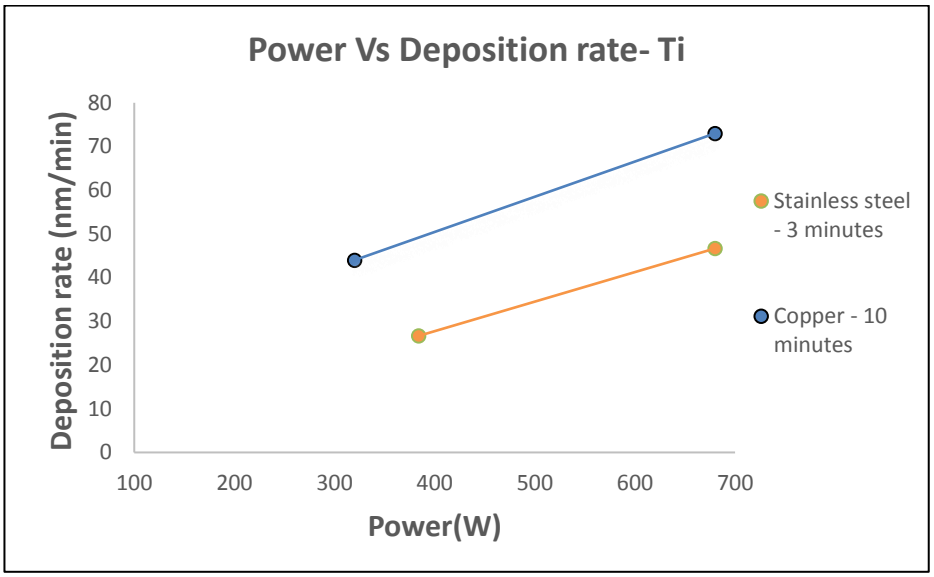

Figure 71. Typical representation of the relation between sputtering power (W) and deposition rate (nm/min) values of Titanium coatings is illustrated in this Figure. As the power value is increased the deposition rate is increased correspondingly.

6.1.2 Relation between argon sputtering pressure and deposition rate

In sputter deposition of titanium thin film coating, the sputtering pressure is varied to study the correlation between deposition rate of coating. The sputtering pressure of argon gas is increased from 5 mtorr to 10 mtorr and further increased to 20 mtorr. The respective deposition rate values are plotted in the below Figure 72. From the graphical representation in Figure 72, it is understood that from 5 mtorr to 10 mtorr the deposition rate of coating is almost linearly constant. However, when the sputtering pressure of argon gas is increased from 10 mtorr to 20 mtorr, the sudden decrease in the deposition rate is observed. The decrease in deposition rate at 20 mtorr is due to the fact at higher sputtering pressure, sputtering atoms mean free path is small, thereby the collision of sputtering atoms between target and substrate with argon particles is increased thus resulting in lower deposition rate of thin film coating [1; 2; 10; 22; 124; 125]. The increase in sputtering pressure also means that the sputtered atoms between the target and substrate is reduced and there is also a possibility that sputtered atoms might be reflected back to the target, which is undesired property for thin film deposition [2; 10; 22; 124]. Figure 72 describes the relationship between sputtering pressure and deposition rate of sputtered Ti coatings.

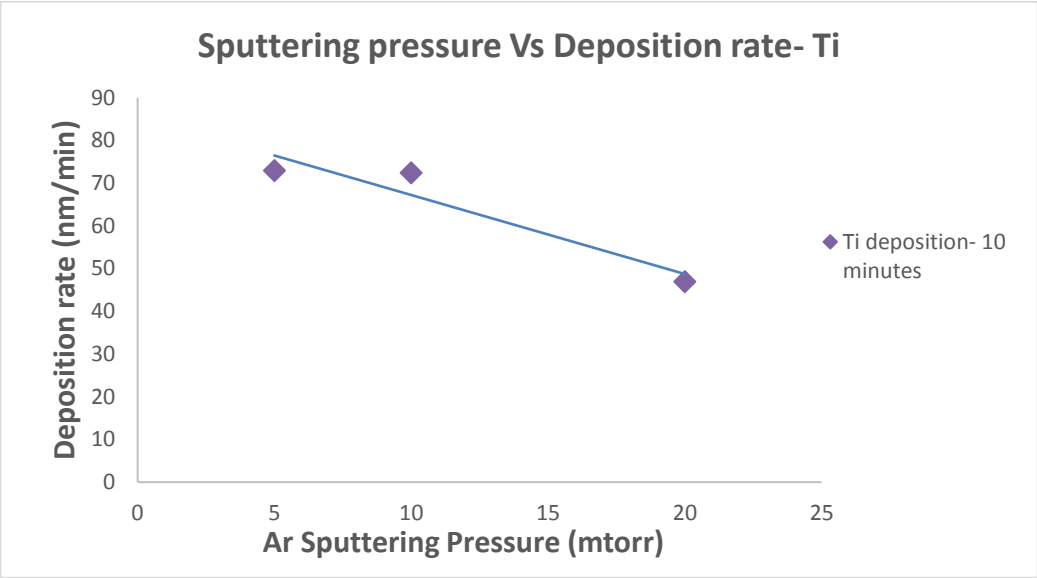

Figure 72. General overview of the relation between sputtering pressure(mtorr) and deposition rate (nm/min) values of Titanium coatings. At lower sputtering pressure the deposition rate is higher, while at higher sputtering pressure the deposition rate is decreased significantly.

6.1.3 Influence of other parameters

The correlation between the deposition time and deposition rate is discussed in this section. In general, the depositions rate should be constant with respect to deposition times, however in this experiments due to unidentified factors, constant deposition rates were not achieved. There is no direct correlation established between deposition time and deposition rate, as the deposition rate increased initially till a certain point and from that point the deposition rate decreases gradually as shown in the below Figure 73. In this experiments, the samples deposited at different deposition times such as 3, 5, 10 and 30 minutes. The initial value of deposition rate for 3 minutes is around 46 nm/min which is increased to approximately to 71 nm/min at 5 minutes deposition time. When the deposition time is increased to 10 minutes, the increase in deposition rate is observed. With further increase to 30 minutes deposition time, rapid decrease in deposition rate is experienced. During this sputtering depositions, it is perceived that higher deposition rates can be observed in between 5 to 10 minutes deposition time. The following Figure 73 clearly depicts the relationship between deposition time and deposition rate of sputtered titanium coating.

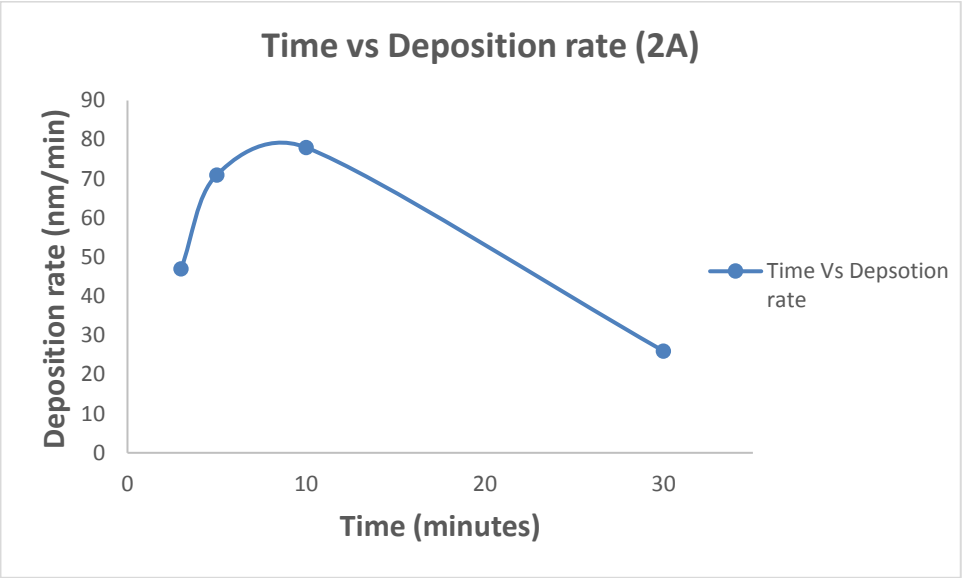

Figure 73. General overview of the correlation between deposition time (minutes) and deposition rate (nm/min) values of sputtered titanium coatings. The high deposition rate of titanium thin film coatings is achieved in between 5 to 10 minutes deposition time.

6.2 Discussion - Magnetron sputtered titanium nitride coatings

The optimization of deposition parameters for sputtered titanium nitride coatings is discussed in this section. The relation between various deposition parameters such as deposition time, current or power, sputtering pressure with respect to deposition rate is explained in the following section.

6.2.1 Relation between sputtering power and deposition rate

The titanium nitride thin film coating is deposited at different power levels, from the Figure 74, it is clear that as the power increased, significant rise in deposition rate is observed. As shown in below Figure 74, at 360 W power applied the rate of deposition is around 15 nm/min. When the power applied is increased to 540 W, it results in slight increase in the deposition rate (19 nm/min). With further increase in power to 760 W, there is rapid increase in the deposition rate and the value is around 35 nm/min. Thus, from this experimental observation at 2 A current (760 W), higher deposition rate for TiN coating is achieved in Nordiko sputtering equipment. Similar kind of experiments are conducted at 6 mtorr sputtering pressure, from the experimental data it is verified that with increase in sputtering power, higher deposition rate can be achieved [126]. However, if the power value is increased to critical value the target material used in the experiments might overheat which in turn result in deterioration to the thin film coating quality obtained. So care needs to be taken in increasing the power value of thin film coatings. Figure 74, explains the relationship between the sputtering power and deposition rate of sputtered Ti coatings

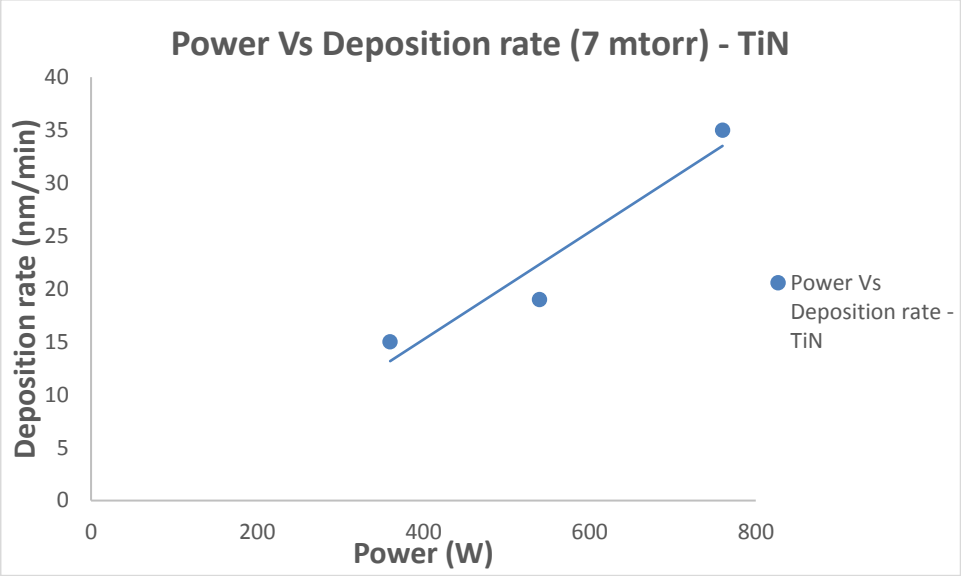

Figure 74. Relationship between sputtering power (W) and deposition rate (nm/min) values of sputtered titanium nitride coatings is represented in this Figure. With increase in power values the deposition rate of sputtered TiN coatings is increased respectively.

6.2.2 Relation between sputtering pressure and deposition rate

The correlation between sputtering gas pressure and deposition rate is discussed in this section. As the sputtering gas used for the titanium nitride thin film sputtering is Argon gas and it is kept constant at 5 mtorr pressure. The reactive gas is nitrogen gas and it is varied from 6 mtorr to 8 mtorr. The relation amongst sputtering pressure and deposition rate is shown in below Figure 75. From the experimental data, the deposition rate at 6 mtorr sputtering pressure is around 32 nm/min, the deposition rate is further increase to 35 nm/min with increasing the sputtering pressure to 7 mtorr. However, when the sputtering pressure is increased to 8 mtorr, comparatively lower deposition rate is obtained due to increase in sputtering pressure [127; 128]. The reason for this behavior is at higher sputtering pressure, the inflow of nitrogen gas is increased thereby the more collisions between them and so decreased deposition rate in general. [127] The increase in nitrogen partial pressure result in decrease of argon partial pressure, which sequentially decreases the ionization [128]. This results in the decrease of the sputtered atoms in the plasma composition so results in reduction of deposition rates [128]. From the Figure 75, it is also clear the obtained deposition rate is approximately in between 30-35 nm/min, which is because the sputtering gas pressure is not increased profoundly, therefore average deposition rate of around 30 nm/min is achieved for TiN sputtering deposition. The following Figure 75, illustrates the association between sputtering pressure and deposition rate of sputtered TiN coatings.

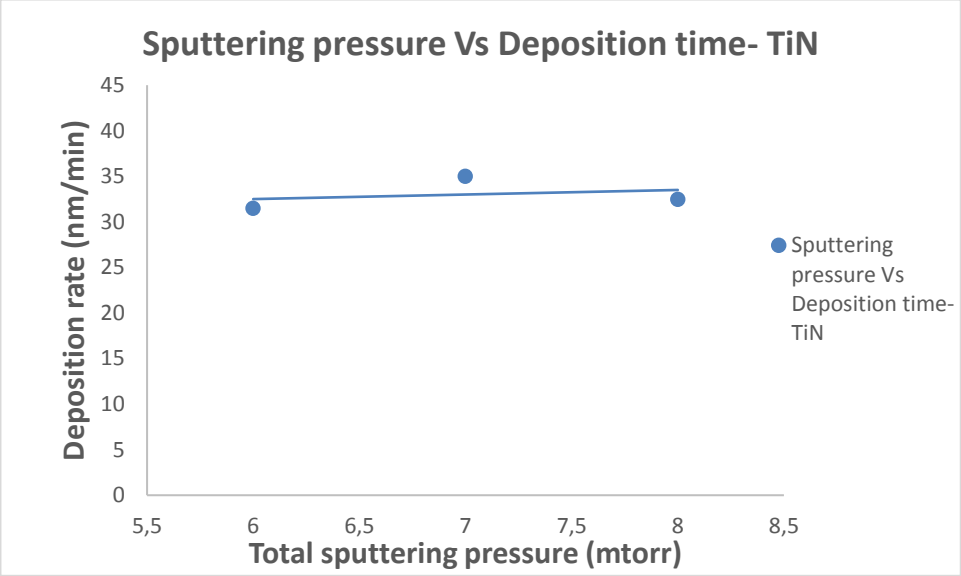

Figure 75. Typical correlation between sputtering pressure (W) and deposition rate (nm/min) values of sputtered titanium nitride coatings is denoted in this Figure. The deposition rate of around 30 nm/min is accomplished in this thesis study.

6.2.3 Influence of other parameters

The deposition rate of TiN coating with respect to deposition time is discussed in this section. From the experimental data obtained at 5 minutes deposition time, the resultant deposition rate is around 34 nm/min. When the deposition time is increased to 10 minutes, the deposition rate is slightly increased to 38 nm/min. With further increase of deposition time, the deposition rate is slightly increased to around 40 nm/min. The above mentioned relation can be easily understood by the following Figure 76. As from the data it is clearly understood that during 10 minutes deposition time, the deposition rate of TiN coating is higher. It is also observed that at 30 minutes deposition time, the deposition rate is slightly higher. Figure 76, illustrates the relationship between deposition time and deposition rate of sputtered titanium nitride coatings.

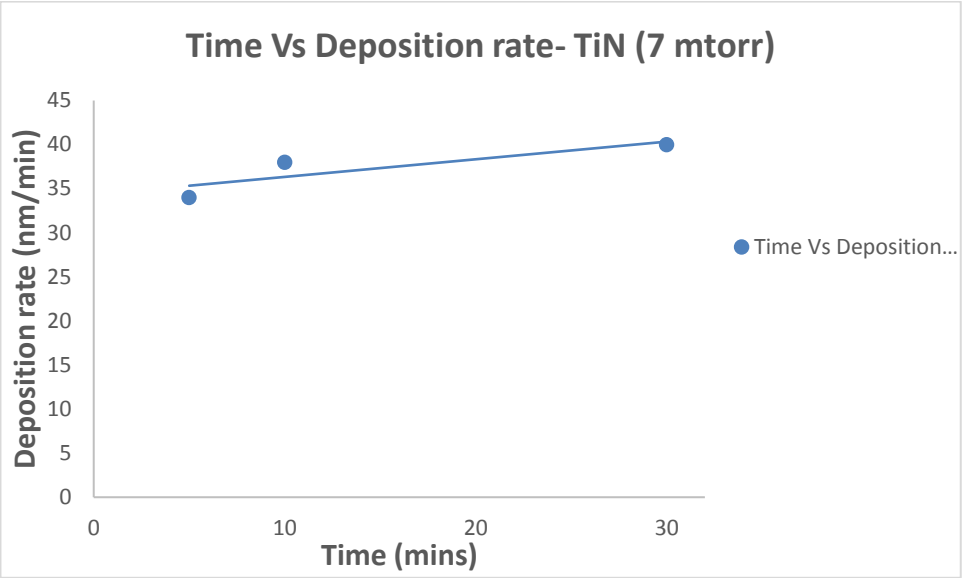

Figure 76. General overview of relation between deposition time (minutes) and deposition rate (nm/min) values of sputtered titanium nitride coatings is illustrated in this Figure. The deposition rate lies almost in similar range when different time of depositions is considered.

6.3 Microstructures

The microstructures play an imperative role in defining the final properties of any thin film coatings. So in this section, the microstructure of titanium and titanium nitride thin film coating is discussed. From the results it is clearly understood that the substrate used in the sputtering process also have minor influence on the final microstructural property of thin films. In this research work, the microstructures obtained are uniform, dense in nature and the grains are columnar all throughout the experiments. Increasing sputtering pressure does not directly influence the microstructure evolution of thin films deposited. With higher substrate temperature the required microstructure of preferred zone structure is obtained.

However, in some cases as in sample S044, the microstructure represents needle like column which are random in nature. Please refer Figure 38, for more information regarding this observation. In this sample slight inclination in microstructure is observed that is due to the fact of sample orientation or clustering or shadowing effect [129].

In this section, the microstructural evolution of sputtered titanium coatings according to the structure zone diagram (SZD) by Thornton are discussed in detail. The sample S012 comprises of pyramid-like surface, dense in nature, fibrous columnar grains which are not distinct, non-porous grains. The samples S015, S018 and S019 exhibits similar kind of microstructures with dense fibrous columnar grains, non-porous, pyramid-like

surface grains with blunt edges. Please refer to section 5.1.1 and Figures 33-36 for more information regarding this. So from the microstructural evaluation, samples S012, S015, S018 and S019 exhibits zone T microstructure in Thornton SZD as the microstructures consists of dense fibrous grains which are not clearly distinct [130]. In general, zone T represents the transition zone of the SZD, where the transition between zone 1 and zone 2 occurs. The samples S030, S031, S048 and S049 also exhibits zone T microstructure which comprises of densely stacked fibrous grains, which are uniform with pyramid-like surface morphology.

The samples which are considered for discussion are S042, S043 and S044, these samples exhibit characteristic features of zone 1 microstructure. The sample S042 comprises of columnar grains which are fine, uniform, well bonded, grain boundaries are separated by small voids and consists of sharp-edge surface morphology. The samples S043 and S044 displays features such as sharp-edge surface morphology, separated by voids, poorly defined columnar grains. The reasons for the formation of zone 1 microstructure as proposed by Thornton is due to the following factors such as mean-free path between the sputtered ions and the gas atoms is reduced, collisions increased, decreasing bombardment of energetic particles, decreasing mobility of adatoms and shadowing effect [1; 2]. The shadowing effect is more effective when there is low surface diffusion of adatoms and these surface shadowing effect contributes to the certain characteristics features of final columnar microstructure of deposited thin films [1; 2; 131]. The sample S042 represents slightly inclined columnar grains which might be due to the shadowing effects, please refer Figure 39 for more information. One of the important factors that contributes to the formation of zone 1 microstructure is increase in argon gas pressure. Typical zone 1 microstructure results in low densification when compared with higher densified zone 2 microstructure. The deposition conditions of the following samples S012, S015, S018, S019, S030, S031, S042, S043, S044, S048 and S049 have taken place at low substrate temperature with no substrate heating involved.

The samples S039 and S055 is considered for discussion with respect to microstructural evaluation and these samples exhibit zone 2 microstructure as intercrystalline boundaries are separating the columnar grains. The columnar grains are dense, well bonded fibrous grains which shows matte smooth appearance. When compared with other samples, the titanium sputtering deposition for S039 and S055 is accomplished at comparatively higher temperatures as S039 is heated for thirty minutes using heating elements present in the sputtering equipment which might result in factors which improves the surface diffusion of adatoms to higher extent. The sample S055 is etched with plasma with 100 W RF for 10 minutes, which might have influence the increase in surface diffusion of atoms.

The microstructural evolution of various sputtered TiN coatings which are deposited during this thesis work is discussed in this following section with respect to extended structure zone model (SZM). The SZD is used to estimate the microstructure of thin films deposited by PVD process. However, for polycrystalline thin films such as TiN, zinc oxide deposition, there are several factors which contribute to the final microstructures obtained. So many researchers have proposed several SZM to incorporate various deposition parameters which influence the microstructures of thin film obtained. The extended SZM by S. Mahieu et al. is used in this work to investigate TiN thin films deposited by magnetron sputtering process and this model basically is an extended version of Thornton SZD.

The clean stainless steel substrate used in this process is bombarded with energetic ions and the TiN sputtering deposition is mostly taken place in low temperature operating conditions. The TiN thin films samples namely S013, S016, S024, S033 and S034 displays the Zone Ib (extended SZD) microstructure. The above mentioned samples exhibits characteristic features such as dense columnar grains which are well bonded, uniform column grains, surface morphology resembles facet in no voids present along the microstructures so the structure resemble denser in nature. The sputtering ions from the target material combines with the reactive gas species and bombard the substrate material continuously. So as the sputtering proceeds, the initially formed columnar grains with voids will be filled by the new sputtered species and this results in densified columnar grains in this zone [132]. The zone Ib microstructure formation is explained in the below Figure 77.

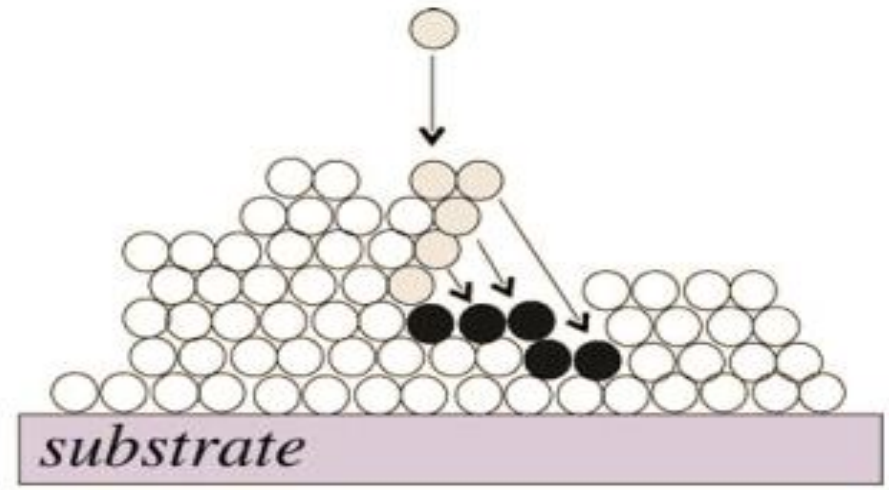

Figure 77. Illustrates the schematic representation of zone Ib formation[132].

The samples which exhibits zone Ic (extended SZD) microstructures are given as follows S014, S017, S023, S025, S026, S029, S032, S035, S040 and S041. The characteristic features which are most predominant in the microstructure is surface morphology is sharply faceted with v shaped surface grains, dense, uniform columnar grains, non-porous, stacking of columns over previously deposited columns is also evident, please refer Figures 49, 57 and 59 for better understanding regarding this feature in microstructure. The reason is when the columns are deposited initially, it will be interacted by the adadtom particles which will be competing with the older columns, so that is the reason there is larger columnar grains over the existing columns in microstructure. This type of columnar growth over existing columnar is due to shadowing effect [132]. The surface diffusion and mobility of adatoms in this zone structure is high when compared with zone Ib [132].

The sample S056 which had been sputter etched by RF power, displays zone T microstructure. The typical features for this microstructures are as follows dense, uniform, well bonded columnar grains with faceted grains, the surface morphology looks smooth in nature. In this microstructure the surface diffusion between columnar grains are more predominant, these feature is not present in zone Ib and Ic structures [132].

6.4 Adhesion and surface roughness

The final microstructures of thin film coatings are profoundly influenced by the packing of columnar grains in the surface which in turn affect the properties such as adhesion strength, surface roughness, hardness, wear and corrosion strength, thermal conductivity. This section mainly focusses on discussing about the properties such as adhesion and roughness property of thin film coating. So in this section the influence of microstructures on these properties are discussed.

The adhesion property of titanium coating is comparatively very low as the samples considered are S030 and S031, which were generally deposited at low temperature conditions. While the sample S055 is sputter etched for 10 minutes. In general, the increase in power will result in improvement in adhesion strength owing to the excess energy present in the deposited film [133]. The increase in power value directly influences the adhesion strength of titanium thin film coating. With higher power better surface diffusion of adatoms is achieved so improved adhesion strength for S031, when compared to sample S030. The sputter etching is an important factor which enhances the adhesion strength of thin film coatings as in this case, S055 is subjected to RF etching with argon ions for 10 minutes. The argon ions remove the surface contaminants, impurities also surface layer to some extent is also removed all these factors contributes to the improved adhesion strength of S055. The sample S055 almost exhibits three times higher adhesion strength when compared with the as deposited

sample S031. With respect to titanium nitride thin film composition, when sputter etching is applied to TiN sample S056, the adhesion strength is improved to 9 MPa which is approximately five times higher when compared with as deposited sample (TiN) S026 adhesion strength value 1.6 MPa. The sputter deposited Ti and TiN thin film coatings generally displayed lower values of adhesion strength. However, it is expected that when substrate etching is involved in sputtering experiments, the adhesion strength property of thin film coatings improved significantly.

The surface roughness (Ra) value decreases in titanium coating when the power value is increased. This phenomenon is because when the power value is increased, it results in enhancement in surface diffusion, so which result in decrease of surface roughness value at least to some extent as shown in Table 10. The surface roughness value of TiN coatings is decreased when sputtering power value is increased because improvement in surface diffusion is achieved. With slight increase in nitrogen sputtering pressure does not have any major impact in resultant surface roughness value. As in this case, when nitrogen partial pressure is increased from 6 mtorr to 7 mtorr, it results in no significant improvement in surface roughness value, please refer table 12. The increase in nitrogen partial pressure is generally results in modifying the topography of thin films surface which generally means the surface roughness is increased considerably. So the structure of the columnar grains results in coarse surface and it effects in higher surface roughness value [134]. The surface roughness value of thin film coating for titanium is around 340 nm (maximum) which is low with respect to surface roughness value of TiN coating 650 nm (maximum), this might be due to the inclusion of nitrogen composition in the gas composition. When substrate etched samples is considered, the adhesion strength is increased significantly, which gives the clear idea with further enhancement in etching process, improved adhesion strength of thin film coating can be achieved.

6.5 Phase structure

According to the database which is used as reference from International center for diffraction data (ICDD), there are some peaks which are not visible in the sputtered titanium and titanium nitride XRD pattern, for instance in Ti diffraction analysis represented in Figure 44 a, the peaks at $2\theta = 39.897^{\circ}$ is not detected. The reason for this observations is due to fact that occupies higher lattice dimensions, so the peak moved towards left side as shown in Figure 44 b. The other reason for this behavior is due to the fact that stresses present in some lattice points, argon ion inclusion in thin film during sputtering process [135]. So all the above mentioned factors or the combined effects might be reason for change of crystal planes detected in this XRD analysis. [135] The low glancing angle is used for XRD analysis, due to the fact that nanometer thickness of Ti thin films is used for observation. This nanometer thickness is relatively low when compared with the other deposition or fabrication techniques, so this might be the reason for missing or shifting of some peaks in XRD pattern. For instance, the

observed peaks are shifted as depicted in peaks at 2θ = 37.777˚and 69.635˚. The reason for the shift is most likely due to well known facts such as stresses occurring during lattice distortions and titanium ions occupying interstitial positions in the crystal system. The crystal orientation of the thin films deposited can also be affected by the substrate used. The different height of peaks and missing peaks are might be due to orientation of the crystal. The reason for short and shallow peaks in this XRD patterns is might be due to low thickness of the coating and the substrate (stainless steel) compositions are observed and it is overlapping with the XRD peaks of titanium at 2θ =50.375˚and 74.679˚. [7] The high intensity peaks for stainless steel peak is observed at 2θ = 43.038˚, 50.375˚, 74.679˚ and 90.998˚ with the crystal planes (1 1 1) and (2 0 0) as explained in various research articles. The titanium nitride and stainless steel composition both exhibited FCC structure. [120; 136] So this might be the reason for some peaks overlap at 2θ = 43.709˚ 50.375˚and 74.679˚.

From the XRD pattern of deposited titanium nitride thin film, high intensity peak is observed at 2θ = 36.673˚, 42.601˚, 61.825˚ and 74.084˚. The Figure 63 a, shows the XRD pattern for sample S032 and various peaks for TiN thin films. The preferred orientation of TiN peaks is observed in crystal planes (2 0 0) at 2θ = 42.601˚. From numerous articles it is also verified that the orientation at (1 1 1) and (2 2 0) crystal plane observed at 36.673˚ and 61.825˚ correspond to titanium nitride peaks which are most predominant [137-139]. The (1 1 1) peaks is mostly observed in FCC structure. The broad peaks observed during XRD pattern might be also due to the peaks which exhibits substochimetric phases of TiN and also due to overlapping of peaks at 43.038˚and 74.679˚. Several research articles claimed that the peaks observed at (2 0 0) is also due to titanium nitride preferred orientation [7; 140-142]. So according to this discussion, the crystallographic orientation of sputtered Ti and TiN is evaluated in detail, however due to the low thickness range of thin films used in this XRD analysis, only limited information regarding the phases present in the composition is attained.

7. CONCLUSIONS

The thin film coating formation of titanium and titanium nitride compositions is successfully deposited using Nordiko sputtering equipment. Typical deposition rates of 30-75 nm/min were able to achieve in this DC magnetron sputtering process. In this thesis work, the correlation between deposition parameters is studied in detail and the important results related to deposition rates of thin film coatings is typically verified. Although well-established relationship between some deposition parameters were not able to verified due to unidentified reasons. The effect of deposition parameters on microstructures and properties such as adhesion strength and surface roughness is successfully studied using several characterization techniques such as FESEM, adhesion strength, optical profilometer and XRD analysis. The effect of substrate etching and heating is studied briefly in this thesis work and the corresponding results demonstrated significant improvement in adhesion strength values. Thus, if substrate etching and substrate heating is extensively studied, it will result in substantial improvement in final microstructures and properties of thin films deposited by sputtering process.

The sputtering equipment used in this experiment work is investigated completely and it can be used for versatile operations. One of the many advantages is that the equipment can be used for RF sputtering when non-conducting materials are involved. A short operational guide regarding the user manual is also prepared in this thesis report.

The short summary of the sputter deposition process with respect to this sputter equipment is stated as follows

1) Titanium depositions

- Higher sputtering power results in higher deposition rates, but care needs to be taken to prevent overheating of target materials.
- Typical deposition rates of around 50-75 nm/min were able to achieve in the sputtering pressure range of 5 to 10 mtorr, with further increase in sputtering pressure, deposition rates tend to decrease considerably.

2) Titanium nitride depositions

- Increased sputtering power directly relates to deposition rate, but precaution needs to be taken to avoid target overheating.
- Increase in nitrogen partial pressure value result in decrease of deposition rates of titanium nitride thin films.

- Typical deposition rates of around 25-35 nm/min were achieved in this sputtering experiments

3) Microstructures

- Columnar microstructures were observed in deposited thin films, however the coatings look dense and well-bonded in nature. According to Thornton structure zone model, zone T and zone 2 is mostly observed in the deposited thin films,

4) Adhesion strength

- Typical adhesion strength of around 3 MPa is achieved for titanium thin films when substrate etching is used in the sputtering process. Likewise, when sputter etching is used for TiN thin film coating, adhesion strength of approximately 9 MPa is accomplished.

5) XRD

- Crystalline phases of titanium and titanium nitride compositions is detected with minor shift observed in the peaks due to higher lattice dimensions.

Recommended sputtering parameters for the Nordiko equipment is given as follows with respect to,

i)Titanium deposition

a) Sputtering power - 300-700 Watts
b) Sputtering pressure - 5-10 mtorr
c) Time - 3-10 minutes; for higher thicknesses longer deposition times are naturally needed

ii) Titanium nitride deposition

a) Sputtering power - 350-800 Watts
b) Argon sputtering pressure - 5-7 mtorr
c) Nitrogen sputtering pressure - 1-3 mtorr
d) Time - 5-30 minutes; for higher thicknesses longer deposition times are naturally needed.

8. SUGGESTIONS FOR FUTURE STUDIES

The sputter deposition process is highly advantageous when it is used to it full potential. With this in mind and the experience gained during this research studies, the future work is planned to conduct with respect to substrate etching and substrate heating process, in order to get more information about the film properties. The Nordiko sputtering equipment is also well suited for RF sputtering process. So more research work is planned to conduct in this RF sputtering field. The manufacturing of alloy compounds by this sputtering equipment is planned to study in the future. The sputtering equipment is running well and available for future research work of sputter coating of different materials.

REFERENCES

[1] F.R. Bunshah, HANDBOOK OF DEPOSITION TECHNOLOGIES FOR FILMS AND COATINGS, second edition ed. Noyes Publications, Mill Road, Park Ridge, New Jersey 07656, 1994, 27-888 p.

[2] Martin, M.P. (ed.). 2009. Handbook of Deposition Technologies for Films and Coatings. Third edition ed. Norwich, N.Y., William Andrew ; Oxford : Elsevier Science [distributor], 2009. 253-294 p.

[3] Handbook on RF sputtering-Instructions manual, Nordiko, Nordiko Limited, Nordiko limited, Brockhampton Lane, Havant, Hants, PO9 1SR, .

[4] P. De Araujo, P. Steyer, J.-. Millet, E. Damond, B. Stauder, P. Jacquot, PVD Aluminium Alloy Coatings: Environmentally Friendly Alternative to Protect Steel Parts Against Corrosion, Surface Engineering, Vol. 19, No. 4, 2003, pp. 304-309.

[5] I. Safi, Recent aspects concerning DC reactive magnetron sputtering of thin films: a review, Surface and Coatings Technology, Vol. 127, No. 2, 2000, pp. 203-218.

[6] G.J. Exarhos, X. Zhou, Discovery-based design of transparent conducting oxide films, Thin Solid Films, Vol. 515, No. 18, 2007, pp. 7025-7052.

[7] Y.L. Jeyachandran, S.K. Narayandass, D. Mangalaraj, S. Areva, J.A. Mielczarski, Properties of titanium nitride films prepared by direct current magnetron sputtering, Materials Science and Engineering: A, Vol. 445–446, 2007, pp. 223-236.

[8] P.M. Martin, Handbook of deposition technologies for films and coatings: science, applications and technology, William Andrew, 2009, .

[9] L.J. VOSSEN, W. KERN, THIN FILM PROCESSES II, First ed. ACADEMIC PRESS INC., San Dielo, CA 92101, 1991, 854 p.

[10] J.L. Vossen, W. Kern, Thin Film Processes. 1978, Academic Press, New York, 1991, 564 p.

[11] Y.L. Jeyachandran, B. Karunagaran, S.K. Narayandass, D. Mangalaraj, T.E. Jenkins, P.J. Martin, Properties of titanium thin films deposited by dc magnetron sputtering, Materials Science and Engineering: A, Vol. 431, No. 1–2, 2006, pp. 277-284.

[12] C. Huang, K. Tay, L. Wu, Aluminum nitride films deposited under various sputtering parameters on molybdenum electrodes, Solid-State Electronics, Vol. 49, No. 2, 2005, pp. 219-225.

[13] J.P. Kar, S. Kim, B. Shin, K.I. Park, K.J. Ahn, W. Lee, J.H. Cho, J.M. Myoung, Influence of sputtering pressure on morphological, mechanical and electrical properties of Al-doped ZnO films, Solid-State Electronics, Vol. 54, No. 11, 2010, pp. 1447-1450.

[14] V. Kolkovsky, K. Lukat, E. Kurth, C. Kunath, Reactively sputtered hafnium oxide on silicon dioxide: Structural and electrical properties, Solid-State Electronics, Vol. 106, 2015, pp. 63-67.

[15] C.M.T. Sanchez, B.R. Plata, M.E.H.M. da Costa, F.L. Freire Jr., Titanium diboride thin films produced by dc-magnetron sputtering: Structural and mechanical properties, Surface and Coatings Technology, Vol. 205, No. 12, 2011, pp. 3698-3702.

[16] A. Besnard, N. Martin, F. Sthal, L. Carpentier, J. Rauch, Metal-to-Dielectric transition induced by annealing of oriented titanium thin films, Functional Materials Letters, Vol. 6, No. 01, 2013, pp. 1250051.

[17] M. Ohring, Plasma and Ion Beam Processing of Thin Films, in: Academic Press (ed.), Materials Science of Thin Films, Second edition ed., Academic Press, 525 B Street, Suite 1900, San Diego, CA 92101-4495, USA, 2002, pp. 205-206.

[18] M.M. Waite, S.I. Shah, D.A. Glocker, Sputtering Sources, SVC Bulletin, No. Spring 2010, 2010, pp. 42-50.

[19] D.V. Ho, THE DESIGN AND MODIFICATION OF A SPUTTER SYSTEM FOR DC REACTIVE SPUTTERING OF ALUMINA AND ZIRCONIA THIN FILMS, Master of Science in Mechanical Engineering, 2011, 1-108 p. Available: http://etd.lsu.edu/docs/available/etd-06302011-115240/unrestricted/Ho_Thesis.pdf.

[20] Home page of SEMICORE, Hughes.M, What Is Sputtering? SEMICORE Equipment, Inc, web page. Available (accessed 17.01.2015): http://www.semicore.com/what-is-sputtering.

[21] Home page of King Fahd University of Petroleum & Minerals, DC/RF Sputtering, King Fahd University of Petroleum & Minerals (KFUPM), web page. Available (accessed 21.05.2015): http://www.kfupm.edu.sa/sites/tsf/AnalyticsReports/sputtering.pdf.

[22] M. Ohring, Materials Science of Thin Films, Second edition ed. Academic Press, 525 B Street, Suite 1900, San Diego, CA 92101-4495, USA, 2002, .

[23] K. Seshan, HANDBOOK OF THIN-FILM DEPOSITION PROCESSES AND TECHNIQUES, Second ed. NOYES PUBLICATION, Intel Corporation Santa Clara, California, 2002, 1-629 p.

[24] M. Ohring, Materials science of thin films, Second ed. Academic press, 2001, 794 p.

[25] M. Jarratt, History of PVD coatings, PVD coatings, web page. Available (accessed 05.05.2015): https://www.pvd-coatings.co.uk/history-pvd-coatings/.

[26] K. Seshan, Handbook of thin film deposition, William Andrew, 2012, .

[27] P.M. Martin, Handbook of deposition technologies for films and coatings: science, applications and technology, Third ed. William Andrew, Norwich, N.Y., 2009, .

[28] Deposition of Metals Using Either E-Beam Evaporation or Sputtering Techniques, Dartmouth College(US), web page. Available (accessed 15.02.2016): https://engineering.dartmouth.edu/microeng/courses/es194/student/jiaying/sem/topic.html.

[29] D. Tabor, Interaction between surfaces: adhesion and friction, Surface physics of materials, Vol. 2, 1975, pp. 509.

[30] K. Koski, J. Hölsä, J. Ernoult, A. Rouzaud, The connection between sputter cleaning and adhesion of thin solid films, Surface and Coatings Technology, Vol. 80, No. 1, 1996, pp. 195-199.

[31] E. Taglauer, Surface cleaning using sputtering, Applied Physics A, Vol. 51, No. 3, 1990, pp. 238-251.

[32] J. Vossen, The preparation of substrates for film deposition using glow discharge techniques, Journal of Physics E: Scientific Instruments, Vol. 12, No. 3, 1979, pp. 159.

[33] E. Hoyt, M. Hoyt, R. Kirby, C. Perkins, D. Wright, A. Farvid, Processing of OFE copper beam chambers for PEP-II high energy ring, Particle Accelerator Conference, 1995., Proceedings of the 1995, IEEE, pp. 2054-2056.

[34] A. Mathewson, The effects of cleaning and other treatments on the vacuum properties of technological materials used in ultra high vacuum, 1987, pp. 102.

[35] M. Taborelli, Cleaning and surface properties, CERN Accelerator School Vacuum in accelerators, 2007, pp. 321.

[36] M. Taborelli, Cleaning and surface properties, CERN Accelerator School Vacuum in accelerators, 2007, pp. 321.

[37] Solvay, Sifren® 46, Cleaning gas for the use in plasma, ion beam or sputter etching in semiconductor devices manufacturing. web page. Available (accessed 11/11): http://www.solvay.com/en/markets-and-products/featured-products/sifren-46.html.

[38] D. Perednis, L.J. Gauckler, Thin film deposition using spray pyrolysis, Journal of electroceramics, Vol. 14, No. 2, 2005, pp. 103-111.

[39] R.F. Bunshah, Handbook of deposition technologies for films and coatings: science, technology, and applications, Second ed. William Andrew, 1994, 888 p.

[40] I. Ben Mbarek, F. Chaabouni, M. Selmi, M. Abaab, B. Rezig, Effect of the substrate temperature on the properties of the RF sputtered TiO2 thin films, physica status solidi (c), Vol. 7, No. 9, 2010, pp. 2311-2315.

[41] S. Kaya, E. Yilmaz, H. Karacali, A. Cetinkaya, A. Aktag, Samarium oxide thin films deposited by reactive sputtering: Effects of sputtering power and substrate temperature on microstructure, morphology and electrical properties, Materials Science in Semiconductor Processing, Vol. 33, 2015, pp. 42-48.

[42] R.N. Anderson, T.E. Deacon, D.K. Carlson, Apparatus and method for substrate heating utilizing various infrared means to achieve uniform intensity. US5179677 A, US 07/651,668, (12.01.1993), .

[43] M. Tahashi, M. Ishihara, K. Sassa, S. Asai, Control of Crystal Orientation in Deposited Films of Bismuth Vaporized in Laser and Resistance Heating Methods under a High Magnetic Field. Materials Transactions, Vol. 44, No. 2, 2003, pp. 285-289.

[44] J. Lam, D. Hodul, Method for microwave plasma substrate heating. U.S. Patent No. 6,030,666, US 08/831,495, (29.02.2000), .

[45] PVD PRODUCTS, Inconel_disc, web page. Available (accessed 11/11): http://www.pvdproducts.com/products/substrate-heaters/attachment/inconel_disc.

[46] S. Jeong, J. Lee, S. Lee, J. Boo, Deposition of aluminum-doped zinc oxide films by RF magnetron sputtering and study of their structural, electrical and optical properties, Thin Solid Films, Vol. 435, No. 1, 2003, pp. 78-82.

[47] X. Li, H. Li, Z. Wang, H. Xia, Z. Xiong, J. Wang, B. Yang, Effect of substrate temperature on the structural and optical properties of ZnO and Al-doped ZnO thin films prepared by dc magnetron sputtering, Optics Communications, Vol. 282, No. 2, 2009, pp. 247-252.

[48] Y. Kim, K. Lee, T. Lee, B. Cheong, T. Seong, W. Kim, Effects of substrate temperature and Zn addition on the properties of Al-doped ZnO films prepared by magnetron sputtering, Applied Surface Science, Vol. 255, No. 16, 2009, pp. 7251-7256.

[49] Z. Zhang, C. Bao, W. Yao, S. Ma, L. Zhang, S. Hou, Influence of deposition temperature on the crystallinity of Al-doped ZnO thin films at glass substrates prepared by RF magnetron sputtering method, Superlattices and Microstructures, Vol. 49, No. 6, 2011, pp. 644-653.

[50] S. Lin, J. Huang, P. Šajgalik, Effects of substrate temperature on the properties of heavily Al-doped ZnO films by simultaneous rf and dc magnetron sputtering, Surface and Coatings Technology, Vol. 190, No. 1, 2005, pp. 39-47.

[51] P. Barna, History of thin films: growth techniques characterization, Research Institute for Technical Physics and Materials Science of HAS, Budapest, Hungary, Autumn School, 2005, .

[52] Z. Xu, W. Chan, Preparation and electrical properties of highly (111) oriented antiferroelectric PLZST films by radio frequency magnetron sputtering, Acta materialia, Vol. 55, No. 11, 2007, pp. 3923-3928.

[53] R. Navamathavan, C.K. Choi, E. Yang, J. Lim, D. Hwang, S. Park, Fabrication and characterizations of ZnO thin film transistors prepared by using radio frequency magnetron sputtering, Solid-State Electronics, Vol. 52, No. 5, 2008, pp. 813-816.

[54] N.H. Al-Hardan, M.J. Abdullah, H. Ahmad, A.A. Aziz, L.Y. Low, Investigation on UV photodetector behavior of RF-sputtered ZnO by impedance spectroscopy, Solid-State Electronics, Vol. 55, No. 1, 2011, pp. 59-63.

[55] Q.M. Wang, K.H. Kim, Microstructural control of Cr–Si–N films by a hybrid arc ion plating and magnetron sputtering process, Acta Materialia, Vol. 57, No. 17, 2009, pp. 4974-4987.

[56] L. Chen, S. Liu, Growth and characterization of indium oxide diodes prepared by reactive magnetron sputtering, Solid-State Electronics, Vol. 50, No. 7–8, 2006, pp. 1355-1358.

[57] Y. Pei, C. Chen, K. Shaha, De Hosson, J Th M, J. Bradley, S. Voronin, M. Čada, Microstructural control of TiC/aC nanocomposite coatings with pulsed magnetron sputtering, Acta Materialia, Vol. 56, No. 4, 2008, pp. 696-709.

[58] C. Sengstock, M. Lopian, Y. Motemani, A. Borgmann, C. Khare, P.J.S. Buenconsejo, T.A. Schildhauer, A. Ludwig, M. Köller, Structure-related antibacterial activity of a titanium nanostructured surface fabricated by glancing angle sputter deposition, Nanotechnology, Vol. 25, No. 19, 2014, pp. 195101.

[59] T. Chang, W. Wang, F. Huang, L. Wang, J. Hwang, Rapid thermal nitridation of titanium on Cu/Si contact system, Solid-State Electronics, Vol. 38, No. 4, 1995, pp. 815-820.

[60] H. Seo, M. Son, J. Kim, I. Shin, K. Prabakar, H. Kim, Method for fabricating the compact layer in dye-sensitized solar cells by titanium sputter deposition and acid-treatments, Solar Energy Materials and Solar Cells, Vol. 95, No. 1, 2011, pp. 340-343.

[61] M.N. Polyakov, T. Chookajorn, M. Mecklenburg, C.A. Schuh, A.M. Hodge, Sputtered Hf–Ti nanostructures: A segregation and high-temperature stability study, Acta Materialia, Vol. 108, 2016, pp. 8-16.

[62] A. Furlan, J. Lu, L. Hultman, U. Jansson, Control of crystallinity in sputtered Cr–Ti–C films, Acta Materialia, Vol. 61, No. 17, 2013, pp. 6352-6361.

[63] A. Kelling, K.R. Mangipudi, I. Knorr, T. Liese, H. Krebs, C.A. Volkert, Investigating fracture of nanoscale metal–ceramic multilayers in the transmission electron microscope, Scripta Materialia, Vol. 115, 2016, pp. 42-45.

[64] R. Banerjee, S.A. Dregia, H.L. Fraser, Stability of fcc titanium in titanium/aluminum multilayers, Acta materialia, Vol. 47, No. 15, 1999, pp. 4225-4231.

[65] J. Chakraborty, K. Kumar, R. Ranjan, S.G. Chowdhury, S. Singh, Thickness-dependent fcc–hcp phase transformation in polycrystalline titanium thin films, Acta Materialia, Vol. 59, No. 7, 2011, pp. 2615-2623.

[66] H. Uchida, S. Inoue, K. Koterazawa, Electrochemical evaluation of pinhole defects in TiN films prepared by rf reactive sputtering, Materials Science and Engineering: A, Vol. 234, 1997, pp. 649-652.

[67] J.F. Pierson, D. Horwat, Addition of silver in copper nitride films deposited by reactive magnetron sputtering, Scripta Materialia, Vol. 58, No. 7, 2008, pp. 568-570.

[68] E. Zalnezhad, A.A.D. Sarhan, M. Hamdi, Investigating the fretting fatigue life of thin film titanium nitride coated aerospace Al7075-T6 alloy, Materials Science and Engineering: A, Vol. 559, 2013, pp. 436-446.

[69] B.F. Chen, W.L. Pan, G.P. Yu, J. Hwang, J.H. Huang, On the corrosion behavior of TiN-coated AISI D2 steel, Surface and Coatings Technology, Vol. 111, No. 1, 1999, pp. 16-21.

[70] H.C. Barshilia, N. Selvakumar, K.S. Rajam, A. Biswas, Optical properties and thermal stability of TiAlN/AlON tandem absorber prepared by reactive DC/RF magnetron sputtering, Solar Energy Materials and Solar Cells, Vol. 92, No. 11, 2008, pp. 1425-1433.

[71] M. Janders, U. Egert, M. Stelzle, W. Nisch, Novel thin film titanium nitride micro-electrodes with excellent charge transfer capability for cell stimulation and sensing applications, Engineering in Medicine and Biology Society, 1996. Bridging Disciplines for Biomedicine. Proceedings of the 18th Annual International Conference of the IEEE, IEEE, pp. 245-247.

[72] P. Patsalas, C. Charitidis, S. Logothetidis, The effect of substrate temperature and biasing on the mechanical properties and structure of sputtered titanium nitride thin films, Surface and Coatings Technology, Vol. 125, No. 1–3, 2000, pp. 335-340.

[73] R. Wuhrer, W.Y. Yeung, Grain refinement with increasing magnetron discharge power in sputter deposition of nanostructured titanium aluminium nitride coatings, Scripta Materialia, Vol. 50, No. 6, 2004, pp. 813-818.

[74] R. Wuhrer, W.Y. Yeung, Effect of target–substrate working distance on magnetron sputter deposition of nanostructured titanium aluminium nitride coatings, Scripta Materialia, Vol. 49, No. 3, 2003, pp. 199-205.

[75] N.J.M. Carvalho, J.T.M. De Hosson, Deformation mechanisms in TiN/(Ti,Al)N multilayers under depth-sensing indentation, Acta Materialia, Vol. 54, No. 7, 2006, pp. 1857-1862.

[76] H.C. Barshilia, Growth, characterization and performance evaluation of Ti/AlTiN/AlTiON/AlTiO high temperature spectrally selective coatings for solar thermal power applications, Solar Energy Materials and Solar Cells, Vol. 130, 2014, pp. 322-330.

[77] S. Massl, W. Thomma, J. Keckes, R. Pippan, Investigation of fracture properties of magnetron-sputtered TiN films by means of a FIB-based cantilever bending technique, Acta Materialia, Vol. 57, No. 6, 2009, pp. 1768-1776.

[78] F. Kauffmann, B. Ji, G. Dehm, H. Gao, E. Arzt, A quantitative study of the hardness of a superhard nanocrystalline titanium nitride/silicon nitride coating, Scripta Materialia, Vol. 52, No. 12, 2005, pp. 1269-1274.

[79] M. Okada, M. Tazawa, P. Jin, Y. Yamada, K. Yoshimura, Fabrication of photocatalytic heat-mirror with TiO 2/TiN/TiO 2 stacked layers, Vacuum, Vol. 80, No. 7, 2006, pp. 732-735.

[80] Z. Lin, M. Zhuo, M. Li, J. Wang, Y. Zhou, Synthesis and microstructure of layered-ternary Ti 2 AlN ceramic, Scripta Materialia, Vol. 56, No. 12, 2007, pp. 1115-1118.

[81] T. Joelsson, A. Hörling, J. Birch, L. Hultman, Single-crystal Ti2AlN thin films, Applied Physics Letters, Vol. 86, No. 11, 2005, pp. 111913.

[82] C. Hwang, M. Juang, M. Lai, C. Jaing, J. Chen, S. Huang, H. Cheng, Effect of rapid-thermal-annealed TiN barrier layer on the Pt/BST/Pt capacitors prepared by RF magnetron co-sputter technique at low substrate temperature, Solid-State Electronics, Vol. 45, No. 1, 2001, pp. 121-125.

[83] L. Chen, S. Wang, Y. Du, J. Li, Microstructure and mechanical properties of gradient Ti (C, N) and TiN/Ti (C, N) multilayer PVD coatings, Materials Science and Engineering: A, Vol. 478, No. 1, 2008, pp. 336-339.

[84] T. An, M. Wen, C.Q. Hu, H.W. Tian, W.T. Zheng, Interfacial fracture for TiN/SiNx nano-multilayer coatings on Si(1 1 1) characterized by nanoindentation experiments, Materials Science and Engineering: A, Vol. 494, No. 1–2, 2008, pp. 324-328.

[85] Thin Film Coating Services | VPE Inc. web page. Available (accessed 11/12/2015): http://www.vpei.com/technologies-processes/thin-film-coating.

[86] What is PVD coating and how does PVD coating work? « Oerlikon Balzers, web page. Available (accessed 11/12/2015): http://www.oerlikon.com/balzers/en/know-how/coating-technologies/pvd-process/.

[87] Copper Facts: Chemical and Physical Properties, web page. Available (accessed 11/11/2015): http://chemistry.about.com/od/elementfacts/a/copper.htm.

[88] Stainless Steel, web page. Available (accessed 11/11/2015): http://www.aalco.co.uk/products/stainless-steel.aspx.

[89] Stainless Steels - Introduction To Grades, Properties and Applications, Supplier Data by Aalco, web page. Available (accessed 11/11/2015): http://www.azom.com/article.aspx?ArticleID=2873.

[90] Article: Melting temperature ranges for stainless steels, web page. Available (accessed 11/11/2015): http://www.bssa.org.uk/topics.php?article=103.

[91] M. Lira-Cantú, A. Morales Sabio, A. Brustenga, P. Gómez-Romero, Electrochemical deposition of black nickel solar absorber coatings on stainless steel AISI316L for thermal solar cells, Solar Energy Materials and Solar Cells, Vol. 87, No. 1–4, 2005, pp. 685-694.

[92] Stainless Steel Alloys 316/316L Datasheet | Fine Tubes, web page. Available (accessed 4/28/2016): http://www.finetubes.co.uk/products/specialist-tube-materials/stainless-steel-tubes/alloys-316-316l-uns-s31600-uns-s31603-werkstoff-nr.-1.4401/.

[93] Stainless Steel - Grade 316L - Properties, Fabrication and Applications (UNS S31603), web page. Available (accessed 4/28/2016): http://www.azom.com/article.aspx?ArticleID=2382.

[94] W. Cheng, D. Chen, C. Wang, High-temperature corrosion of Cr–Mo steel in molten LiNO3–NaNO3–KNO3 eutectic salt for thermal energy storage, Solar Energy Materials and Solar Cells, Vol. 132, 2015, pp. 563-569.

[95] M. Kotilainen, Temperature-Induced Ageing Mechanisms and Long-Term Stability of Solar Thermal Absorber Coatings, Tampereen teknillinen yliopisto.Julkaisu-Tampere University of Technology.Publication; 1222, 2014, .

[96] Titanium - Element information, properties and uses | Periodic Table, web page. Available (accessed 11/12/2015): http://www.rsc.org/periodic-table/element/22/titanium.

[97] Titanium Facts - Uses, Properties, Element Ti, Strength, Jewelry, Alloys, web page. Available (accessed 11/12/2015): http://www.sciencekids.co.nz/sciencefacts/metals/titanium.html.

[98] Total Materia - Titanium Properties, web page. Available (accessed 11/12/2015): http://www.totalmateria.com/page.aspx?ID=TitaniumProperties&LN=EN.

[99] Facts About Titanium, web page. Available (accessed 11/12/2015): http://www.livescience.com/29103-titanium.html.

[100] Chapter 6 Vacuum Pumps, Rochester Institute of Technology University, web page. Available (accessed 13.04.2016): https://people.rit.edu/vwlsps/LabTech/Pumps.pdf.

[101] N. Hilleret, Mechanical pumps, CERN EUROPEAN ORGANIZATION FOR NUCLEAR RESEARCH-REPORTS-CERN, 1999, pp. 25-36.

[102] EM40/80 Rotary Vacuum Pumps - Products - Edwards, Edwards Limited, web page. Available (accessed 13.04.2016): https://www.google.com/url?sa=t&rct=j&q=&esrc=s&source=web&cd=1&cad=rja&uact=8&sqi=2&ved=0ahUKEwi_6M_VyYvMAhVjD5oKHYV8BaQQFggcMAA&url=https%3A%2F%2Fshop.edwardsvacuum.com%2FViewers%2FDocument.ashx%3Fid%3D1362%26lcid%3D2057&usg=AFQjCNEaBGs82puQUOLNIcbbGWFzI_CQVQ&sig2=YVXp8ktelelWjoBmT6O5vg.

[103] M.E. Joaquim, B. Foley, Inside a vacuum diffusion pump, American Laboratory, Vol. 35, No. 6, 2003, pp. 30-32.

[104] Agilent Varian HS-20 High Vacuum Diffusion Pump, VacuumFamily.COM, web page. Available (accessed 14.04.2016): http://www.vacuumfamily.com/pro_Agilent-Varian-HS-20-High-Vacuum-Diffusion-Pump_15851.htm.

[105] Dow Corning DC-704 Diffusion Pump Oil, web page. Available (accessed 11/16/2015): http://www.vacuumoil.com/dc704.htm.

[106] M. Goettemoeller, C. Morris, S. Rowell, Consolidated Vacuum Corporation (CVC) Vacuum Evaporation System
STANDARD OPERATING PROCEDURE, University of Washington, web page. Available (accessed 15.04.2016): http://www.ee.washington.edu/research/microtech/cam/SOP/PDFfiles/CVCVacSys.pdf.

[107] Chapter 7: Oil Vapor Diffusion Pumps, Vacuum Technology, web page. Available (accessed 15.04.2016): http://lpc1.clpccd.cc.ca.us/lpc/tswain/chapt7.pdf.

[108] Description of a Basic Vacuum System, Brigham Young University, web page. Available (accessed 15.04.2016): https://www.cleanroom.byu.edu/metal.parts/vacuum.pdf.

[109] S. Sultana, RF Magnetron Sputtering system
Make: Anelva Sputtering Unit Model SPF-332H, Centre for Excellence in Nano-Electronics, Indian Institute of Science, Bangalore-12., web page. Available (accessed 15.04.2016): http://www.nano.iisc.ernet.in/RF%20sputtering%20manual_2010.pdf.

[110] ULTRA Series field emission scanning electron microscope for material science research, web page. Available (accessed 12/16/2015): http://www.zeiss.com/microscopy/en_us/products/scanning-electron-microscopes/ultra-materials.html#ultra-plus.

[111] Elcometer 110 PATTI Pneumatic Adhesion Tester - Test Method, web page. Available (accessed 12/17/2015): http://www.sciteex.com.pl/elcometer/produkts/testmethods/110.htm.

[112] F. Roux, S. Amtablian, M. Anton, G. Besnard, L. Bilhaut, P. Bommersbach, J. Braillon, C. Cayron, A. Disdier, H. Fournier, J. Garnier, A. Jannaud, J. Jouhannaud, A. Kaminski, N. Karst, S. Noël, S. Perraud, O. Poncelet, O. Raccurt, D. Rapisarda, A. Ricaud, D. Rouchon, M. Roumanie, E. Rouviere, O. Sicardy, F. Sonier, K. Tarasov, F. Tardif, M. Tomassini, J. Villanova, Chalcopyrite thin-film solar cells by industry-compatible ink-based process, Solar Energy Materials and Solar Cells, Vol. 115, 2013, pp. 86 92.

[113] M. Kotilainen, M. Honkanen, K. Mizohata, P. Vuoristo, Influence of temperature-induced copper diffusion on degradation of selective chromium oxy-nitride solar absorber coatings, Solar Energy Materials and Solar Cells, Vol. 145, 2016, pp. 323-332.

[114] Elcometer 110,P.A.T.T.I.® Pneumatic Adhesion Tester, Operating Instructions, Elcometer Limited, web page. Available (accessed 17.12.2015): http://www.elcometer.com/images/stories/PDFs/InstructionBooks/110.pdf.

[115] Elcometer 110,P.A.T.T.I.® Pneumatic Adhesion Tester, Operating Instructions, Operating Instructions, 2008/2010, pp. 2-22.

[116] Surface profile measuring systems - Tampere University of Technology, web page. Available (accessed 12/17/2015): http://www.tut.fi/en/about-tut/departments/materials-science/research/research-equipment/surface-analysis/surface-profile-measuring-system/index.htm.

[117] XRD - Tampere University of Technology, web page. Available (accessed 12/21/2015): http://www.tut.fi/en/about-tut/departments/materials-science/research/research-equipment/structural-analysis/xrd/index.htm.

[118] PANalytical - Empyrean, web page. Available (accessed 12/21/2015): http://www.panalytical.com/Empyrean.htm.

[119] R. Chang, F. Chen, C. Chuang, Y. Tung, Residual stresses of sputtering titanium thin films at various substrate temperatures, Journal of nanoscience and nanotechnology, Vol. 10, No. 7, 2010, pp. 4562-4567.

[120] F. Borgioli, A. Fossati, E. Galvanetto, T. Bacci, Glow-discharge nitriding of AISI 316L austenitic stainless steel: influence of treatment temperature, Surface and Coatings Technology, Vol. 200, No. 7, 2005, pp. 2474-2480.

[121] A. Fossati, F. Borgioli, E. Galvanetto, T. Bacci, Glow-discharge nitriding of AISI 316L austenitic stainless steel: influence of treatment time, Surface and Coatings Technology, Vol. 200, No. 11, 2006, pp. 3511-3517.

[122] J.H. Kang, K.J. Kim, Structural, optical, and electronic properties of cubic TiNx compounds, Journal of Applied Physics, Vol. 86, No. 1, 1999, pp. 346-350.

[123] A.S. Reddy, H. Park, V.S. Reddy, K.V.S. Reddy, N.S. Sarma, S. Kaleemulla, S. Uthanna, P.S. Reddy, Effect of sputtering power on the physical properties of dc magnetron sputtered copper oxide thin films, Materials Chemistry and Physics, Vol. 110, No. 2–3, 2008, pp. 397-401.

[124] A.S. Reddy, S. Uthanna, P.S. Reddy, Properties of dc magnetron sputtered Cu2O films prepared at different sputtering pressures, Applied Surface Science, Vol. 253, No. 12, 2007, pp. 5287-5292.

[125] S. Achache, A. Alhussein, S. Lamri, M. François, F. Sanchette, C. Pulgarin, J. Kiwi, S. Rtimi, Sputtered Gum metal thin films showing bacterial inactivation and biocompatibility, Colloids and Surfaces B: Biointerfaces, Vol. 146, 2016, pp. 687-691.

[126] S. Konstantinidis, J. Dauchot, M. Ganciu, A. Ricard, M. Hecq, Influence of pulse duration on the plasma characteristics in high-power pulsed magnetron discharges, Journal of Applied Physics, Vol. 99, No. 1, 2006, pp. 013307.

[127] T. Yeh, J. Wu, L. Hu, The properties of TiN thin films deposited by pulsed direct current magnetron sputtering, Thin Solid Films, Vol. 516, No. 21, 2008, pp. 7294-7298.

[128] S.M. Borah, A.R. Pal, H. Bailung, J. Chutia, Optimization of plasma parameters for high rate deposition of titanium nitride films as protective coating on bell-metal by reactive sputtering in cylindrical magnetron device, Applied Surface Science, Vol. 254, No. 18, 2008, pp. 5760-5765.

[129] A. Barranco, A. Borras, A.R. Gonzalez-Elipe, A. Palmero, Perspectives on oblique angle deposition of thin films: From fundamentals to devices, Progress in Materials Science, Vol. 76, 2016, pp. 59-153.

[130] T. Mäntylä, P. Vuoristo, A. Telama, P. Kettunen, Electrical insulating properties and thermal stability of rf-sputtered alumina coatings, Thin Solid Films, Vol. 126, No. 1-2, 1985, pp. 43-49.

[131] K. Bordo, H. RUBAHN, Effect of deposition rate on structure and surface morphology of thin evaporated Al films on dielectrics and semiconductors, Materials Science, Vol. 18, No. 4, 2012, pp. 313-317.

[132] S. Mahieu, P. Ghekiere, D. Depla, R. De Gryse, Biaxial alignment in sputter deposited thin films, Thin Solid Films, Vol. 515, No. 4, 2006, pp. 1229-1249.

[133] S. Gangopadhyay, R. Acharya, A. Chattopadhyay, S. Paul, Effect of substrate bias voltage on structural and mechanical properties of pulsed DC magnetron sputtered TiN–MoSx composite coatings, Vacuum, Vol. 84, No. 6, 2010, pp. 843-850.

[134] R. Wuhrer, S. Kim, W. Yeung, Effect of nitrogen partial pressure on the surface morphology and properties of reactive dc magnetron sputtered (Ti, Al) N coatings, Scripta Materialia, Vol. 37, No. 8, 1997, pp. 1163-1169.

[135] B.G. Priyadarshini, S. Aich, M. Chakraborty, Substrate bias voltage and deposition temperature dependence on properties of rf-magnetron sputtered titanium films on silicon (100), Bulletin of Materials Science, Vol. 37, No. 7, 2014, pp. 1691-1700.

[136] Y. Wang, D.O. Northwood, An investigation into TiN-coated 316L stainless steel as a bipolar plate material for PEM fuel cells, Journal of Power Sources, Vol. 165, No. 1, 2007, pp. 293-298.

[137] P. Kelly, C. Beevers, P. Henderson, R. Arnell, J. Bradley, H. Bäcker, A comparison of the properties of titanium-based films produced by pulsed and continuous DC magnetron sputtering, Surface and coatings technology, Vol. 174, 2003, pp. 795-800.

[138] P. Mayrhofer, F. Kunc, J. Musil, C. Mitterer, A comparative study on reactive and non-reactive unbalanced magnetron sputter deposition of TiN coatings, Thin Solid Films, Vol. 415, No. 1, 2002, pp. 151-159.

[139] R. Wuhrer, W. Yeung, A comparative study of magnetron co-sputtered nanocrystalline titanium aluminium and chromium aluminium nitride coatings, Scripta Materialia, Vol. 50, No. 12, 2004, pp. 1461-1466.

[140] B. Subramanian, C. Muraleedharan, R. Ananthakumar, M. Jayachandran, A comparative study of titanium nitride (TiN), titanium oxy nitride (TiON) and titanium aluminum nitride (TiAlN), as surface coatings for bio implants, Surface and Coatings Technology, Vol. 205, No. 21, 2011, pp. 5014-5020.

[141] P. Kelly, T. Vom Braucke, Z. Liu, R. Arnell, E. Doyle, Pulsed DC titanium nitride coatings for improved tribological performance and tool life, Surface and Coatings Technology, Vol. 202, No. 4, 2007, pp. 774-780.

[142] D. Nolan, S.W. Huang, V. Leskovsek, S. Braun, Sliding wear of titanium nitride thin films deposited on Ti–6Al–4V alloy by PVD and plasma nitriding processes, Surface and Coatings Technology, Vol. 200, No. 20, 2006, pp. 5698-5705.